SEPARATION AND IDENTIFICATION OF COMPLEX MIXTURES USING CHROMATOGRAPHY MASS SPECTROMETRY

A Thesis
Presented to
The Academic Faculty

by

Hannah L. Barks

In Partial Fulfillment
of the Requirements for the Degree
Master of Science in the
School of Chemistry and Biochemistry

Georgia Institute of Technology
May 2010

SEPARATION AND IDENTIFICATION OF COMPLEX MIXTURES

USING CHROMATOGRAPHY MASS SPECTROMETRY

Approved by:

Dr. Thomas M. Orlando, Advisor
School of Chemistry & Biochemistry
Georgia Institute of Technology

Dr. Nicholas V. Hud
School of Chemistry & Biochemistry
Georgia Institute of Technology

Dr. Facundo M. Fernandez
School of Chemistry & Biochemistry
Georgia Institute of Technology

Dr. Jean-Marie D. Dimandja
School of Chemistry
Spelman College

Dr. Alfred H. Merrill, Jr.
School of Biology
Georgia Institute of Technology

Date Approved: April 2nd, 2010

This is dedicated to….

my parents (Dana E. Anthony and David T. Barks) for their enduring faith in my ability to fulfill my dreams and the patience to let me decide what I think is the best for me no matter what that may bring.

ACKNOWLEDGEMENTS

I wish to thank my coworkers who helped me gather the information and the data for this thesis. Specifically I would like to thank Ragan Buckley for developing experiments and running side-by-side experiments with me. For almost every LC-MS/MS sample I ran, she did an equivalent HPLC-UV run, which gave us ways to compare data and methods throughout each step of project.

I would also like to thank Nicholas V. Hud for starting this project and the ongoing collaboration I enjoyed through the Origins Group (Chemical Bonding Center, Center for Chemical Evolution). This group, funded by the National Science Foundation, supported my work and also allowed me to collaborate with many people I would not have otherwise been able to meet, such as Dr. Jean-Marie D. Dimandja from Spelman College, Dr. Greg Springsteen from Furman University, and Dr. Ernesto DiMauro from Universita Sapienza. The collaboration with Dr. J Dimandja led to many experiments using GC×GC-MS which are described in this thesis. I greatly appreciate all of the time and patience that Dr. Dimandja showed me throughout our time working together and I hope I get a chance to work with him again. I would also like to thank Amanda Bryant for her work preparing standards and samples of the formamide mixtures for analysis via GC×GC-MS. Dr. Greg Springsteen's work done on the equilibrium between formamide and ammonium formate was very helpful in determining the bulk composition of my samples. Further, Dr. Springsteen's work led to extensive analysis by Ragan Buckley and myself on the role of ammonium formate and water in the formation of nucleic acid bases. Dr. Ernesto DiMauro's previous work on formamide reactions and the possible

products allowed him to supervise and show us exactly which "catalysts" gave the most products, which products were most likely present on earth, and which products could lead to possible glycosylation of nucleobases.

Dr. Nicholas V. Hud also introduced me to his group members who were very helpful throughout the formamide project. The group members with whom I collaborated most are Dr. Irena Mamajanov, Dr. Heather Bean, Christina Graves, and Ragan Buckley. Dr. Irena Mamajanov conducted extensive hydrogen cyanide (HCN) and diaminomaleonitrile (DAMN) experiments during her time at Brandeis University and was very helpful in determining what the possible intermediates in the formation of nucleic acid bases could be. Dr. Heather Bean was very helpful at the beginning of the project, assisting in the design of experiments to detect possible products of the formamide reactions (including the use of HPLC-UV and LC-MS/MS in our analysis). Christina Graves was also a great help throughout the formamide project due to her conducting extensive formamide heating reactions with different possible "catalysts" and who helped catalog the prebiotic chemical inventory. Lastly, I would like to acknowledge the extensive collaboration with Ragan Buckley; not only did she run almost every formamide sample using HPLC-UV that I ran using LC-MS/MS, she also performed nuclear magnetic resonance (NMR) experiments on samples to determine the bulk composition of the samples, specifically looking at the amount of formamide, water, and ammonium formate after reactions were complete.

I would also like to thank the members of Dr. Thomas M. Orlando's group for listening to multiple presentations on formamide reactions and the use of different separation and detection techniques to determine the composition of these reaction

mixtures. I would especially like to thank Michele M. Dawley for starting this experiment with me using reflectance FTIR measurements to determine if there were any functional group changes in the reactions after heating and to determine the types of surface reactions that may be occurring in the formamide reactions. I would also like to thank members of the Thomas M. Orlando research group. Gregory A. Grieves for his help in finding and modifying the appropriate labview programs to moderate the temperature in for the prebiotic synthesis of purines, Joshua M. Symonds for his help in drawing the reaction center so I could give the plans to the Physics Machine Shop, and Dr. Thomas M. Orlando for his continued guidance through this project and for my time at Georgia Institute of Technology.

None of this work would have been possible without the continued guidance and recommendations from the mass spectrometry facility at the Georgia Institute of Technology. The training I received from David Bostwick on the LC-MS/MS was invaluable, as was his continued interest and willingness to help me throughout the progression of my research. I would also like to thank Dr. Cameron Sullards for his continued guidance in the field of mass spectrometry and for his help in determining the appropriate methods for effectively quantifying the amount of purine that was produced in each pre-biotic synthesis sample.

The advice and the instrumentation obtained from Dr. J. Michael Nicovich from the Dr. Paul Wine research group, was invaluable especially since he showed me how to detect the different wavelengths that were being emitted by the mercury pen-ray lamps I was using.

I would also like to thank Lisa Vaughan, Christopher Kub, Carlos Zuniga, Jennifer Steeb, Nathan Jarnigan, James McNary, Jason McClain, Stacy Elwood, Michael Poston, Kristin Shepherd, Aleks Aleksandrov, Torri Rose, Alice Johnson, Kim Allen, and Alex Jonke for their continued support throughout my time at the Georgia Institute of Technology, my time at Tech would not have been the same without them.

I would also like to thank my baby sister, Malana, for coming to visit me and checking my reactions with me throughout her visit, and showing me that my life was not as boring as I had previously thought.

TABLE OF CONTENTS

Page

LIST OF TABLES

Page

LIST OF FIGURES

Page

LIST OF SYMBOLS AND ABBREVIATIONS

AICN	Aminoimidazole carbonitrile
AICA	Aminoimidizole carboxamide
AP	Atmospheric Pressure
$CaCO_3$	Calcium Carbonate
CID	Collision Induced Dissociation
DAMN	Diaminomaleonitrile
EI	Electron Ionization
ESI	Electrospray Ionization
GC	Gas Chromatography or Capillary Gas Chromatography
2DGC	2 Dimensional Gas Chromatography (usually referring to Heartcut method)
GC×GC2	Gas Chromatography with two different types of columns directly connected
HPLC	High Pressure Liquid Chromatography
MDS	Multidimensional Scattering
MRM	Multiple Reaction Monitoring
MS	Mass Spectrometry
MS/MS	Tandem Mass Spectrometry
$Na_4P_2O_7$	Sodium Pyrophosphate
nm	Nanometer
PCA	Principal Component Analysis
PEEK	Poly-ether-ether-ketone
SRM	Selected Reaction Monitoring
TIC	Total Ion Chromatogram
TOF	Time-of-flight
UV	Ultraviolet

SUMMARY

A variety of nucleobases have previously been identified as products from formamide solutions heated to 160 °C in the presence of various mineral catalysts. Here, for the first time, the formation of adenine, hypoxanthine, and guanine from formamide solutions with only heating to 130 °C and UV-irradiation (in the absence of an inorganic catalyst) is shown. Experimental support for "classical" HCN pathways for purine nucleobase production also being active in heated and UV-irradiated formamide reactions is also shown. This thesis goes on to demonstrate that the product distributions change drastically when the temperature is increased from 130 °C to 160 °C, specifically that the amount of hypoxanthine increases with the addition of UV light, and the amount of adenine greatly increases when the temperature is increased from 130 °C to 160 °C. Along with showing the formation of purines, the identification of pyrimidines was also achieved using GC×GC-MS along with the identification of other nucleobases to be studied in the future. GC×GC-MS was also used to study additional samples, specifically bio-oils, where the types of compounds in the system were easily identifiable and allowed for a direct comparison between different types of bio-oils (Douglas-fir Bark, Pine Bark, and a Pine Bark-Wood mixture).

CHAPTER 1

INTRODUCTION

1.1 Abstract

A great deal of research has been devoted to modeling the formation of nucleobases on early earth and the methods that will be used for the analysis of these molecules throughout the thesis. The chapter begins with an overview of the importance of determining the chemical origin of life and then describes the different reactions that have previously been used to produce the building blocks of life using pre-biotically relevant conditions.

1.2 Previous research in pre-biotic synthesis

The prebiotic origin of ribonucleic acid (RNA) is of great importance due to the hypothesis that the earliest form of life used RNA or proto-RNA for information storage and catalysis (RNA World Hypothesis).[1] For these reasons, and the fact that adenine can be synthesized by a variety of model prebiotic reactions, it is widely speculated that nucleobases were likely part of the very first proto-RNA polymers. These simpler molecules then went on to form RNA or a molecule similar to RNA (proto-RNA) and eventually gave rise to the RNA world. The robustness of nucleic acid base pairing in molecular recognition suggests that even the earliest genetic polymers of life may have used a similar mechanism for information storage and transfer, perhaps even with the same canonical nucleobases that are used in contemporary life. It has also been widely speculated that the first genetic polymers would have assembled from preexisting building blocks (i.e. nucleobases, sugars, phosphate) through condensation-dehydration

reactions.[2-5] Thus, the abiotic synthesis of the RNA nucleobases and related molecules is of great interest with regards to understanding the chemical origin of life.

Deoxyribonucleic acid (DNA), the cell's repository for genetic information, and ribonucleic acid (RNA), the chemical intermediate between DNA and proteins, encode their information of purine (adenine and guanine) and pyrimidine bases (cytosine, thymine, and uracil). In DNA and RNA, each base is bonded to a sugar, and the sugars are linked by phosphate to form information-carrying polymers. Although there are currently five main nucleic acid bases many alternative bases may have been present at the chemical origin of life. Steven Benner proposed that early life on earth may have started with an expanded set of nucleobases, some of which have been lost or replaced over time due to Darwinian natural selection.[6] The hypothesis that RNA preceded the emergence of proteins and that the first self-replicating system was made of RNA or proto-RNA is called the "RNA World Hypothesis."[1] Due to the unlikely formation of RNA directly from the "prebiotic soup," many chemists believe that RNA was not the first self – replicating molecule to form, but was instead preceded by simpler molecules.

The formation of organic compounds under conditions which could be accepted as primitive have been studied extensively throughout the past century. The first successful synthesis of organic compounds under plausible primordial conditions was accomplished by Stanley Miller in 1953.[7] This experiment was performed in a sealed glass bulb that contained materials thought to have been present on early earth: water hydrogen gas, ammonia, and methane. The mixture was heated simulating the action of the sun, and the resulting vapor was subjected to electrical discharges to simulate the

effect of lightening. This experiment yielded racemic mixtures of several proteinogenic amino acids, hydroxyl acids, urea, and other organic molecules.

Miller's experiment was followed a few years later by the formation of adenine from the aqueous polymerization of HCN under basic conditions. This result was first demonstrated by Juan Oro and coworkers in 1961.[8] Oro's synthesis of adenine via the reaction of concentrated solutions of ammonium cyanide are refluxed and adenine is reflected in yields of as much as 0.5 %, along with two main side products, aminoimidizole carboxamide and a cyanide polymer. The mechanism for the formation of purines has been postulated extensively with a variety of different reactants including HCN, formamide, and formamidine.[7-30] The most studied mechanism has been the formation of adenine from HCN, the proposed pathway for this reaction is shown in Figure 1.1.

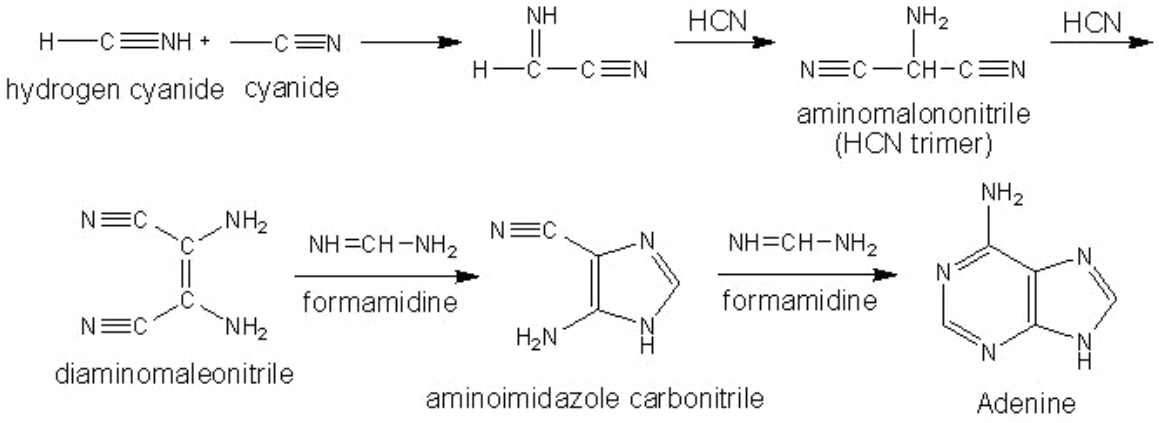

Figure 1.1. Putative mechanism for the formation of adenine from hydrogen cyanide

The limiting reaction in this mechanism is the step in which the HCN tetramer (diaminomaleonitrile) combines with formamidine to form aminoimidizole carbonitrile. Orgel and Ferris (1966) showed that this step can be bypassed via a two-photon photochemical rearrangement of diaminomaleonitrile.[11] This process has been shown to

proceed readily to give high yields of aminoimidizole carbonitrile from diaminofumaronitrile. Once the aminoimidizole carbonitrile has formed it is readily converted to adenine (Figure 1.2).

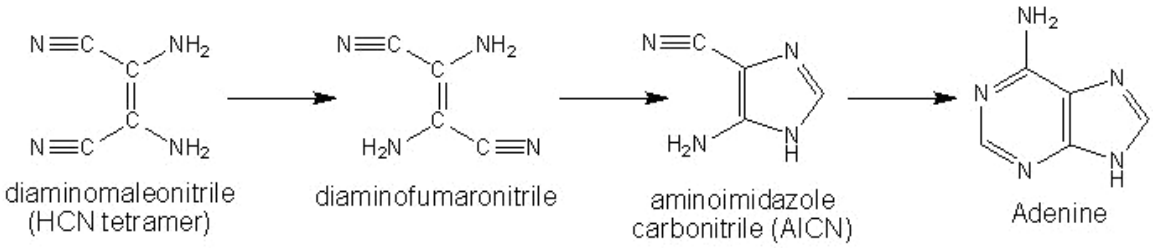

Figure 1.2. Putative pathway for the formation of adenine from diaminomaleonitrile

Along with the production of adenine, other purines could have been generated from aminoimidizole carbonitrile, including diaminopurine and isoguanine. Aminoimidazole carbonitrile (AICN) is easily converted to aminoimizole carboxamide (AICA) that can then lead to the formation of hypoxanthine, guanine, and xanthine.[31,32]

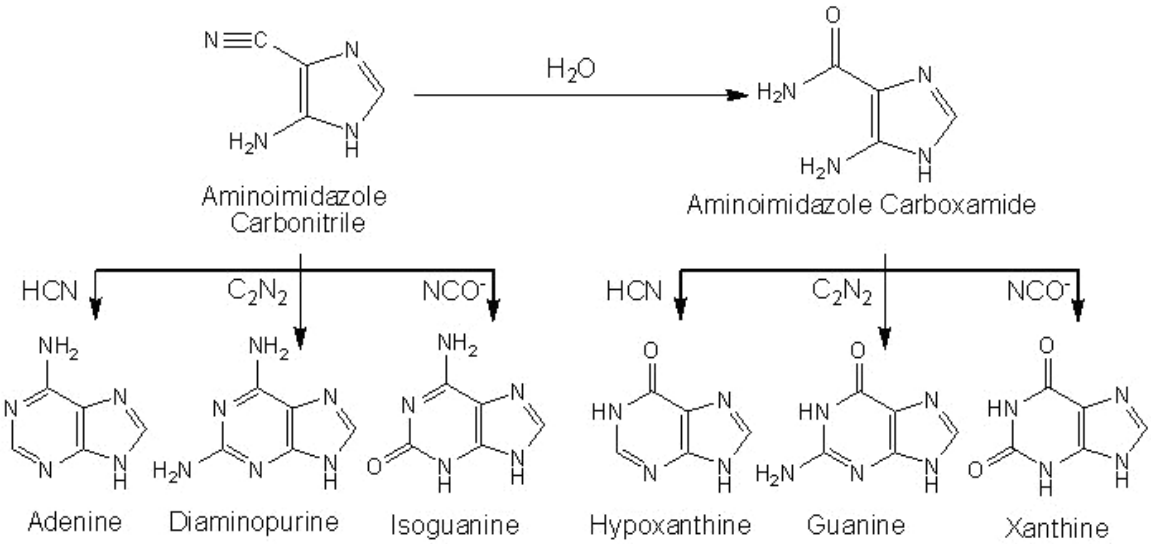

Figure 1.3. Putative pathways to the formation of purines from AICN

The formation of adenine only requires the addition of an HCN molecule to the AICN molecule. The formation of diaminopurine only would require the addition of a C_2N_2 molecule, while the formation of isoguanine requires the addition of a NCO^- ion. The same molecules can be added to AICA to form hypoxanthine, guanine, and xanthine, respectively (Figure 1.3). Guanine has also been observed from the polymerization of ammonium cyanide along with the formation of the purines produced from AICN and AICA that are listed above. Guanine and isoguanine are formed from the hydrolytic deamination of diaminopurine, which can be seen readily from the polymerization of ammonium cyanide.[31]

Since the nitrogenous bases are more stable than the ribose, it is highly likely that the nitrogenous bases were synthesized first so that when the ribose was synthesized the linkage between the two could be made before the sugar decomposed. It also seems likely that the inclusion of a phosphate occurred after the formation of the nucleoside because the conditions required for the phosphate addition are harsh, but once the nitrogenous base has the ribose attached to the base, the sugar is stabilized so that the nucleoside can withstand the rigorous conditions necessary for the phosphate addition.[32]

A linkage between hydrogen cyanide chemistry and formamide chemistry is made due to the fact that formamide is the hydrolysis product of hydrogen cyanide as shown in Figure 1.4.[31]

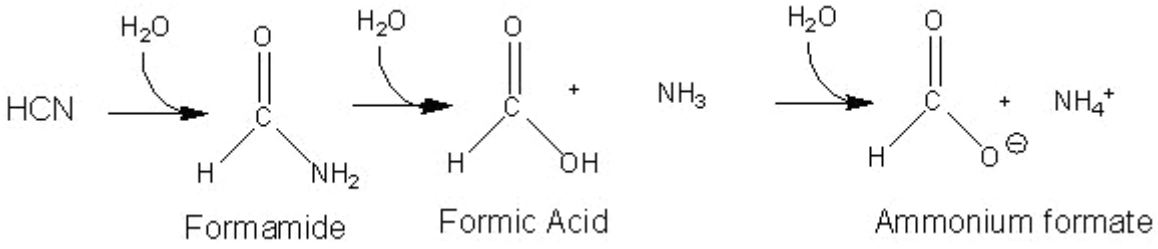

Figure 1.4. Formation of ammonium formate and formamide from hydrogen cyanide

In dilute solutions of hydrogen cyanide, formamide slowly hydrolyzes to formamide and then to formic acid and ammonia, which readily convert into the very soluble salt ammonium formate. AICN can be converted directly to adenine by exposure to hydrogen cyanide. AICN can then be hydrolyzed to form AICA, which can then be converted to hypoxanthine by treatment with hydrogen cyanide.[8,10-12,33] The formation of adenine from AICN and hypoxanthine from AICA has been shown by Zubay and coworkers when the respective precursor and ammonium formate are heated at 75 °C and allowed to evaporate to dryness (Figure 1.5).[29,32] The pathways proposed by Zubay and coworkers for the production of AICN and AICA are shown below.

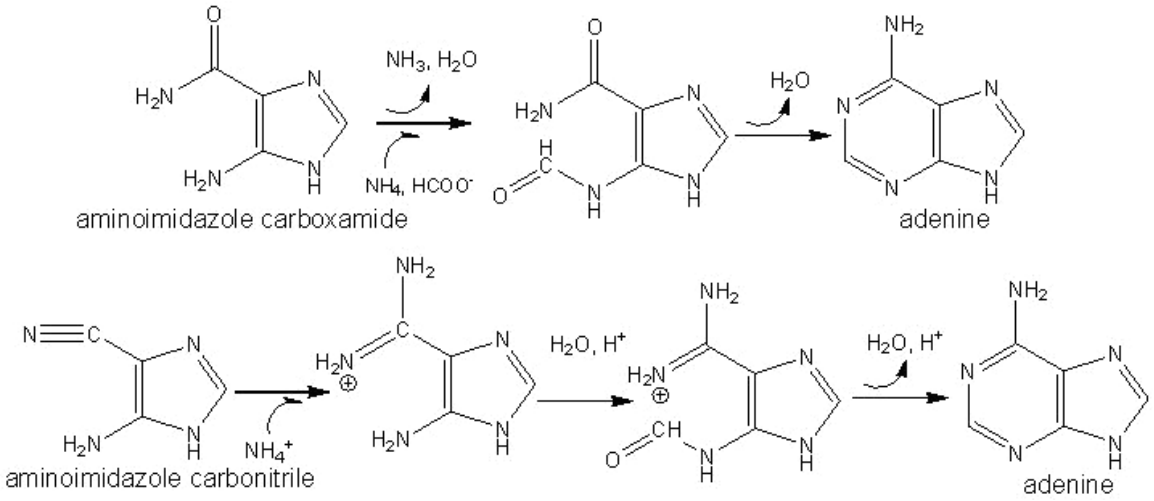

Figure 1.5. Formation of adenine and hypoxanthine from AICN and AICA

Formamide is attractive as a potential prebiotic starting material for the purine bases; it stands out because it contains the four essential elements of life (carbon, hydrogen, oxygen, and nitrogen) and because of its likely prebiotic availability, relative stability, versatile reactivity, and low volatility compared to water.[34] Formamide meets

the requirements of abundance and diffusion in the universe, analysis of the molecular composition of comets and asteroids and of interstellar clouds shows that the two compounds made of the four more common biologically relevant elements H, C, N, and O are isocyanate and formamide.[35-43] For example, formamide was detected in the gas phase of the interstellar medium,[41] in the long period comet Hale-Bopp,[42] and tentatively in the solid phase of grains around the young stellar object W33A.[43]

Formamide also meets the requirements for stability. Since the pivotal experiment by Oro on the synthesis of adenine from HCN, numerous studies have been devoted to assess the role of HCN intermediates in the origin of primordial nucleic acids. With HCN chemistry, two main issues remain unresolved: (1) the thermodynamic instability of HCN under hydrolytic conditions and (2) the narrow panel of nucleobases, limited only to purines that can be formed via HCN condensation processes. HCN chemistry in homogenous solution first requires dissolution in water. After the dissolution process polymerization and hydrolysis of HCN compete, and the resulting concentrations are determined. Hydrolysis to formamide predominates in dilute solutions while polymerization takes over at higher concentrations. Since HCN is more volatile than water it cannot be concentrated by simple evaporation at pH lower than its pK_a (9.2 at 25 °C). This suggests that eutectic freezing is a valid means for HCN to reach a sufficient concentration for polymerization.

While eutectic freezing is a valid pathway for the formation of the purines from HCN, it is assumed that the eutectic freezing of formamide will not lead to the formation of purines. However, this assumption does not take into consideration that (1) formamide can be formed from prebiotic compounds diffused over the early Earth other than HCN

and (2) formamide is liquid under a wide range of temperature and pressure values, with a boiling point of 210 °C and very limited azeotropic effects.[44]

Therefore, formamide, unlike HCN, can be very easily envisioned as a prebiotic molecule using the drying lagoon model. The drying lagoon model implies that the formamide would become concentrated if the water were to dry because of the high boiling point of formamide compared to water and the fact that water and formamide do not form an azeotrope. Formamide can be very easily concentrated by evaporating off any lower boiling point compounds leaving behind the pure formamide.

A pre-biotic reaction mixture based on formamide as the main component is tuned by the components surrounding the formamide solution. One of the main differences between formamide and HCN is that formamide has all of the necessary components within the molecule to form both the purine and pyrimidine nucleobases. The resulting inventory of products depends on the specific physical and chemical properties that the solution has been subjected to along with the type of the catalysts present in the reaction medium.

Saladino, Di Mauro and coworkers have described formamide thermochemistry in detail, cataloging the variety of potentially prebiotic compounds generated when neat formamide is heated in the presence of montmorillonites and other clays, phosphate minerals, cosmic dust analogues, and iron-sulfur minerals.[19-23,30] These investigators have identified a variety of purines and pyrimidines among mineral-catalyzed formamide reaction products, as well as acyclonucleosides, some simple amino acids, and other small molecules of prebiotic importance, such as carbodiimide and urea.

Previous studies of thermal formamide reactions have identified (AICA) as a reaction product.[19,20,22] However, the roles of this compound and other (HCN) condensation products – including (AICN) and (DAMN)[8,10-12,23] – have not been explored in the context of prebiotic nucleobase formation by formamide chemistry. In light of the fact that HCN is related to formamide by the loss of a water molecule, and that the formation of AICA and AICN from DAMN is promoted by photoisomerization, it seemed promising that photons could promote nucleobase formation in heated formamide reactions.

Complex organic compounds are formed if and only if the mixture is heated strongly, irradiated with ultraviolet light, acted upon by a an electric discharge, or subjected to the action of some other form of energy or a combination of energy sources. It is clearly important to decide which forms of energy contributed most to the synthesis of organic compounds on the primitive earth. This is not an easy matter until one can be certain about the composition of the primitive atmosphere. A reducing atmosphere, such as is thought to have been present on the primitive earth is highly stable unless it is acted upon by a source of energy.

The sun supplies far more energy to the earth than any other source. Each year about 260,000 calories of radiant energy are incident on each square centimeter of the atmosphere.[45] This amount of energy is sufficient to boil away a layer of water twelve feet deep covering the whole surface of the earth. However, not all of this energy is useful because light can bring about chemical reactions only it is absorbed by one of the components of the reaction mixture; light passing through a mixture of gases without being absorbed can have no photochemical influence on the gases.[33,45]

An atmosphere containing methane, ammonia, nitrogen, and water of the kind that might have existed on the primitive earth could have absorbed 40 calories per square centimeter per year, that is, less than 0.02 % of the total solar energy.[33,45] This would not have been enough to cause very extensive organic synthesis. However, it has been shown that if hydrogen sulfide and formaldehyde were present in sufficient quantities in the atmosphere, they could have absorbed a much larger amount of ultraviolet energy and made it available for the synthesis of organic compounds.[33,45]

The amount of ultraviolet light reaching the surface of the earth is very small compared to the amount that reaches the top layer of the atmosphere. The surface of the earth and the lower atmosphere are protected by a layer of ozone in the upper atmosphere. Ozone, unlike the other components of the atmosphere, absorbs ultraviolet light strongly and prevents it from reaching the earth. There was no ozone on the primitive earth because it is formed from molecular oxygen, and molecular oxygen cannot survive in a reducing atmosphere. The dim young sun would have provided a much higher flux of UV irradiation than the modern sun.[33,45]

Concentration by evaporation is highly plausible in prebiotic ocean circumstances especially at the point when the oceans started to recede from the land. The recession of oceans would have led to the concentration of high boiling point chemicals in tidal pools and is most likely the method in which formamide came to exist in pools on early earth.

Some of the chemistry on earth is driven by the sunlight. Most of the natural rotational, vibrational, and electronic transitions are caused by absorption of sunlight. The maximum flux of solar radiation received by the earth is in the ultraviolet (UV), visible (VIS), and near infrared (NIR) regions with a maximum in the visible region.[46] The solar

flux outside the earth's atmosphere can be approximated by radiation coming from a black body at 5800 K.[24,47] the average incoming light intensity per unit area normal to the direction of the sunlight is 1368 Wm^{-2}. The effective incoming solar radiation per unit area is divided by 4, or 342 Wm^{-2}. Of this incoming radiation, about 67 Wm^{-2} is absorbed by O_3, CO_2, H_2O, O_2 and by aerosols and clouds in modern earth conditions.[47] Because there would have almost certainly been a reducing atmosphere on early earth, oxygen would have been consumed by the many reducing molecules abundant in the atmosphere. This means that O_2 was most likely not a part of the early atmosphere and the photodissociation of O_2 to atomic oxygen to form O_3 was not a very likely process due to the absence of O_2 in the atmosphere.[24] Therefore, most of the light coming from the sun was not blocked by the O_3, CO_2, H_2O, O_2, or aerosols during early life conditions where a reducing atmosphere was present and that UV photons with wavelengths <300 nm could have penetrated a prebiotic atmosphere lacking an ozone layer.[24]

Surprisingly, the potential for UV photons to promote nucleobase production from formamide has received only limited attention. In particular, Saladino and coworkers identified thymine, for the first time, among the products of a thermal-photochemical reaction of formamide in the presence of TiO_2.[48] Subsequently, Senanayake and Idriss reported the formation of all five canonical nucleobases (adenine, cytosine, guanine, thymine, and uracil) after ultra high vacuum photolysis of formamide deposited on a TiO_2 single crystal surface[25]. These studies of formamide photochemistry, while enticing, rely on high temperatures and/or ultra high vacuum conditions that were unlikely to be present on the early Earth.[19-22,25,48-50]

Early earth conditions where prebiotic formamide occurred most likely involved the reaction of formamide with clays. These reactions could have been brought on by the fact that dissolved components of clays were in the formamide solutions, the clays could have provided the containers in which the formamide reactions occurred, or as they could have been solid suspensions in the formamide solutions. Clays are complex mineral assemblages formed from dissolved aluminosilicates. The minerals form templates for the deposition of layers of mineral, leading to the idea that the first organisms may have been mineral-based. These clays are capable of binding organic material via ionic and van der Waals interactions and may have been the locations for early prebiotic synthesis.[19-22,51] Early minerals would have also supplied anions and cations for the formation of small prebiotic molecules such as amino acids and nucleic acid bases. Minerals have both a reactive and protective quality for the formation and stabilization of small prebiotic molecules. Both the surface of the clays and the interlamellar spaces of clays might serve as a favorable environment to concentrate the organic building blocks of life related syntheses such as the formation of peptides and polynucleotides. Minerals have a high surface area, large absorption constants and ion-exchanging capacity as employed as catalysts in the synthesis of prebiotic molecules. Inorganic oxides have shown to be of value in a large range of abiotic catalytic transformations due to acidic or basic properties, to cation-exchange capacity, and to the possibility to accommodate copious amounts of water or other polar molecules. Minerals have the ability to:

- Tune the selectivity of prebiotic syntheses
- Act as a template for the formation of prebiotic molecules

- Act as benign environments to protect newly formed biomolecules from degradation
- Act as catalytic environments to lower the activation energies for the formation of products
- Contain and concentrate prebiotic molecules

These properties make the use of "mineral catalysts" very useful for the formation, containment, and protection of prebiotic biomolecules.[52]

The minerals involved in the formation of prebiotic molecules may act as a template providing directionality, a surface on which accumulation occurs, and as a catalytic material, reducing the activation energy for the formation of the reaction intermediate. Neat formamide reacted with different mineral catalysts will yield different product distributions as seen in studies by Saladino and DiMauro.[19-23] Formamide chemistry is a rich source for standard and nonstandard purine bases. Particular groups of catalysts produce similar products and certain catalysts will either promote or inhibit the production of prebiotic molecules due to the specific binding sites, molecular configuration, and intercalation sites that each mineral catalyst possesses. Different cations or anions will produce different products and different product distributions.

CHAPTER 2

EXPERIMENTAL TECHNIQUES

2.1 Abstract

A short review of the methods used to separate, identify, and quantify the products obtained from the pre-biotic reactions namely; high-pressure liquid chromatography (HPLC), high-pressure liquid chromatography with UV detection (HPLC-UV), liquid chromatography two dimensional mass spectrometry (LC-MS/MS), and two dimensional gas chromatography mass spectrometry (GC×GC-MS) are discussed in this chapter.

2.2 HPLC

High-performance liquid chromatography (or high pressure liquid chromatography, HPLC) is a form of column chromatography used to separate, identify, and quantify compounds. HPLC uses a column that holds chromatographic packing material (stationary phase), a pump that moves the mobile phase(s) through the column, and a detector that shows the retention times of the molecules. Retention times vary depending on the differential interactions of analytes with the stationary phase and mobile phases, the molecules being analyzed, and the solvent(s) used.

The sample (or analyte) is introduced into the column via the mobile phase. The analyte's motion through the column is slowed by chemical or physical interactions with the stationary phase as it travels through the column. The amount time that the analyte is retained depends on the nature of the analyte, as well as the stationary phase and mobile phase composition. The choice of solvents, additives, and gradient depend on the nature of the stationary phase and the analyte.

Normal phase HPLC (NP-HPLC), or adsorption chromatography, separates analytes based on the adsorption to the stationary surface chemistry and by polarity. NP-HPLC uses a polar stationary phase and a non-polar, non-aqueous mobile phase, and is the most effective method for separating non-polar analytes. In NP-HPLC the adsorption strength increases with increased analyte polarity thereby increasing elution time.

Reversed phase HPLC (RP-HPLC or RPC) is another widely used method especially since the advent of zwitterionic columns. RP-HPLC has a non-polar stationary phase and an aqueous, moderately polar mobile phase. With these stationary phases, retention time is longer for molecules which are more non-polar, and shorter for more polar compounds.

The ZIC-HILIC column is an especially useful HPLC column because it has a zwitterionic stationary phase covalently attached to porous silica. The permanent and hydrophilic zwitterion functionality makes the column suitable for application in Hydrophilic Interaction Chromatography (HILIC). Weak electrostatic interactions between charged analytes and the neutral zwitterionic stationary phase on this column result in a unique selectivity for analytes that are poorly retained on reversed phase columns, such as small polar molecules like nucleic acid bases (See Figure 2.1).

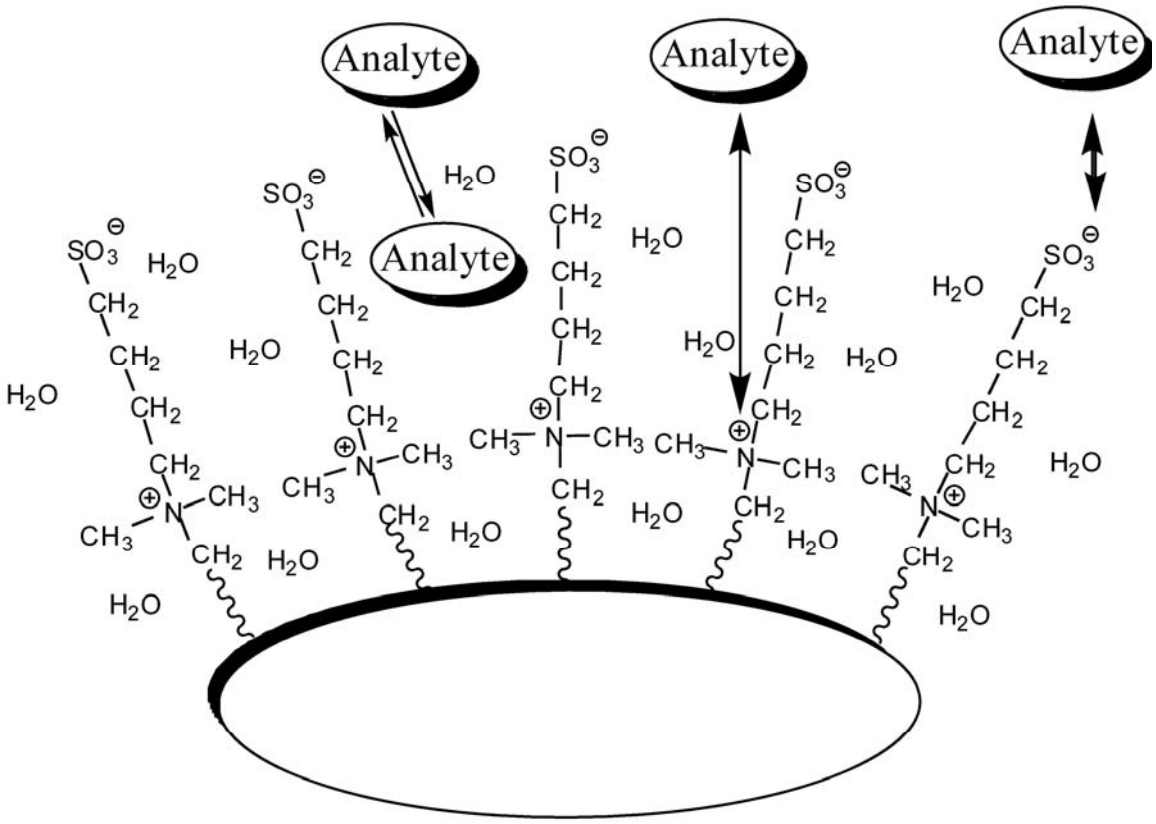

Figure 2.1. ZIC-HILC chromatography column electrostatic interactions induced by the water layer built up on the column and the zwitterionic reactions that take place on the positive and negative charges on the stationary phase

A ZIC-HILIC chromatography column allows for the ideal separation of polar and hydrophilic molecules due to the hydrophilic and electrostatic interactions that the analyte has with the stationary phase of the column. In particular, since polar and hydrophilic molecules are not retainable in a simple fashion on a reverse phase liquid chromatography column, a ZIC-HILIC column is a good HPLC column for the separation of purines.

1.3.1 HPLC-UV

The most common method to detect molecules as they elute from the HPLC column is UV-Vis detection. UV detectors work by measuring the amount of UV light that is absorbed by the chromophores in any given sample. UV detectors usually operate in the range 190 to 1100 nm range. Many molecules absorb wavelengths in this range, including substances that have double bonds, molecules that have conjugated double bonds.

1.3.2 LC-MS/MS

Another common method to detect molecules as they are eluted from the HPLC column is mass spectrometry (MS). The mass spectrometry method used in this study is a multiple reaction monitoring which involves the use of a triple quadrupole mass spectrometer. There is one main issue when going from HPLC to a mass spectrometer and that is the analytes must be vaporized and ionized before they are injected into the mass spectrometer. A common method to vaporize and ionize analytes is electrospray ionization.

In electrospray ionization, a potential is applied to the capillary that induces a charge separation in the eluent, eventually the charge builds up at the tip of the capillary forming a Taylor cone and causing the ejection of a charged droplet. Due to the flow of nitrogen alongside the Taylor cone, the solvent evaporates from the droplet as it moves through the chamber until it reaches the Rayleigh Limit and coulomb explodes to form smaller solvated ions.[53]

At this point the solvated ions must still go into the gas phase, or form desolvated ions. There are two main models for the formation of these desolvated ions. The first model is the charged residue model[54] that proposes that the electrospray droplets repeatedly evaporate and explode as the charge on the surface exceeds the Rayleigh limit forming successively smaller droplets containing a portion of the charge and ultimately

leading to the formation of ions. The second model is the ion evaporation model[55] that proposes that ions are ejected directly out of the droplet due to the high electric field on the surface of the droplet.

Once the ions have been ionized and vaporized they are ready to be analyzed using the triple quadrupole. There are four main ways to operate a triple quadrupole; neutral ion loss scan, product ion scan, precursor ion scan, and multiple reaction monitoring (also called selected reaction monitoring).

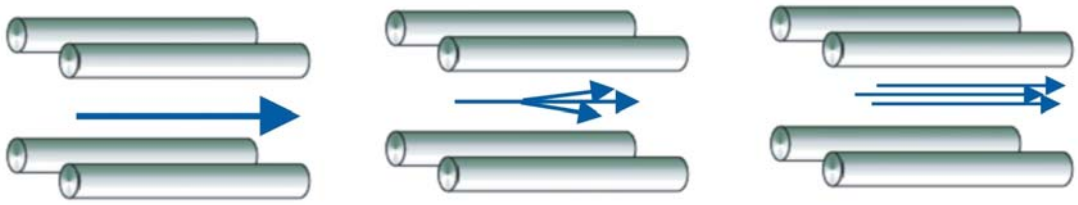

Figure 2.2. Example of product ion scan

In a product ion scan, the precursor ion is focused in the first quadrupole and transferred into the second quadrupole (the collision cell) where it interacts with a collision gas and fragments. The fragments are then measured by scanning the third quadrupole (Figure 2.2).

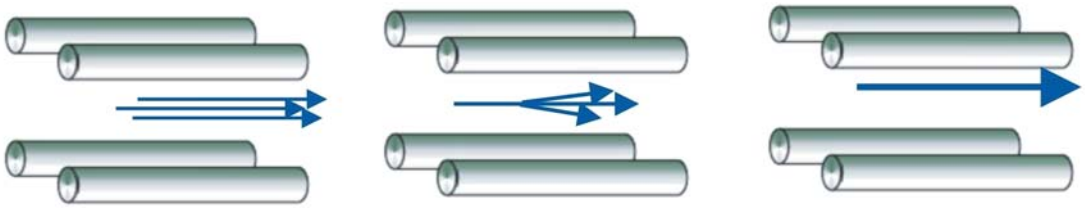

Figure 2.3. Example of precursor ion scan

In a precursor ion scan the third quadrupole is held constant to measure one particular fragment ion and the first quadrupole is scanned (Figure 2.3).

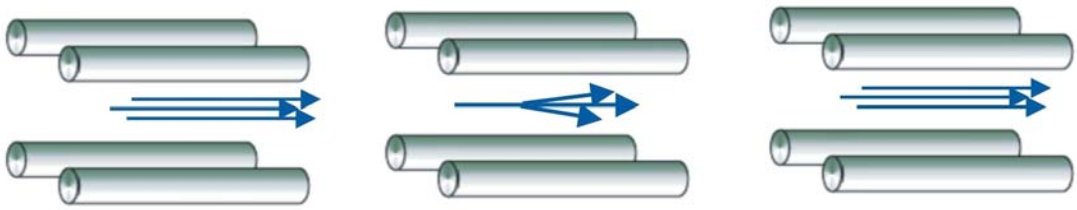

Figure 2.4. Example of neutral ion scan

In a neutral ion loss scan the first quadrupole is scanned, but the third quadrupole is scanned to produce a spectrum of precursor ions that undergo a particular neutral loss (Figure 2.4).

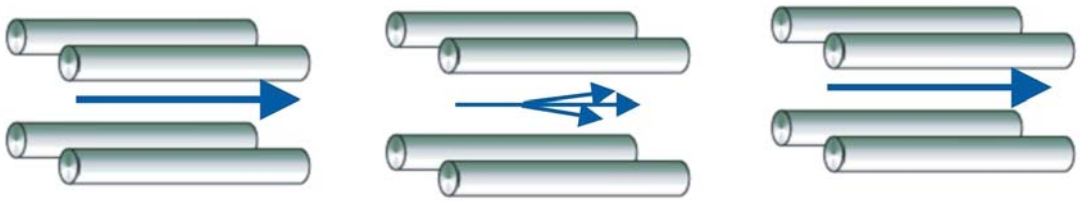

Figure 2.5. Example of multiple (or selected) reaction monitoring

In multiple reaction monitoring, the first quadrupole is held constant to measure a predetermined precursor ion, the second quadrupole is used as a collision cell, and the third quadrupole is held constant to detect the predetermined product ion (Figure 2.5). In all of these methods the second quadrupole is used as a collision cell. The pressure in this chamber is higher and the ions coming from the first quadrupole collide with a neutral gas (usually argon) and fragment via collision induced dissociation, these fragments are then accelerated out of the collision cell and enter the third quadrupole.

1.4 GC×GC-MS

Biomolecules can be classified in four primary groups: carbohydrates, lipids, nucleic acids, and proteins. These large molecules are typically best suited to be analyzed by a combined chromatographic/spectrometric technique such as liquid chromatography with mass spectrometric detection (LC/MS). These polymers can be broken down into their constituent monomeric units (i.e. monosaccharides, fatty acids, nucleobases, amino acids, etc.), which are smaller molecules that can be volatilized and analyzed by gas chromatography/mass spectrometry (GC/MS). GC/MS-based analyses have been reliable for the analysis of known prebiotic compounds in appreciable concentrations, and offer the advantage of higher resolution and faster analysis times when compared to LC/MS.

While capillary one-dimensional gas chromatography has been used to analyze prebiotic mixtures, GC×GC-MS has not been used. The capillary GC analyses are plagued by the complex nature of the samples that result in long GC run times along with extensive peak co-elution. The peak co-elution also presents a challenge for complete quantitative analysis. Additional GC methods that help eliminate the issues of long run times and peak co-elution are multidimensional gas chromatography methods.

These methods include (1) the heart cut method which is conventionally two columns that are connected in a series through a flow-switch interface that directs specific portions of the primary column eluent into the secondary column and (2) comprehensive two-dimensional gas chromatography which uses a valve-less on-column interface between the two GC columns and a high speed second dimension to combine the advantages of high separation power with shorter analysis times. This method greatly

increases the separation power of capillary GC and clearly resolves the selected constituents in a GC chromatogram, but are limited to the analysis of a few discrete regions of the chromatogram and the analysis time is increased even more than that of the capillary one-dimensional gas chromatogram.

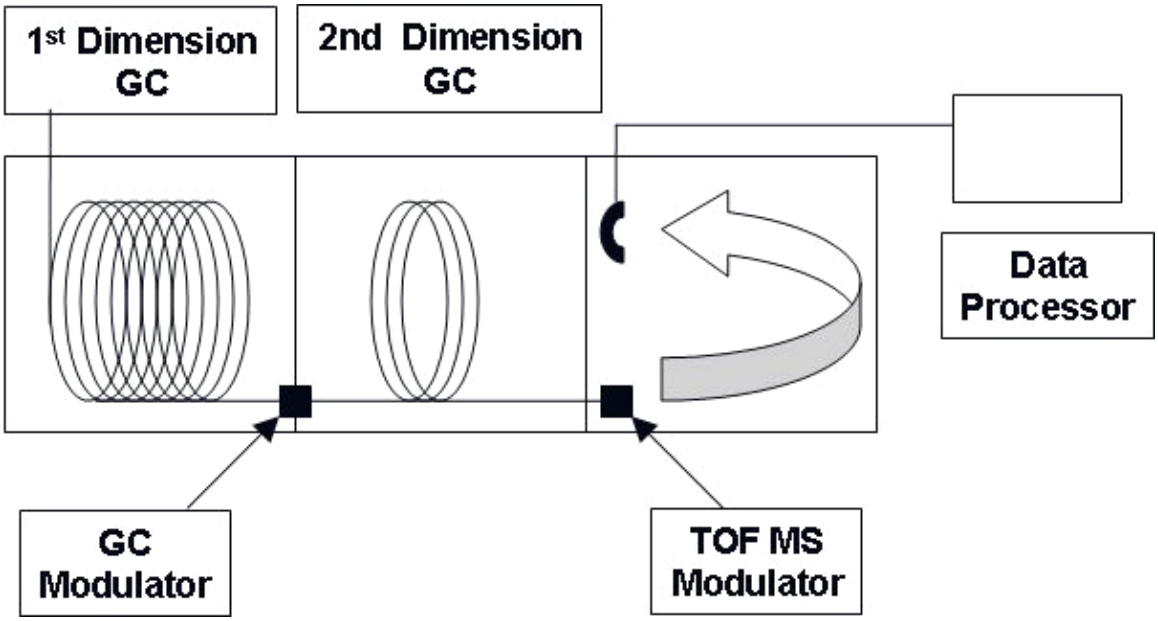

Figure 2.6. Diagram of GC×GC-TOF/MS system

In the GC×GC system the first dimension provides a separation similar to the separation obtained in one dimensional gas chromatography and a modulator inbetween the two columns accumulates the effluent from the first column and re-injects the effluent into the second column (See Figure 2.6)[56-59]. The modulator produces concentration pulses at regular time intervals and the second dimension of the column separates each pulse into its components thereby giving a secondary chromatogram. When the secondary chromatogram is being analyzed the modulator is accumulating sample for the pulse. This means that every component in the sample is subjected to both degrees of

separation.[56-59] The chromatograms from the second dimension are taken at very small intervals which allows for the continuous monitoring of the separation in both dimensions. Three dimensional data are recorded (first and second dimension retention time, and signal intensity) and provide a way to view the peak profiles in either dimension or both dimensions simultaneously.

The Time-of-Flight instrument separates ions with the same kinetic energy but different m/z, because the heavier ions require more time to travel a fixed distance. To accelerate ions to through the time-of-flight a voltage is applied to the backplate and the ions are expelled from the ion source into the drift region, where there is no electric or magnetic field and no further acceleration. Ideally, all ions have the same kinetic energy, which is ½ mv^2, where m is the mass of the ion and v is the velocity. If ions have the same kinetic energy, but different masses, the lighter ones travel faster than the heavier ones. In its simplest incarnation, the time-of-flight mass spectrometer is just a long, straight, evacuated tube with the source at one end and the detector at the other end. Ions expelled from the source drift to the detector in order of increasing mass, because the lighter ones travel faster.

GC×GC-TOF MS has shown to be a promising new analytical tool for the screening of small organic biomolecules such as amino acids[60,61], carbohydrates[62], organic acids[63], lipids[64], as well as other compounds of interest to exobiologists such as polyaromatic hydrocarbons and tholins in meteorites[65-67]. GC×GC-TOF MS combines the superior compound resolution power and ordered structural separations of GC×GC with the fast scanning and spectral deconvolution capabilities of TOF MS for enhanced analyses of complex samples. Nitrogen-containing organic compounds are the only

subunit of important biomolecular compounds that have not yet been separated by GC×GC-TOF MS.

CHAPTER 3

SYNTHESIS OF PURINES FROM SIMPLE HEATING OF NEAT FORMAMIDE AND FORMAMIDE MIXTURES

3.1 Abstract

A detailed description of how the reaction center is setup and how the formamide samples are heated and subsequently analyzed is presented in this chapter. Saladino, Di Mauro and coworkers have described formamide thermochemistry in detail, cataloging the variety of potentially prebiotic compounds generated when neat formamide is heated in the presence of montmorillonites and other clays,[21] phosphate minerals,[49] cosmic dust analogues,[22] and iron-sulfur minerals.[50] These investigators have identified a variety of purines and pyrimidines among mineral-catalyzed formamide reaction products, as well as acyclonucleosides, some simple amino acids, and other small molecules of prebiotic importance, such as carbodiimide and urea.[30,49,50] This work has also demonstrated mineral-specific product profiles, both in terms of yields and identities of compounds.[19-22,30,48-50] This chapter shows the sensitivity and selectivity of LC-MS/MS over the methods used by DiMauro and coworkers and also shows the analysis of different purines as they are allowed to react over time while being heated.

3.2 Materials and Methods

3.2.1 Materials

All solvents were HPLC grade and purchased from EMD Chemicals. Mineral catalysts, AICA, DAMN, and HPLC buffer reagents were purchased from Sigma-Aldrich or Fisher Scientific and used as received. Authentic nucleobase standards were purchased

from Sigma Aldrich, allopurinol from MP Biomedical, and AICN from TCI America. Water was purified using a Milli-Q System.

3.2.2 Prebiotic synthesis reaction conditions

The solutions studied were neat formamide and formamide containing 4.4% by weight sodium pyrophosphate or calcium carbonate. These salts were present as solid particles. Since formamide is a strong solvent for ions, we cannot rule out some dissolution of sodium pyrophosphate and calcium carbonate, especially at elevated temperatures.

Reactions were carried out in a custom-built four well isothermal (± 0.5 ºC) aluminum heating block (See Figure 3.1). Glass-covered quartz test tubes were inserted into wells within the block. All reaction solutions were prepared immediately prior to being placed in the thermally-equilibrated reaction center. Reactions were stirred with Teflon-coated magnetic stir bars throughout the reaction time period. The reaction center was heated using silicon heating tape and a Labview program was set up to monitor the temperature and temperature controller was constructed using a solid state relay. The temperature program was set to maintain the desired temperature, any time the temperature proceeded past the desired temperature the relay would switch and the heating tape would be turned off, and any time the temperature went below the desired temperature the heating tape would be turned off.

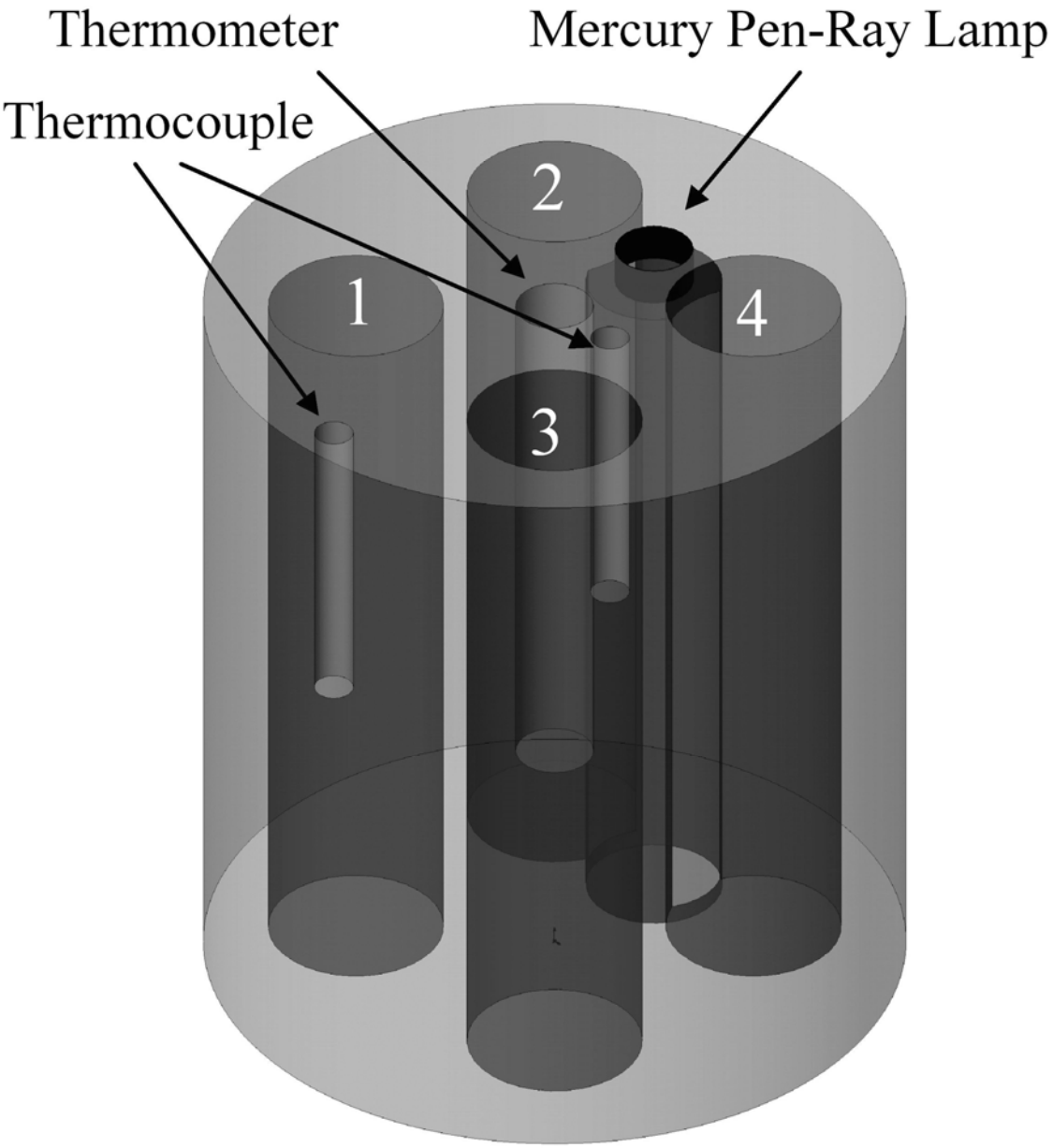

Figure 3.1. Reaction center setup: Temperature is maintained in the reaction center using a Labview program that monitors the temperature through the thermocouple feeds and heats the reaction center using silicon heating tape that is wrapped around the reaction center. Four test tubes are placed in the reaction center. These test tubes are placed in slots 1,2,3, and 4. Test tubes 1 and 3 are simply heated; whereas, test tubes 2 and 4 are heated and irradiated at the same time.

3.2.3 HPLC-UV sample preparation and analysis

Reverse-phase HPLC was performed on an Agilent 1200 Series RRLC system with a diode array detector. A Phenomenex Synergi Polar RP column was used for separations. Mobile phase consisted of sodium phosphate buffer (20 mM at pH 7) and acetonitrile in methanol (10 % v/v).

Using two methods of analysis provided additional verification of product identity, while allowing the selection of desired ions (in LC-MS/MS) and the ability to view the UV-Visible spectrum of any product peak in a chromatogram (by HPLC). Due to the different detection methods and detection limits of these two methods of analysis, significantly different chromatographic conditions were employed. For HPLC analyses, 200 μL aliquots of formamide reaction mixtures were dried under vacuum in a Savant SpeedVac concentrator and resuspended in 500 μL water, sonicated and then centrifuged to remove insoluble solid products. Supernatant aliquots were diluted and, in some cases, spiked with authentic standard compounds, prior to HPLC analysis. Reverse-phase HPLC was performed on an Agilent 1200 Series RRLC system with diode array detector. A Phenomenex Synergi Polar RP column with 4 μM particle size, 4.6 x 250 mm, was used for separations; the column was maintained at 30 °C with a 0.75 mL/min flow rate. Solvent A was 20 mM sodium phosphate buffer at pH 7; solvent B was 10 % acetonitrile in methanol (v/v). Mobile phase composition was: 0-12 min, 5-10% B; 12-16 min, 10-20% B; 16-18 min, 20-40% B; 18-19 min, 40-5% B; 19-30 min, 5% B.

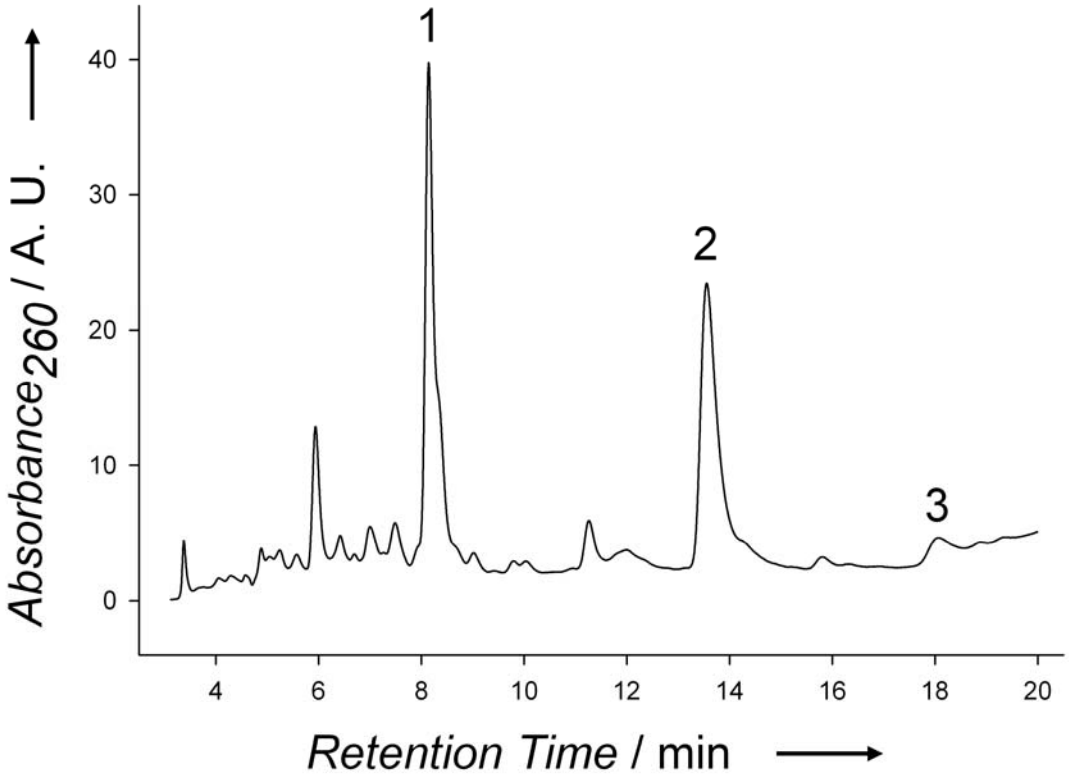

Figure 3.2. HPLC chromatogram of formamide reactions irradiated with UV light (254 and 365 nm) and heated at130 °C for 48 hours. Offsets added for clarity. Products observed include hypoxanthine (1), purine (2), and adenine (3).

A representative HPLC-UV chromatogram is shown in Figure 3.2, in this figure the complexity of the samples can be observed, notice the numerous peaks before and directly after purine (1). It is important to note here that the analysis of most of data only involved the identification of three compounds: purine, adenine, and hypoxanthine. Prepared solutions of at least five different concentrations of each standard compound were used to construct standard calibration curves. Spiking of reaction products with standard compounds was also performed to confirm retention time.

3.2.4 LC-MS/MS sample preparation and analysis

For LC-MS/MS analysis, 200 μL aliquots of formamide reaction mixtures were dried under vacuum at 60 °C using a Savant SpeedVac, resuspended in 200 μL water, agitated with a vortex mixer, and subjected to centrifugation to remove insoluble products. 5 μL aliquots of the supernatants were mixed with 285 μL of acetonitrile and an internal standard (isoguanine for guanine concentration determination; 2-aminopurine for determination of adenine, hypoxanthine, and purine concentration). Analyses were performed using an Agilent 1100 binary HPLC system coupled to a Micromass Quattro LC triple quadrupole mass spectrometer.

HILIC is very similar to NPLC except that HILIC uses semi-aqueous mobile phases. The ability to use an aqueous mobile phase as the strong solvent in HILIC allows for better solubility and separation of the analyte compared to NPLC and RPLC.

A PEEK 100 x 2.1 mm Merck SeQuant ZIC-HILIC HPLC column with 5 μm particle size and 200 Å porosity was used for separations. The column was maintained at 30 °C with a flow rate of 0.1 mL/min and an injection volume of 30 μL. Solvent A was neat acetonitrile; solvent B was 2.5 mM ammonium formate and 25 mM formic acid in water. The following gradient was employed: 0-20 min, 5-20% B; 21-30 min, 20% B; 30-31 min, 20-5% B; 31-40 min, 5% B.

Table 3.1. LC-MS/MS MRM parameters used for optimal detection of nucleobase standards

Nucleobase Standard	***Precursor Ion Mass***	***Product Ion Mass***	***Collision Voltage*/V**	***Cone Voltage*/V**	***Retention Time*/min**
Guanine	151.8	134.8	25	40	21.5
Isoguanine	151.8	134.8	25	40	30.6
Hypoxanthine	136.9	109.8	30	50	14.1
Adenine	135.9	118.7	35	50	12.4
2-aminopurine	135.9	118.7	35	50	11.1
AICA	126.9	54.8	50	20	15.1
Purine	120.9	93.9	20	40	7.6
AICN	108.8	81.8	20	20	5.7
DAMN	108.8	81.8	10	20	6.2

The Micromass Quattro LC triple quadrupole mass spectrometer is operated in multiple reaction monitoring mode to allow for the best separation of purines. In this process, the first quadrupole (MS1) is held constant to measure a particular precursor ion, the second quadrupole is used as a collision cell, where the precursor ion interacts with a collision gas and fragments. In the third quadrupole (MS2) is held constant to detect the predetermined product ion. The capillary voltage was maintained at 2.75 kV. The source block temperature was maintained at 100 ºC and the desolvation temperature at 150 ºC. The MRM parameters are shown in Table 3.1 and a total ion chromatogram, a combined selected ion chromatogram, and the selected ion chromatograms for a representative reaction are provided in Figure 3.3.

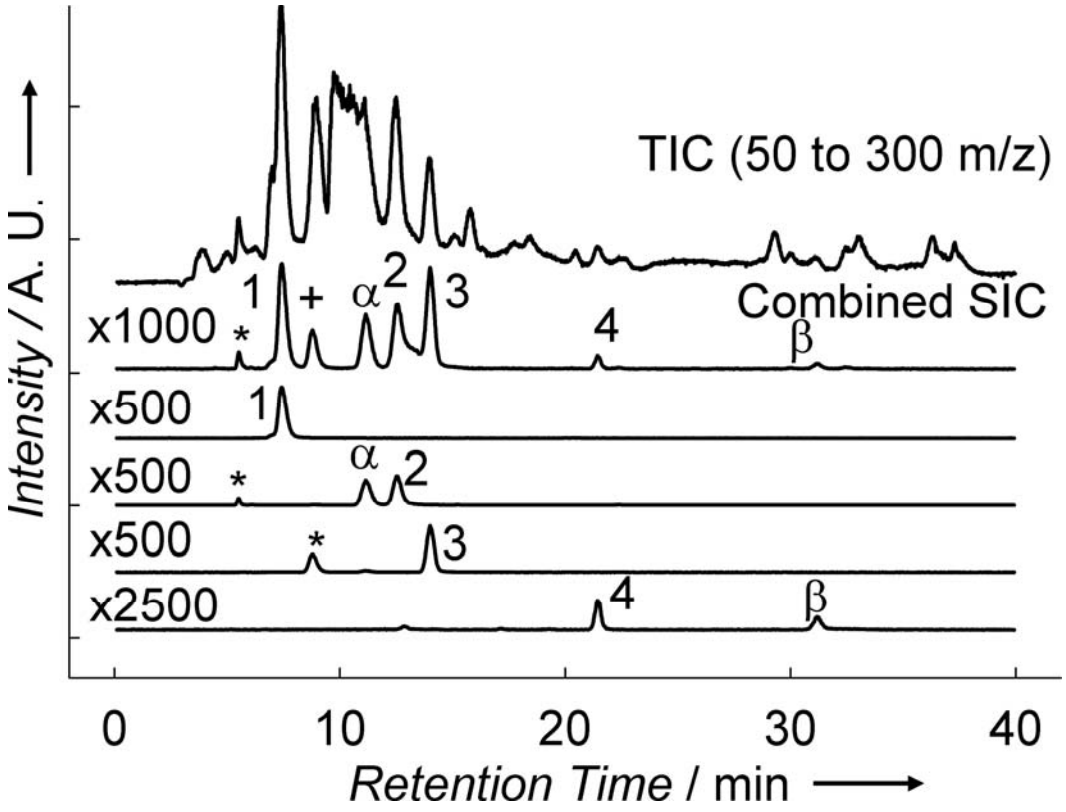

Figure 3.3. LC-MS selected ion chromatograms of formamide reaction products from a representative reaction sample (neat formamide reacted at 130 °C for 48 h). Products observed include purine (1), adenine (2), hypoxanthine (3), and guanine (4). The peaks labeled (α) and (β) are the internal standards 2-aminopurine and isoguanine, respectively. Peaks labeled (*) are products that have the same mass but a different retention time as the selected ions in each respective trace. Offsets are added for clarity. TIC = total ion chromatogram; SIC = selected ion chromatogram.

Prepared solutions of at least five different concentrations of each standard compound were used to construct standard calibration curves. Spiking of reaction products with standard compounds was also performed to confirm retention time, precursor ion and product ion identification.

Internal standards are used to account for variation between experiments. The two internal standards used in this experiment are 2-aminopurine for the determination of adenine, hypoxanthine, and purine concentration and isoguanine for the determination of

guanine concentration. The internal standard analysis method used involves (1) infusion of the standard into the mass spectrometer to determine the cone voltage, precursor ion mass, collision voltage, and product ion mass, (2) injection of the internal standard to determine the retention time, (3) injection of internal standards (10 μL of 95:5 isoguanine: 2-aminopurine) with standards (5 μL) to construct the standard calibration curves – standard calibration curves are constructed with analyte peak area / internal standard peak area vs. known analyte concentration, (4) injection of the exact same amount of internal standard (10 μL of 95:5 isoguanine: 2-aminopurine) into each sample (5 μL), and (5) taking the desired analyte peak area divided by the internal standard peak area and using the internal standard calibration curve to discern the analyte concentration.

The main advantages of using a liquid chromatography triple quadrupole analysis technique are (1) co-eluting peaks can be isolated by mass selectivity and are not constrained by chromatographic resolution, (2) greater sensitivity is achieved when using multiple reaction monitoring, (3) the method has high sample capacity and throughput, and (4) peaks are identified not only by retention time but also by the precursor and product ion.

3.2.4 NMR sample preparation and analysis

NMR spectroscopy was performed on a 400 MHz Varian Mercury Vx. Samples were acquired as single, unlocked transients in formamide. A TMS (tetramethylsilane) reference was included in a flame-sealed capillary insert. Sixteen spectra were acquired with TMS set to 0 ppm; these were then averaged in the Igor Pro data analysis software package to produce a single spectrum.

3.3 Results and Discussion

3.3.1 Neat formamide

To explore the possible intermediates of the heat induced purine nucleobase formation process, DAMN and AICN (putative precursors to adenine), and AICA (putative precursor to hypoxanthine and guanine) were each added to neat formamide at 10 mM before heating. The progression of selected product yields was also monitored for neat formamide over a 96 hour period. Recall that the thermal reactivity of the neat formamide was limited to the formation of purine and no adenine, hypoxanthine or guanine. Figure 3.4 shows the measured yields of adenine as a function of time and as a function of dosed DAMN, AICA or AICN. It is clear that the adenine yield from heating 10 mM DAMN and 10 mM AICA in neat formamide for 48 h at 130 °C is relatively modest. In contrast, heating 10 mM AICN in neat formamide leads to the formation of adenine. This thermal reaction reaches steady state after about 48 h, and then stays constant within experimental error.

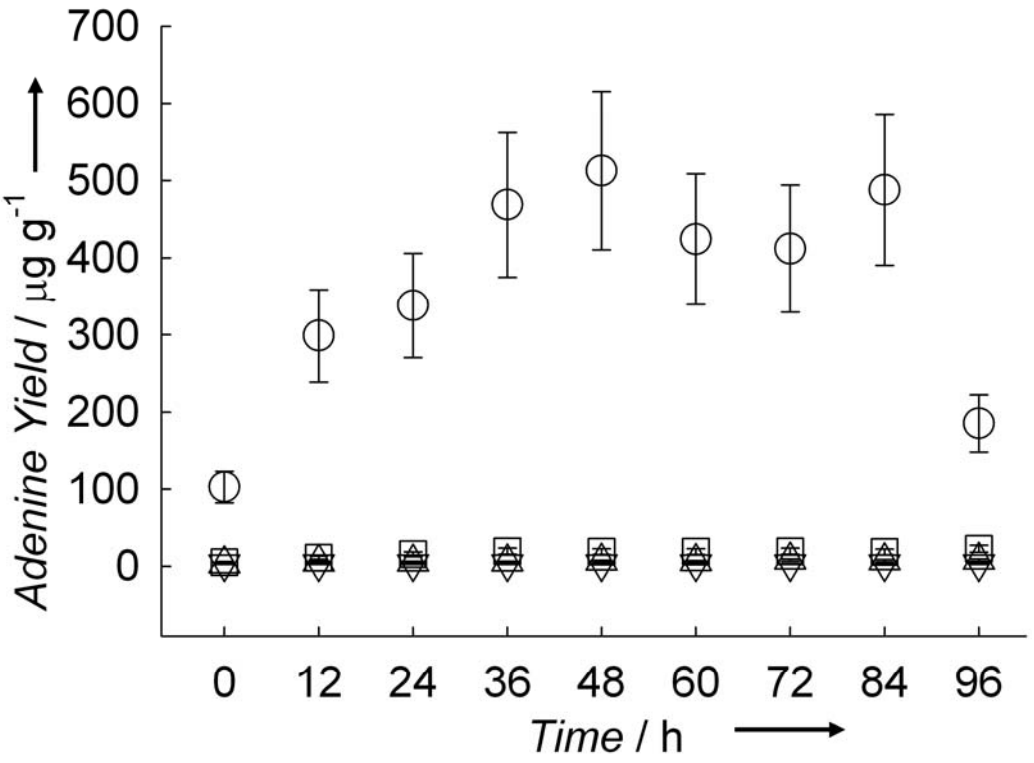

Figure 3.4. Production of adenine with the temperature maintained at 130 ºC. Solutions of neat formamide (▽), and formamide with 10 mM DAMN (□), 10 mM AICN (○), 10 mM AICA (△).

Heating neat formamide or a formamide solution containing 10 mM AICN to 130 ^{o}C yields very little hypoxanthine via thermal processes (Figure 3.5). In contrast, the addition of 10 mM AICA causes direct formation of hypoxanthine. The amount of hypoxanthine quickly rises to approximately 240 μg hypoxanthine/ g formamide in 12 hours, and then remains constant with sustained heating. Our analysis has also revealed the formation of hypoxanthine from AICA when this suspected intermediate is dried from a formamide solution under vacuum at temperatures as low as 60 °C, and then reconstituted in water prior to analysis.

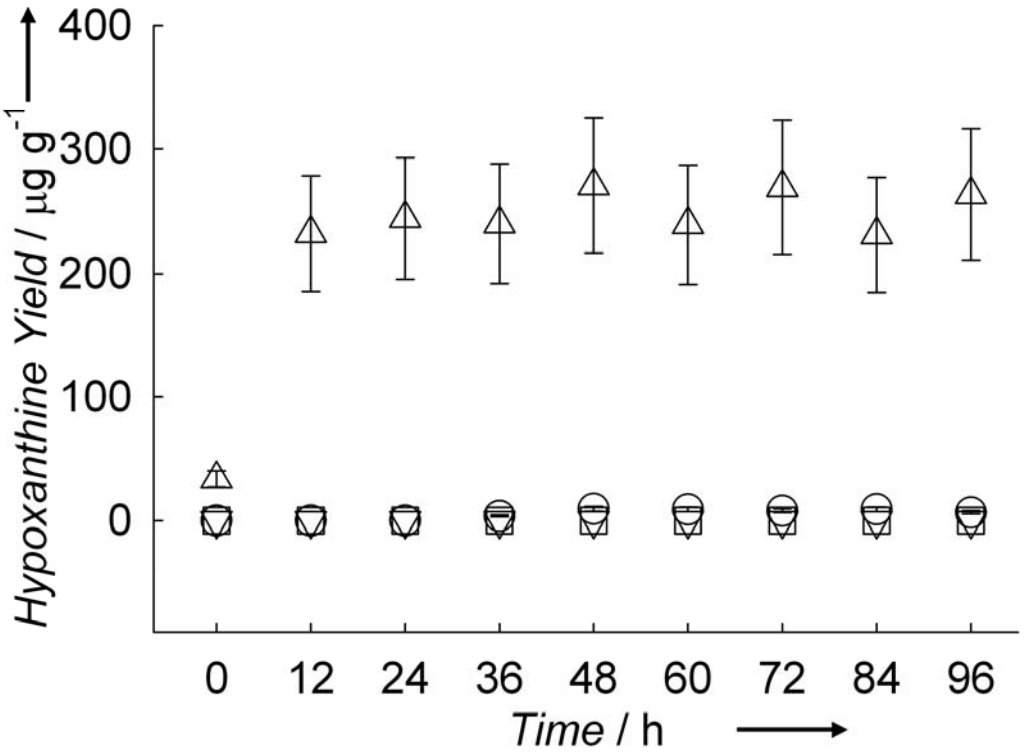

Figure 3.5. Production of hypoxanthine with the temperature maintained at 130 ºC. Solutions of neat formamide (▽), and formamide with 10 mM DAMN (□), 10 mM AICN (○), 10 mM AICA (△).

3.3.2 Formamide reacted in the presence of inorganic salts

Thermal reactions of formamide, neat or in the presence of calcium carbonate or sodium pyrophosphate, were carried out at 130 ºC. Consistent with previous reports of similar reactions performed at higher temperature (160 ºC), purine ($C_5N_4H_4$) was the only nitrogenous base detected in neat formamide reactions that were heated for 48 h (Figure 3.6).[20]

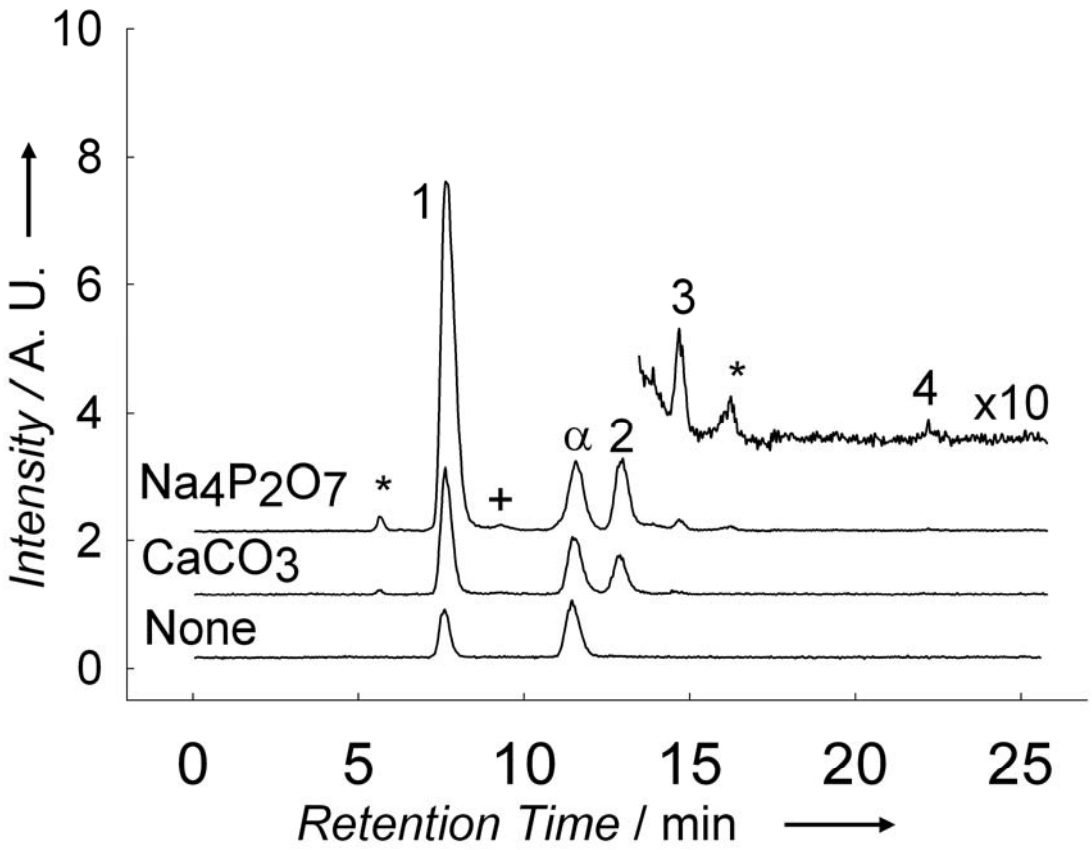

Figure 3.6 Combined selected ion chromatograms of formamide reactions heated to 130 °C for 48 h, in the presence and absence of catalysts. Offsets added for clarity; the inset is magnified by a factor of 10. Products observed include purine (1), adenine (2), hypoxanthine (3), and guanine (4). The peak labeled (α) is the internal standard 2-aminopurine. Peaks labeled (*) have the same product and precursor ion mass as adenine but are not adenine. Peaks labeled (+) are tentatively assigned as allopurinol based upon comparison with existing standards.

The presence of calcium carbonate or sodium pyrophosphate enhanced purine yield and enabled the production of adenine and a small amount of hypoxanthine. The inset in Figure 3.6 also shows that a small amount of guanine is formed when formamide is reacted in the presence of sodium pyrophosphate.

3.3.3 Reaction of formamide after the evaporation of water

The reactions have been carried out with solutions of neat formamide because, for practical experimental considerations, it is the obvious starting point to study the effects of UV-irradiation on nucleobase production from formamide. However, it is difficult to imagine a scenario in which neat formamide collected on the prebiotic Earth, as water was most likely present[68,69] and more abundant than formamide, and as the two liquids are miscible. Nevertheless, given the lower volatility of formamide, and the fact that azeotropic mixtures are not formed by water and formamide,[34] one could imagine scenarios in which primarily aqueous pools containing a small amount of formamide existed on the early Earth. During hot and dry periods, water evaporation could have given rise to ever more concentrated solutions of formamide.

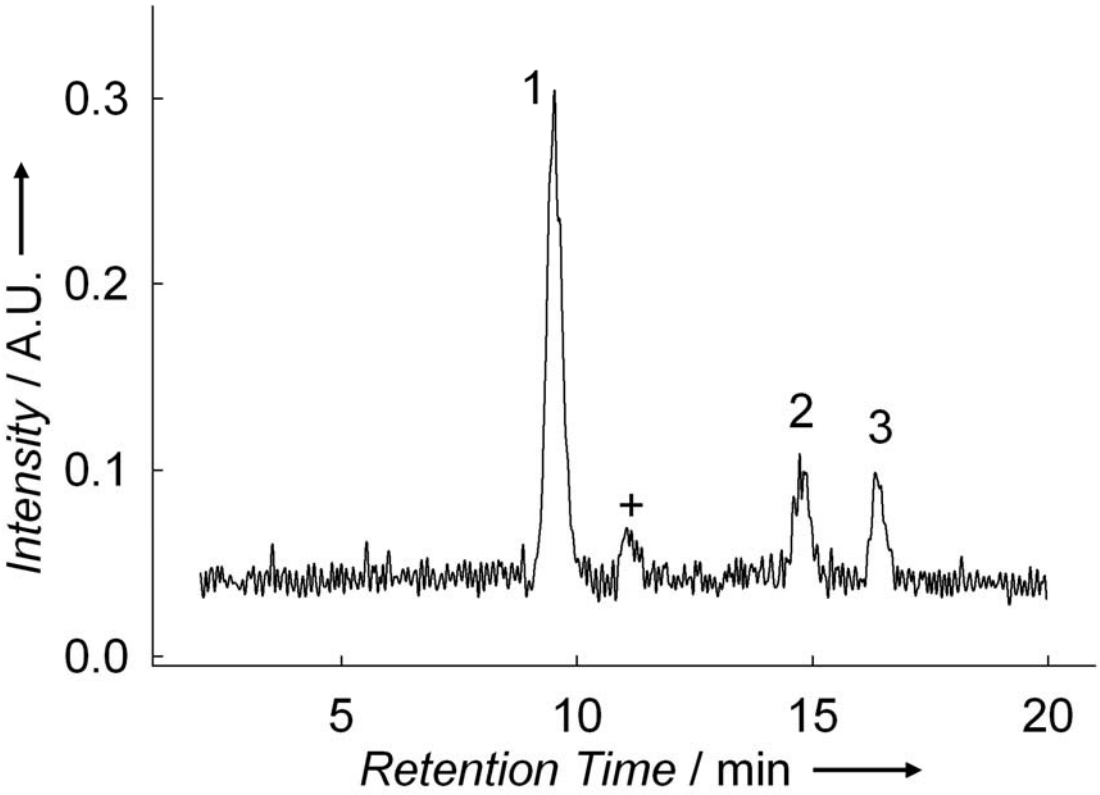

Figure 3.7. Nucleobase production from heating 10 mol % formamide in water at 100 °C for 96 hours. Products observed include purine (1), adenine (2), and hypoxanthine (3). The peak labeled (+) has the same mass as hypoxanthine and is tentatively identified as allopurinol based on comparison with an authentic standard.

Tests have been conducted to determine the likelihood that formamide pools were left behind after water evaporated from the surface. These tests to determine whether this "drying pool" model can give rise to solutions of neat formamide not only saw the evaporation of water but also the formation of nucleobases. In one such experiment, 10 mol % formamide in water was heated to 100 °C for 96 hours (Figure 2.7). In addition to running a 10 mol % formamide reaction, a neat formamide reaction was also run that yielded no products, while the 10 mol % formamide in water reaction produced purine, adenine, and hypoxanthine without the addition of UV light. This is the first time that the production of adenine and hypoxanthine have been observed without the addition of a

catalyst or UV light. These results show that water is indeed one of the main reactants in the formation of purines.

While the yields of these nucleobases are lower than those observed for the neat formamide reactions at 130 °C, the confirmation of nucleobase production from an initially mixed water-formamide solution supports the prebiotic relevance of the experiments presented above, and further relaxes the requirements for prebiotic purine nucleobase production. It should also be noted that the mixed-solvent, salt-free, non-irradiated reaction produced hypoxanthine and adenine; whereas under the same reaction conditions these products were not observed in neat formamide reactions, given the previously reported observation that ammonium formate facilitates adenine production[14,29] and our observation that ammonium formate was produced over the course of heating and water evaporation, it is possible that the *in situ* formation of ammonium formate is an important factor in nucleobase production in this mixed-solvent system.

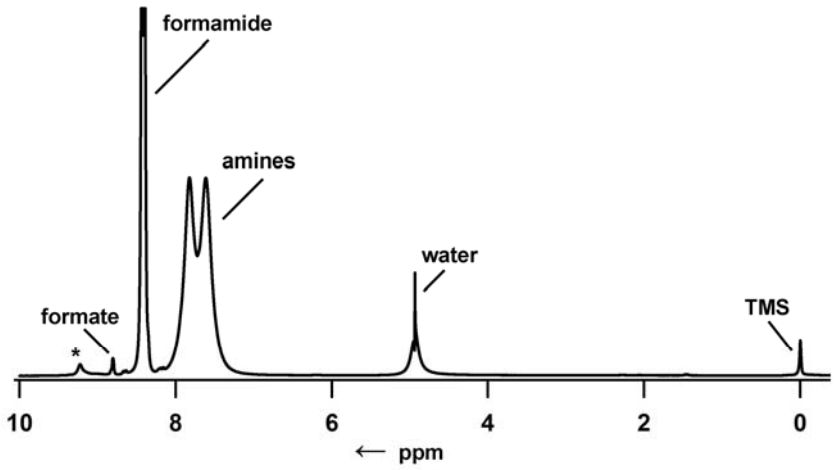

Figure 3.8 NMR spectrum of formamide heated for 24 h at 130 degrees C. The Peak labeled * is an unidentified reaction product. TMS = tetramethylsilane. In this figure the formamide peak is cut off to better see the smaller peaks.

Along with the formation of purines from these reactions, a decrease in solution was observed. Aliqouts from the sample were extracted at predetermined time intervals and the gradual evaporation of water was observed. The NMR results show the hydrolysis of formamide to ammonium formate at a rate of approximately 1% per 24 h (Figure 3.8).

3.4 Conclusions

The heating of neat formamide yields purine, while heating formamide in the presence of possible intermediates leads to the formation of specific purines. For example, heating formamide in the presence of AICN leads to the formation of adenine, heating formamide in the presence of AICA leads to the formation of hypoxanthine, and heating formamide in the presence of DAMN leads to the formation of a small amount of adenine. The addition of inorganic salts to the neat formamide reaction leads to the formation of specific products for each type of salt that is added. When neat formamide is reacted in the presence of calcium carbonate purine, adenine, and a small amount of hypoxanthine are formed. When neat formamide is reacted in the presence of sodium pyrophosphate purine, adenine, hypoxanthine, and a small amount of guanine are formed.

CHAPTER 4

SYNTHESIS OF PURINES FROM SIMPLE HEATING OF NEAT FORMAMIDE AND FORMAMIDE MIXTURES WHILE BEING IRRADIATED THE UV LIGHT

4.1 Abstract

The lack of an ozone layer on early led to the bombardment of early earth with a wide range of UV wavelengths. The UV lamp (mercury Pen-Ray lamp) that is used for this first set of experiments has a primary emission at 254 nm, but it also emits photons with wavelengths centered at 365 nm and 185 nm. In this chapter the products observed when the samples were heated and irradiated with the mercury Pen-Ray lamp described above are analyzed. While wavelengths below 300 nm would have reached the early earth surface due to the lack an ozone layer, carbon monoxide in the atmosphere would have screened wavelengths below 195 nm.[10] Therefore, the likelihood that wavelengths below 195 nm reached the early earth's surface is small. Due to the fact that wavelengths below 195 nm would most likely not have reached early earth additional experiments using custom made mercury Pen-Ray lamps were conducted. In this chapter, these experiments and their results are discussed.

4.2 Materials and Methods

4.2.1 Pre-biotic synthesis reaction conditions

The reactions were carried out as stated in Chapter 2, but two of the tube wells were slotted to allow calibrated exposure to a low pressure mercury lamp (Pen-Ray, primary emission at 254 nm with additional wavelengths being emitted at 185 nm and 365 nm). Wavelengths of 254 nm and 185 nm were chosen as energetic photons that

conceivably would have penetrated through an atmosphere lacking an ozone layer, which cuts off below 280 nm.

In the second set of reactions the wavelengths below 195 nm were cut off because only a few photons below 195 nm would have been able to reach early earth due to the vast amount of atmospheric molecules in the early atmosphere interacting with the photons before they reached the earth's surface.[10]

4.2.2 HPLC-UV sample preparation and analysis

The HPLC analyses were carried out as described in Chapter 2, a short synopsis of the materials and methods involved in this process follows. Reverse-phase HPLC was performed on an Agilent 1200 Series RRLC system with a diode array detector. A Phenomenex Synergi Polar RP column was used for separations. Mobile phase consisted of sodium phosphate buffer (20 mM at pH 7) and acetonitrile in methanol (10 % v/v).

4.2.3 LC-MS/MS sample preparation and analysis

The LC-MS/MS analyses were carried out as described in Chapter 2, a short synopsis of the materials and methods involved in this process follows. LC-MS was carried out using a Merck SeQuant ZIC-HILIC HPLC column on an Agilent 1100 binary HPLC system coupled to a Micromass Quattro LC triple quadrupole mass spectrometer. Mobile phase consisted of acetonitrile (neat) and ammonium formate 2.5 mM) and formic acid (25 mM) in water.

4.3 Results and Discussion

4.3.1 Neat formamide irradiated with UV light

4.3.1.1. UV irradiation with 185, 254, and 365 nm photons

The progression of selected product yields was also monitored for neat formamide over a 96 hour period. Product yields all tend to reach a maximum value and then decrease over this time frame when the samples are irradiated with UV light. The decrease of product yield may be the result of the formation of insoluble high molecular weight products that are not subjected to analysis (see Figure 3.3 for a comparison between full scan and MRM data). To explore the possible intermediates in the UV-enabled purine formation process, DAMN and AICN, reported precursors to adenine and AICA, precursor to hypoxanthine, xanthine, and guanine[8,10-12,15-17,19,21-23,26,29] were each added to neat formamide at 10 mM before heating and UV-irradiation.

The following experiments were conducted with isoguanine as the internal standard and not 2-aminopurine. Instead of using 2-aminopurine, standard calibration curves were constructed with a set of standards ran before and after each set of sample runs.

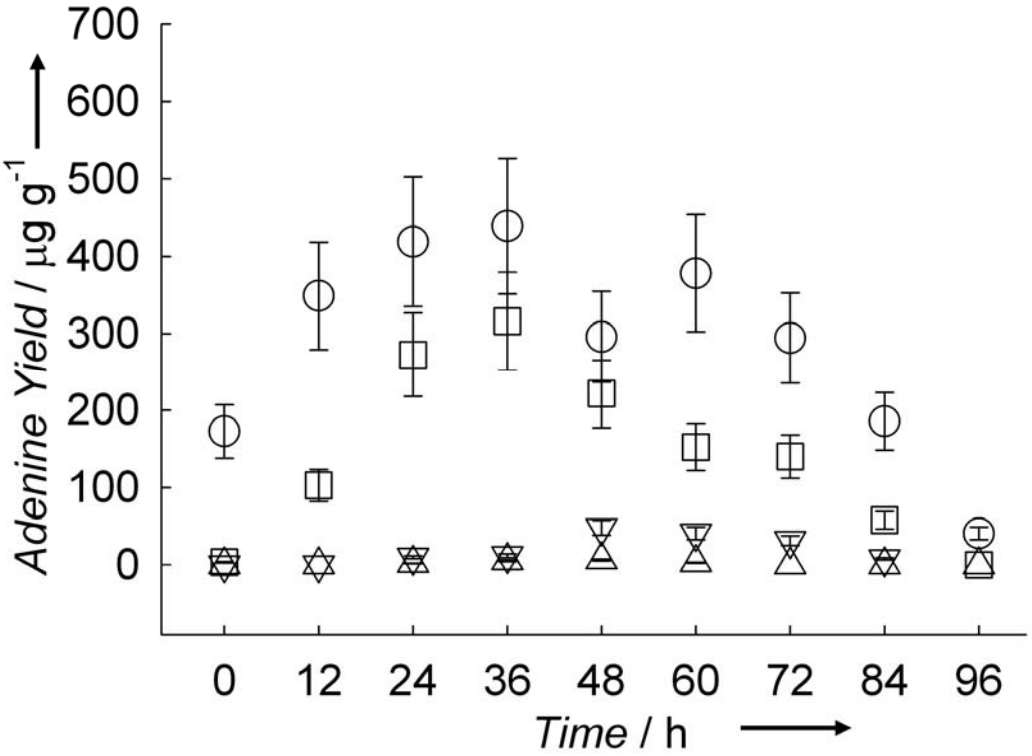

Figure 4.1. Production of adenine with UV irradiation (185, 254, and 365 nm). Solutions of neat formamide (▽), and formamide with 10 mM DAMN (□), 10 mM AICN (○), or 10 mM AICA (△) were maintained at 130 ºC.

The most striking observation in the UV irradiated samples is the clear UV-induced increase in the adenine yield due to the addition of DAMN (Figure 4.1). The adenine yield increased approximately 6-fold with the addition of the DAMN, and 8-fold with the addition of AICN. Also note in these reactions that the amount of adenine peaks at around 48 hours. This may be due to the UV light photodecomposing the AICN or adenine or stimulating the formation of other chemical species.

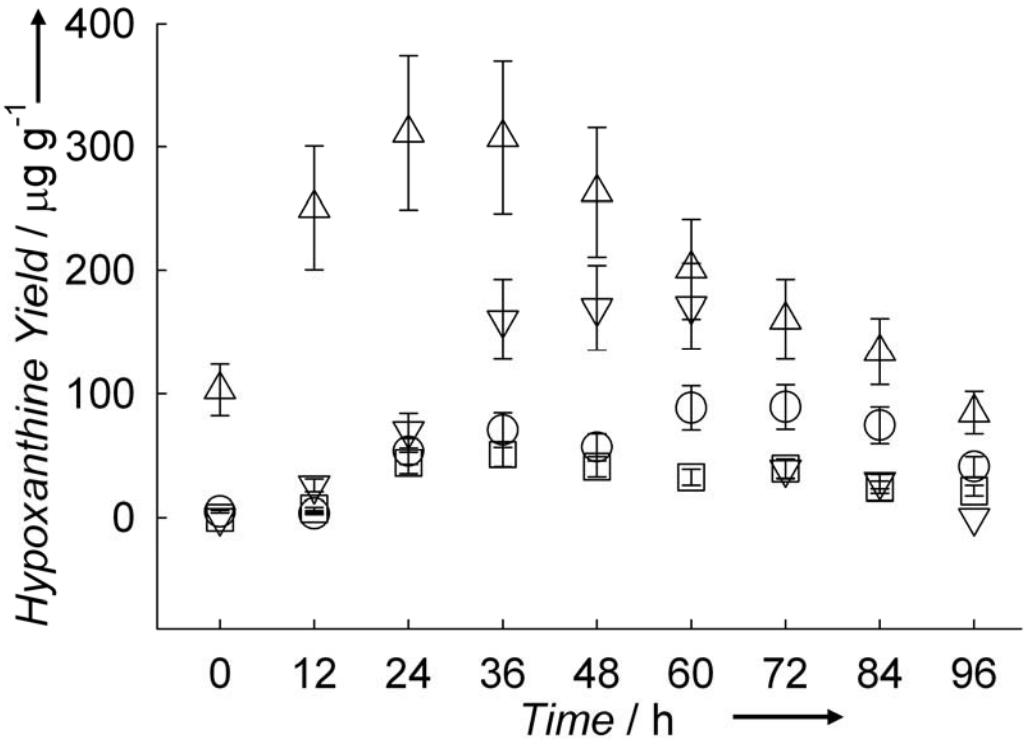

Figure 4.2. Production of hypoxanthine with UV irradiation (185, 254, and 365 nm). Solutions of neat formamide (▽), and formamide with 10 mM DAMN (□), 10 mM AICN (○), 10 mM AICA (△) were maintained at 130 ºC.

The production of hypoxanthine is greatly enhanced when formamide is irradiated with UV light, whether or not there are any intermediates spiked into the formamide at the beginning of the reaction (Figure 4.2). In thermal-only counterpart of this reaction the only intermediate that increased the hypoxanthine yield dramatically was that of AICA. It can be seen in this reaction that there is a definite UV-light induced pathway from formamide to hypoxanthine due to the increased presence of hypoxanthine in the reaction when UV light is introduced to the system. The fact that DAMN, AICN, and AICA increase the amount of adenine and hypoxanthine is consistent with DAMN, AICN, and AICA acting as intermediates under our reaction conditions.

4.3.1.2. UV irradiation with 254 and 365 nm photons

Figure 4.3 monitors the yield of adenine as a function of time and as a function of dosed DAMN, AICA or AICN under heating and UV irradiation conditions. The most striking observation is the clear UV-induced increase in the adenine yield due to the addition of DAMN. Similar adenine yields are observed for UV-irradiated samples dosed with AICN and AICA, as compared to the thermal-only reactions. However, in the case of the AICN containing solution, there appears to be a photo-induced reduction of the adenine yield at longer reaction times. After 48 h, the UV light may photo-decompose the AICN or adenine or stimulates the formation of other chemical species.

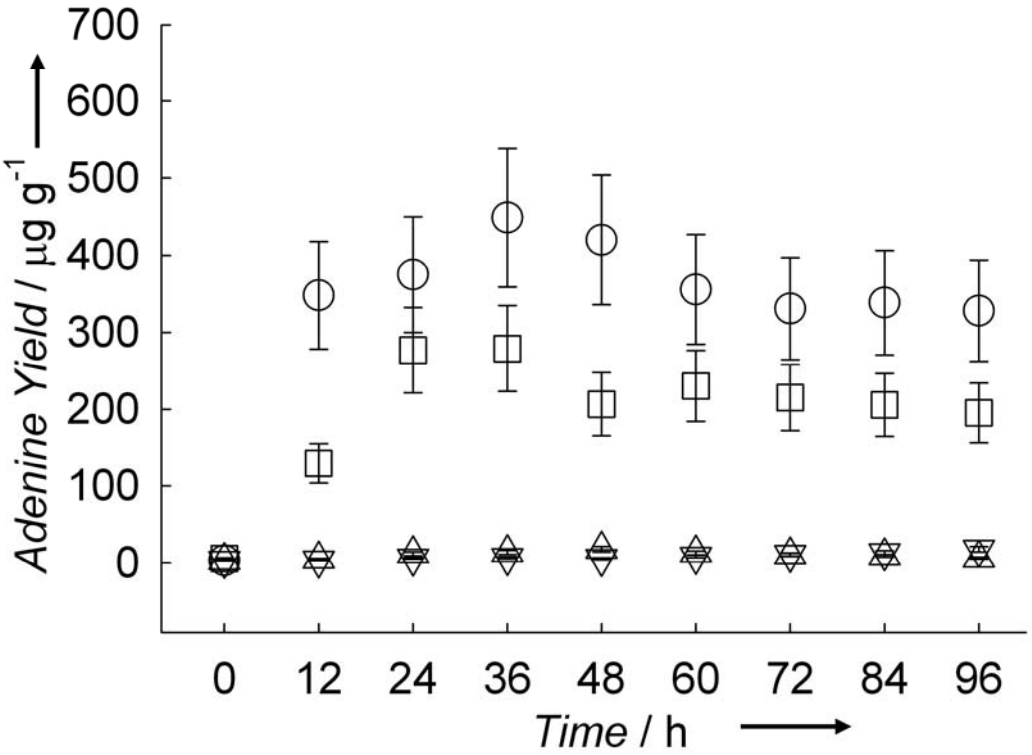

Figure 4.3. Production of adenine with UV irradiation (254 and 365 nm). Solutions of neat formamide (▽), and formamide with 10 mM DAMN (□), 10 mM AICN (○), or 10 mM AICA (△) were maintained at 130 ºC.

Recall that the amount of adenine produced when 10 mM DAMN is heated in formamide for 48 h at 130 °C was relatively modest, reaching around 20 μg adenine/ g formamide. In contrast, the amount of adenine produced when using heat and UV light increases the yield 15-fold (Figure 4.3). This observation suggests that with respect to adenine formation, there may be a photochemical step involving DAMN. This step is most likely the formation of the diaminofumaronitrile (DAFN), the *trans* isomer of DAMN (see Figure 1.2).

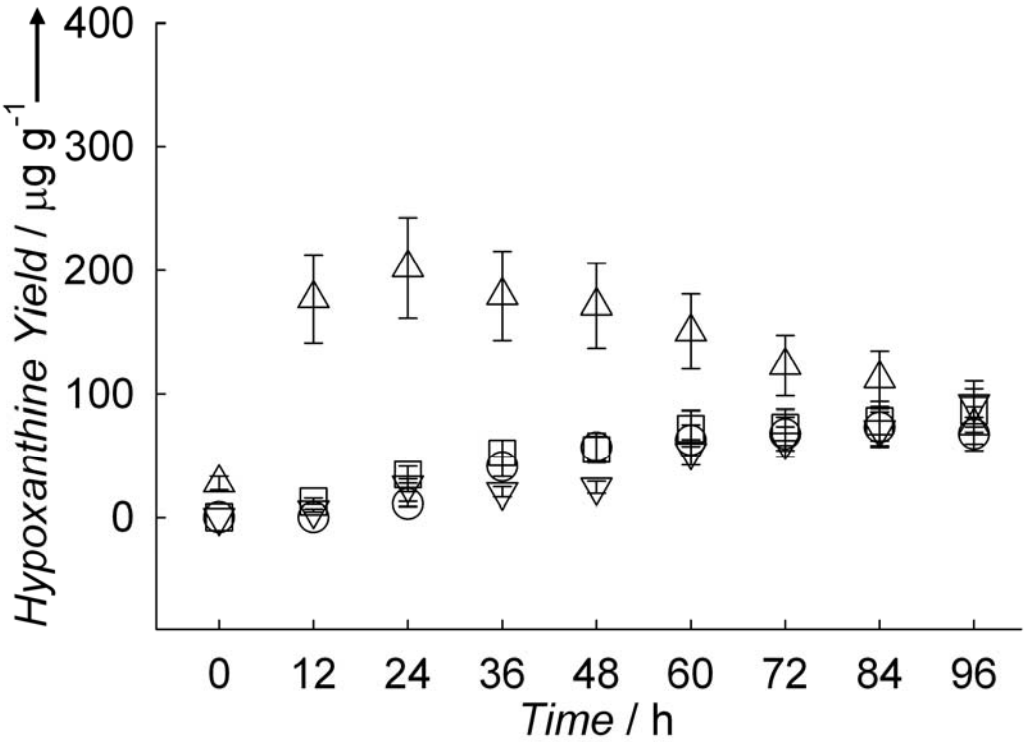

Figure 4.4. Production of hypoxanthine with UV irradiation (254 and 365 nm). Solutions of neat formamide (▽), and formamide with 10 mM DAMN (□), 10 mM AICN (○), 10 mM AICA (△) were maintained at 130 ºC.

Figure 4.4 shows that hypoxanthine yields for all UV-irradiated and heated formamide solutions studied, whether spiked with a putative intermediate or not, reach a plateau of 75 μg hypoxanthine/ g formamide. Solutions spiked with 10 mM AICA

initially exhibited greater hypoxanthine yield, reaching a maximum yield at 24 hours (similar to the thermal-only experiments), but declining over time in the UV-irradiated samples. Interestingly, the yields of the 10 mM AICA formamide reactions decreased, after 96 hours, to around the same yield as all other formamide samples investigated, suggesting that a yield of around 100 μg hypoxanthine/ g formamide is a steady state yield. This observation is consistent with an increased importance of pathways mediated by DAMN and AICN relative to the decreased importance of the AICA path.

The primary pathways are thought to involve diaminomaleonitrile (DAMN, **4**), diaminofumaronitrile (DAFN, **5A**), aminoimidazolecarbonitrile (AICN, **5B**), and aminoimidazolecarboxamide (AICA, **5C**) as intermediates (Figure 4.5).[10-12,19-23,26,29,32] In these pathways DAMN and DAFN are proposed precursors to purine (**6A**) and adenine (**6B**), AICN (**5B**) is a proposed precursor to adenine (**6B**) and AICA (**5C**) is a proposed precursor to hypoxanthine (**6C**) and guanine (**6D**). Previously, Zubay and Mui demonstrated the direct formation of adenine from AICN and the direct formation of hypoxanthine from AICA.[29]

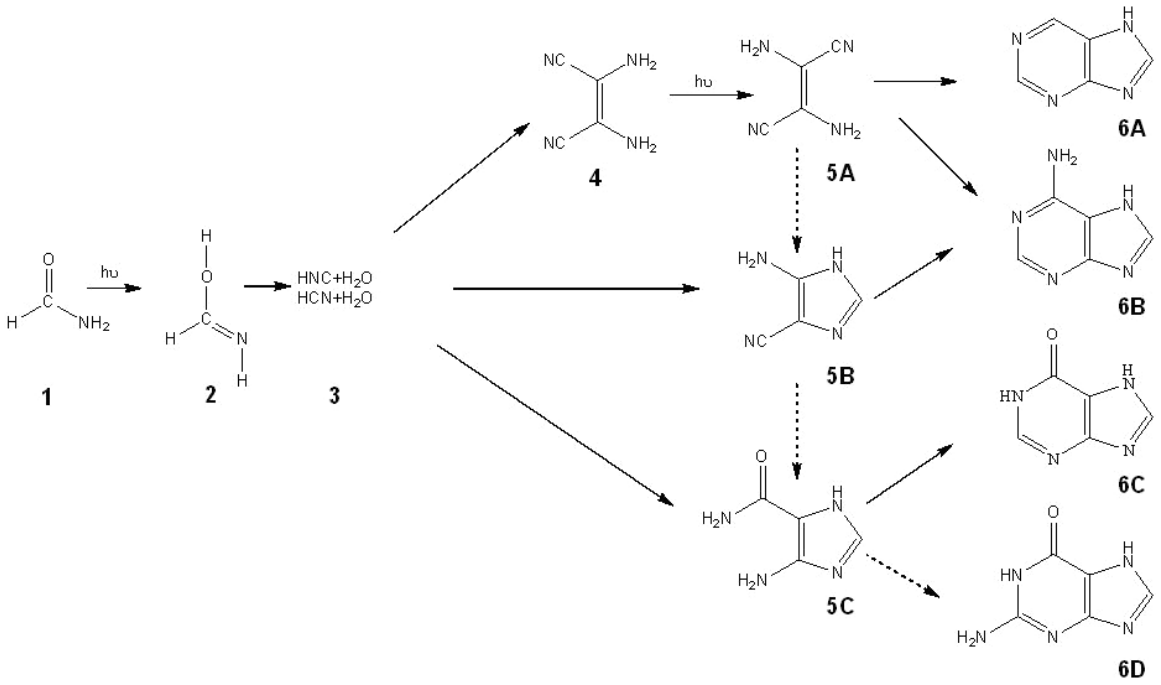

Figure 4.5. Putative chemical pathways from formamide (1) to purines. Energy input in the form of heat and/or UV irradiation is believed to isomerize formamide to formimidic acid (2) which is further broken up into hydrogen cyanide and/or hydrogen isocyanide and water (3). Further thermal or photochemical transformations are believed to generate the reactive intermediates diaminomaleonitrile (DAMN, 4), diaminofumaronitrile (DAFN, 5A), aminoimidazolecarbonitrile (AICN, 5B), and aminoimidazolecarboxamide (AICA, 5C). These intermediates react further to form purine nucleobases including purine (6A), adenine (6B), hypoxanthine (6C), and guanine (6D). All reactions were carried out in an isothermal heating block maintained at 130 °C for 48 h unless otherwise noted. Solutions of formamide (neat, 4 mL) or formamide containing calcium carbonate or sodium pyrophosphate (4.4% by weight), or a spiked intermediate (DAMN, AICA, or AICN; 10 mM). Some reactions were exposed to a low pressure mercury lamp (Pen-Ray, primary emission at 254 nm; no emission below 200 nm).

As previously mentioned, other photochemical processes cannot be ruled out. For example, the observation that UV light stimulates the production of adenine when 10 mM of DAMN is added to formamide points to DAMN as a potentially important photoactive species. This concept is not new and previous work has indicated that DAMN may photoisomerize to DAFN which can lead to the formation of AICN through a ring-closure mechanism.[12] The observation that addition of AICA has an effect on the time dependent photochemical yields of hypoxanthine indicates a potential photochemical role of AICA. NH_3 or radicals produced photochemically from formamide[70] could react with formamidine to generate intermediates such as AICA[18]. NH_3 tends to be the dominant product for surface decompositions, thus the minerals may serve to facilitate the formation of NH_3 or NH_4^+. These molecules may be very important "reactants" in the formation of nucleobases.

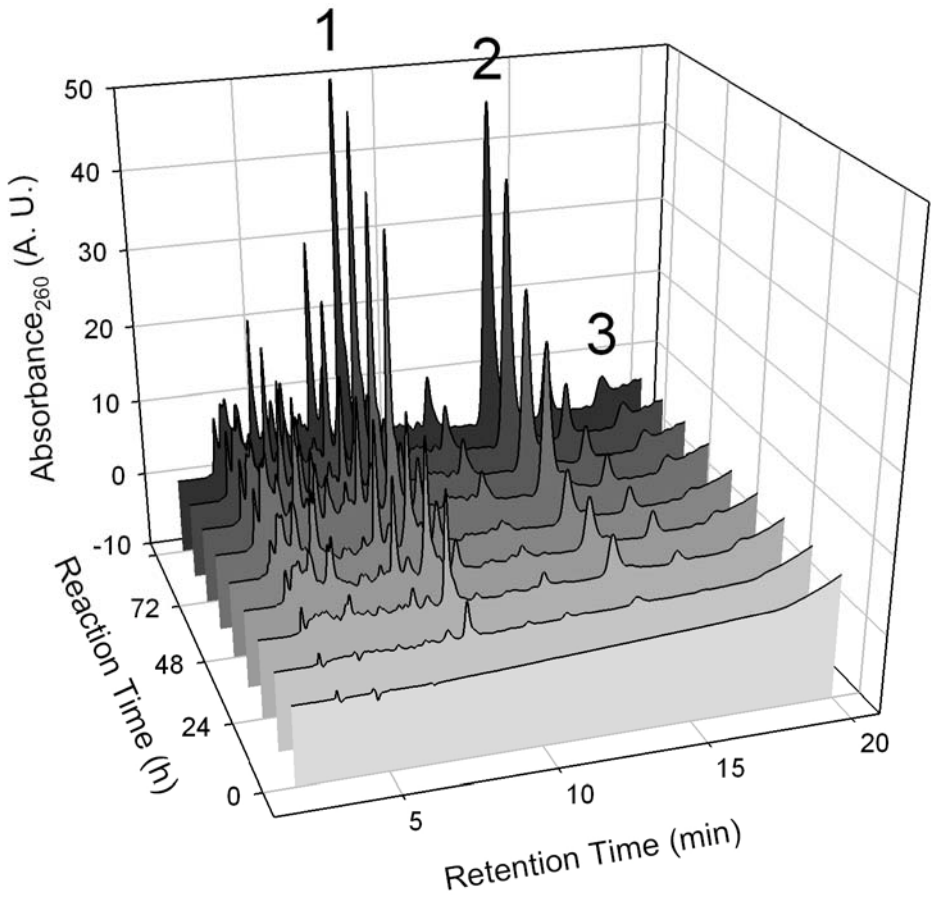

Figure 4.6. HPLC-UV chromatograms of formamide reactions with irradiated with UV light (254 and 365 nm) and heated at 130 °C monitored over a 96 hour time period. Offsets added for clarity. Products observed include hypoxanthine (1), purine (2), and adenine (3).

When formamide is irradiated a wide variety of products are produced. The type of products formed throughout a period of 96 hours changes, as noted in Figure 4.1 through 4.4. These changes in products can be seen very well in the HPLC-UV chromatograms because HPLC-UV is not as selective as the multiple reaction monitoring LC-MS/MS analyses and allows for the observation of products that are not specifically selected for (see Figure 4.6).

4.3.2 Formamide reacted in the presence of inorganic salts

4.3.2.1. UV irradiation with 185, 254, and 365 nm photons

Thermal and UV-irradiated reactions of formamide, neat or in the presence of calcium carbonate or sodium pyrophosphate, were carried out at 130 ºC. Each of the reactions shows very similar products, with only changes in relative yields. The primary products observed in the UV irradiated reactions were **1** purine, **2** allopurinol, **3** adenine, **4** hypoxanthine, and **5** guanine (Figure 4.7). Detection of guanine and hypoxanthine strongly suggests AICA is present as an intermediate.

The following experiments were conducted with isoguanine as the internal standard and not 2-aminopurine. Instead of using 2-aminopurine, standard calibration curves were constructed with a set of standards ran before and after each set of sample runs.

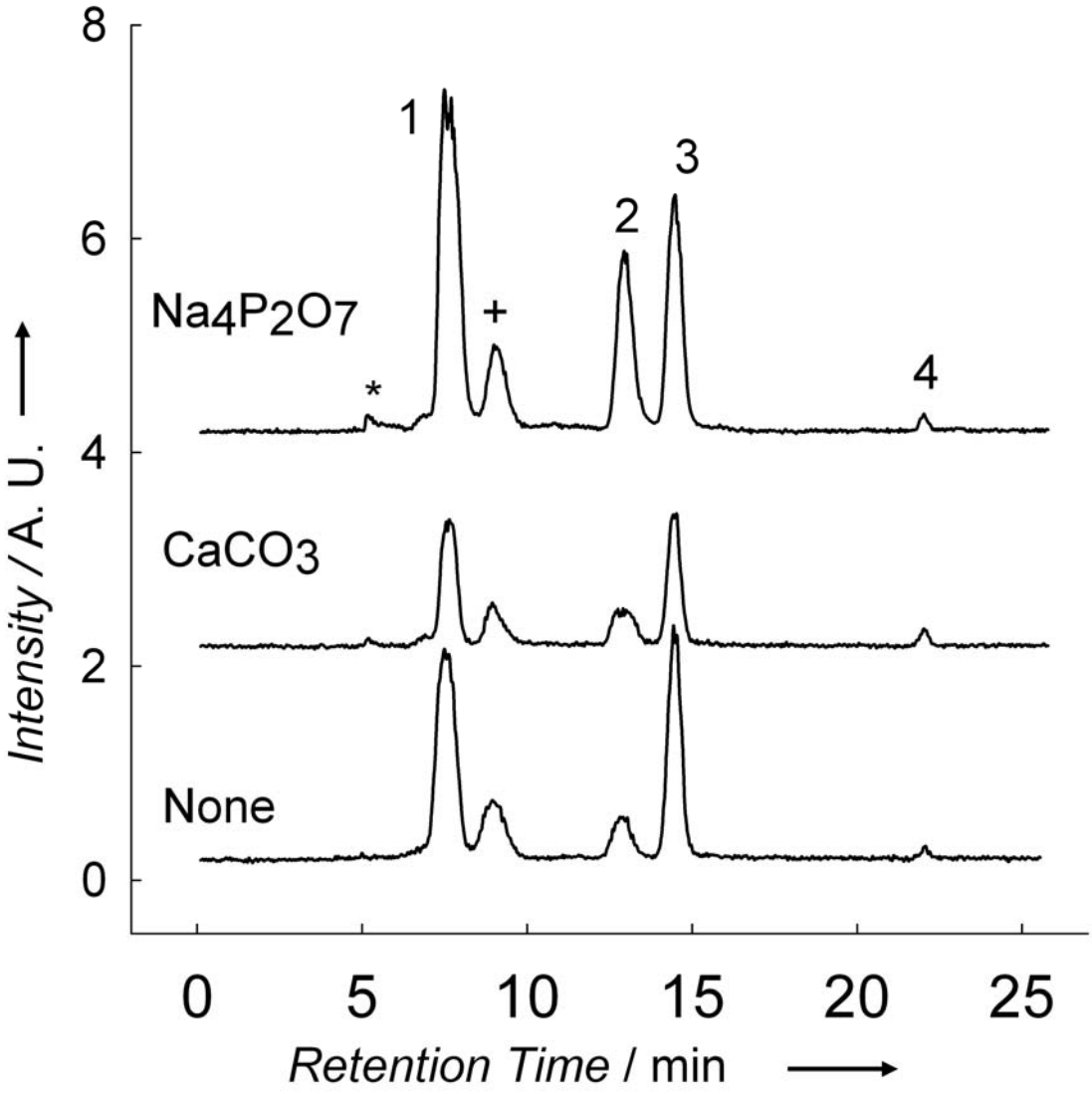

Figure 4.7. Combined selected ion chromatograms of formamide reactions with irradiated with UV light (185, 254, and 365 nm) and heated to 130 °C for 48 h, in the presence and absence of mineral catalysts. Offsets added for clarity. Products observed include purine (1), adenine (2), hypoxanthine (3), and guanine (4). The peak labeled (*) have the same product and precursor ion mass as adenine but are not adenine. The peak labeled (+) are tentatively assigned as allopurinol based upon comparison with existing standards.

In this reaction one or more thermally-generated intermediates likely act as chromophores and are able to access new pathways to other products. The presence of dissolved salts and catalytic surfaces continues to enhance the yields, and the relative

ratio, but not the diversity of products. Solvated ion-complexes and mineral surfaces are not likely involved in direct photoexcitation, unlike semiconductors such as TiO2.[25] The lack of specificity of mineral seen here indicates that possibly a wide range of minerals could have a dramatic effect on formation of prebiotic compounds on early earth without need to invoke any particular set of conditions for availability of heterogeneous interfaces.

4.3.2.2. UV irradiation with 254 and 365 nm photons

UV-irradiation of formamide samples, with 254 nm light and a small amount of 365 nm light, increased the yield and diversity of purine nucleobases produced during heating at 130 °C for all samples tested. The primary nucleobases observed in all the UV-irradiated samples were purine, adenine, hypoxanthine, and guanine.

UV irradiation of neat formamide produces purine, adenine, hypoxanthine, and guanine (Figure 4.8), whereas only purine production is observed under purely thermal conditions. Other important differences are observed; i) there is a significant increase in the hypoxanthine yield for UV-irradiated formamide samples containing minerals and/or their dissolved ions relative to no UV irradiation and ii) the yields of all the products increase by more than a factor of three when UV light is used. While the purine nucleobases are the focus of this study, these compounds represent a subset of all products generated in the formamide reactions.

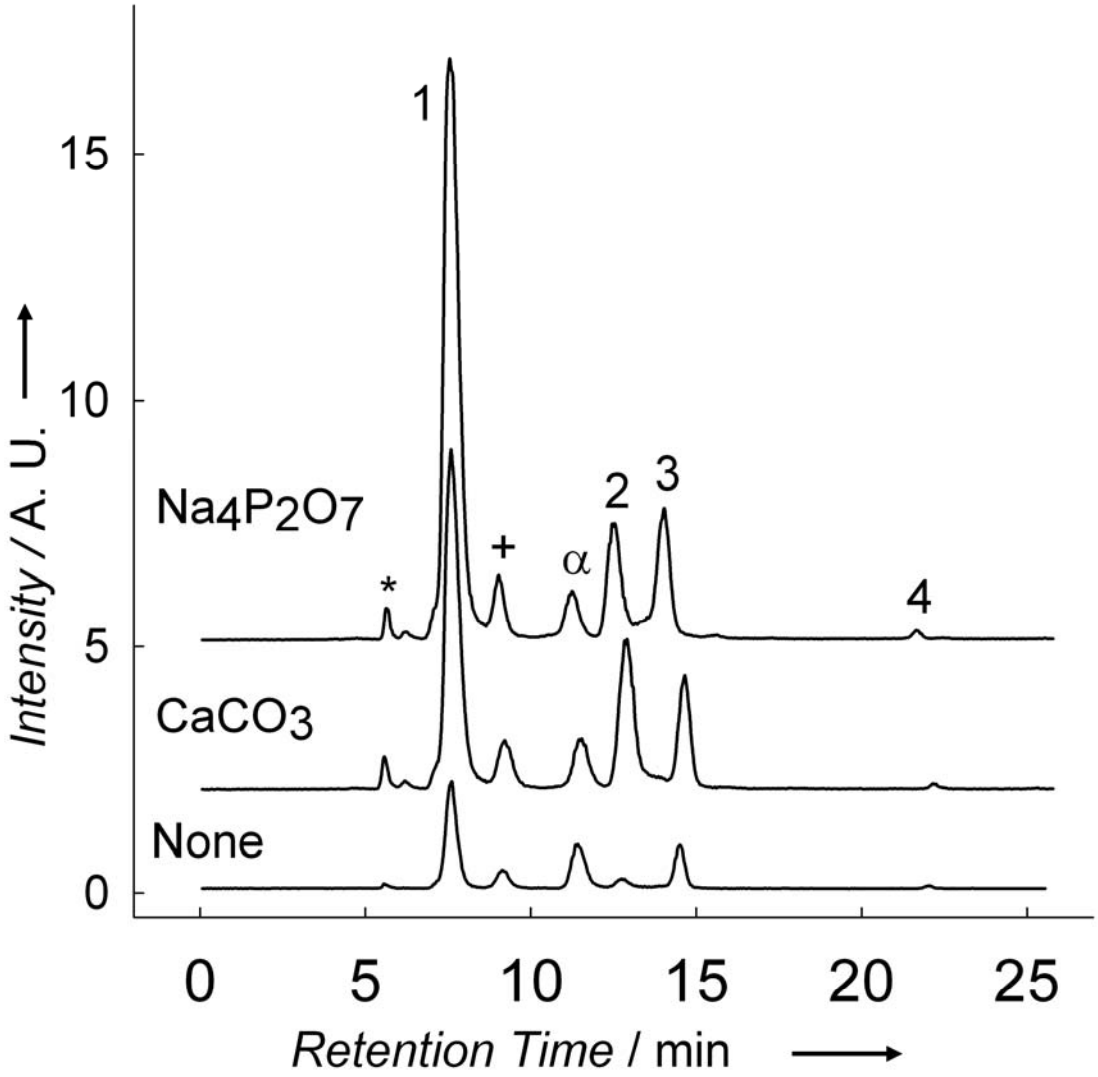

Figure 4.8. Combined selected ion chromatograms of formamide reactions with irradiated with UV light (254 and 365 nm) and heated to 130 °C for 48 h, in the presence and absence of catalysts. Offsets added for clarity. Products observed include purine (1), adenine (2), hypoxanthine (3), and guanine (4). The peak labeled (α) is the internal standard 2-aminopurine. Peaks labeled (*) have the same product and precursor ion mass as adenine but are not adenine. The peak labeled (+) is tentatively assigned as allopurinol based upon comparison with existing standards.

The amount of hypoxanthine produced in the reaction where 185 nm photons are used for 48 hours is significantly larger than that produced when the 185 nm photons are not present. This means that the 185 nm photons lead to the faster production of

hypoxanthine in these formamide reactions, although as seen when the neat formamide reaction was monitored over a time period of 96 hours, this yield decreases over time.

4.3.3 Formamide heated at different temperatures and irradiated in the presence and absence of inorganic salts

The following experiments were conducted with isoguanine as the internal standard and not 2-aminopurine. Instead of using 2-aminopurine, standard calibration curves were constructed with a set of standards ran before and after each set of sample runs.

The standard for performing formamide experiments was set by Dr. Ernesto DiMauro and coworkers who ran their experiments at 160 °C. For a direct comparison to their work, experiments at 160 °C using the custom-built reaction center and LC-MS/MS as the detection method were conducted. For the neat formamide reacted at 130 °C for 48 hours the introduction of UV light greatly enhances the yield of purine and leads to the production of adenine, hypoxanthine, and guanine. Without UV light the only purine detected is purine. Increasing the temperature from 130 °C to 160 °C greatly enhances the purine and adenine yields and hypoxanthine and guanine are both formed without UV light when the reaction is heated at 160 °C (Figure 4.9). Additionally the increase in yield observed at 130 °C when the sample is irradiated with UV light is not observed in the 160 °C experiments.

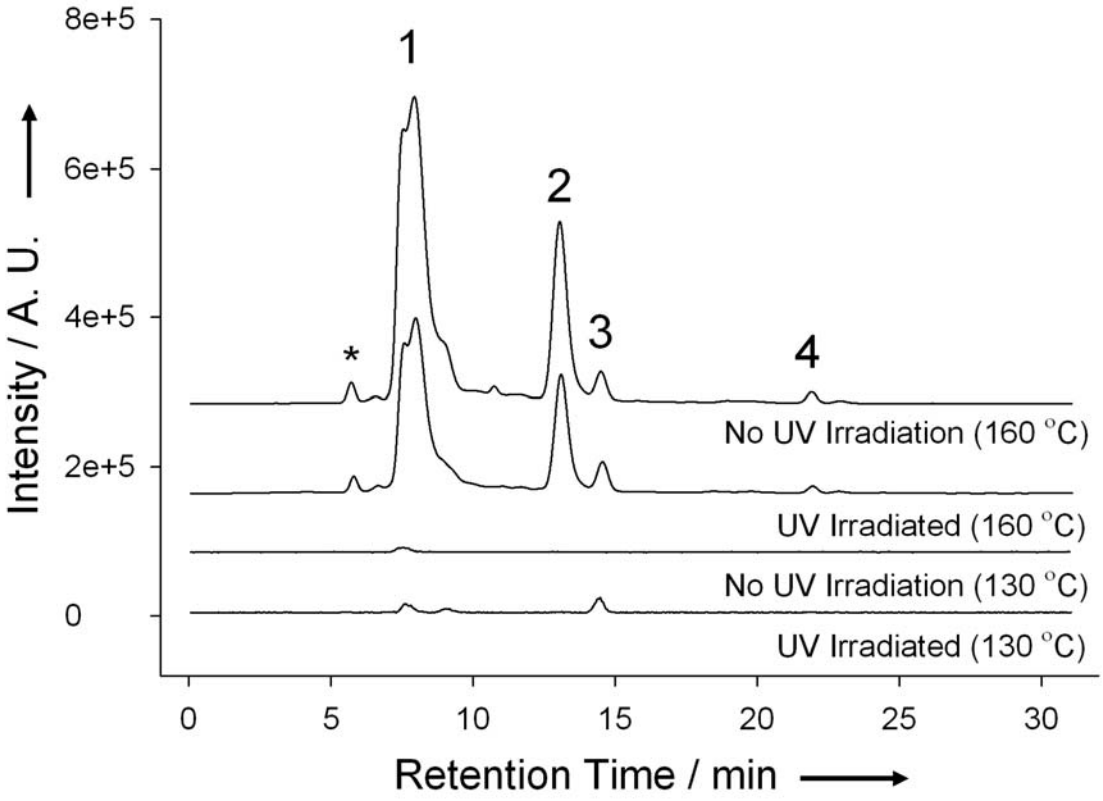

Figure 4.9. Combined selected ion chromatograms of formamide reactions with irradiated with UV light (185, 254, and 365 nm) and heated to 130 °C or 160 °C for 48 h, in the absence of mineral catalysts. Offsets added for clarity. Products observed include purine (1), adenine (2), hypoxanthine (3), and guanine (4). The peak labeled (*) has the same product and precursor ion mass as adenine but is not adenine.

The same increase in products made can be seen when inorganic salt is added to the neat formamide reaction, when formamide is reacted in the presence of calcium carbonate without UV irradiation at 130 °C (Figure 4.10). The only products that are formed at 130 °C without the addition of UV light are purine, adenine, and hypoxanthine. When UV light is added the amount of hypoxanthine greatly increases. When the same neat formamide solution is reacted at 160 °C for 48 hours the amount of products formed greatly increases.

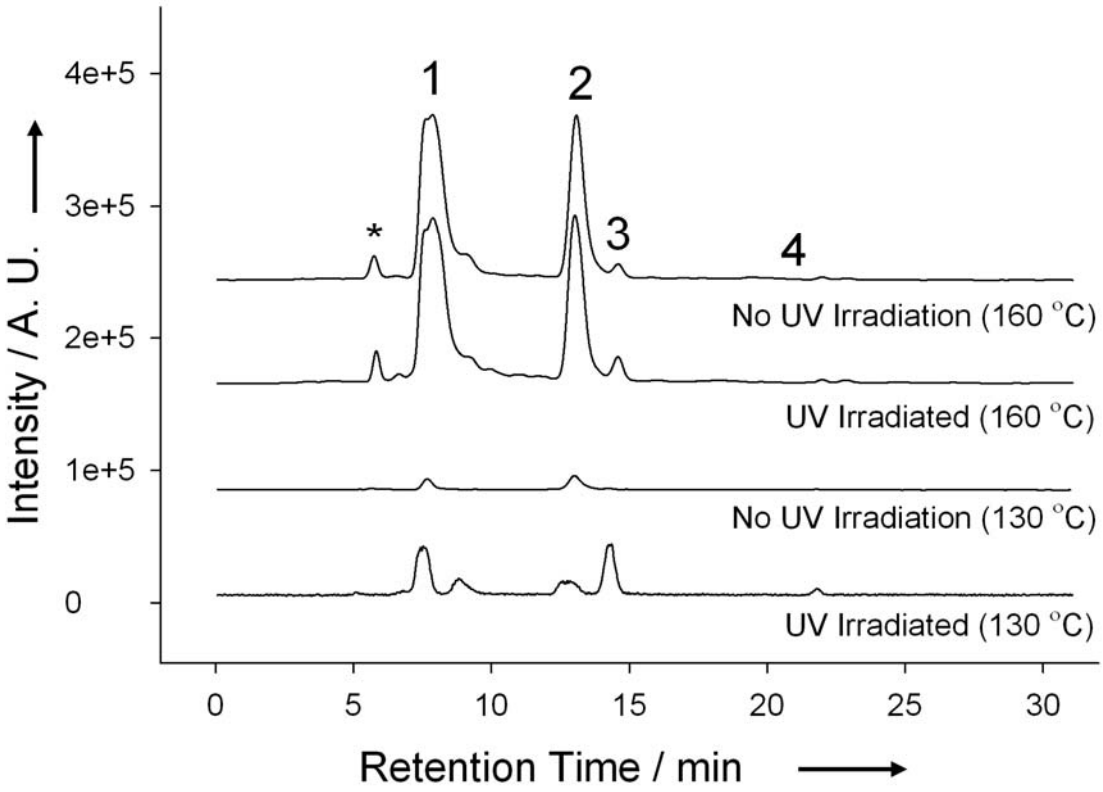

Figure 4.10. Combined selected ion chromatograms of formamide reactions with irradiated with UV light (185, 254, and 365 nm) and heated to 130 °C or 160 °C for 48 h, in the presence of calcium carbonate. Offsets added for clarity. Products observed include purine (1), adenine (2), hypoxanthine (3), and guanine (4). The peak labeled (*) has the same product and precursor ion mass as adenine but is not adenine.

When the sample is heated to 160 °C the product distribution changes, the adenine yield is increased relative to that of hypoxanthine. This result shows that there is a definite temperature threshold for the reaction but that the temperature that the reaction is conducted at has differing effects on the product yield and distribution. For example, when the reaction is heated at 130 °C with UV irradiation a larger amount of hypoxanthine is formed than any other product, but when the reaction is simply heated or heated and irradiated at 160 °C the major products are adenine and purine. This suggests that the production of hypoxanthine is directly correlated to UV irradiation.

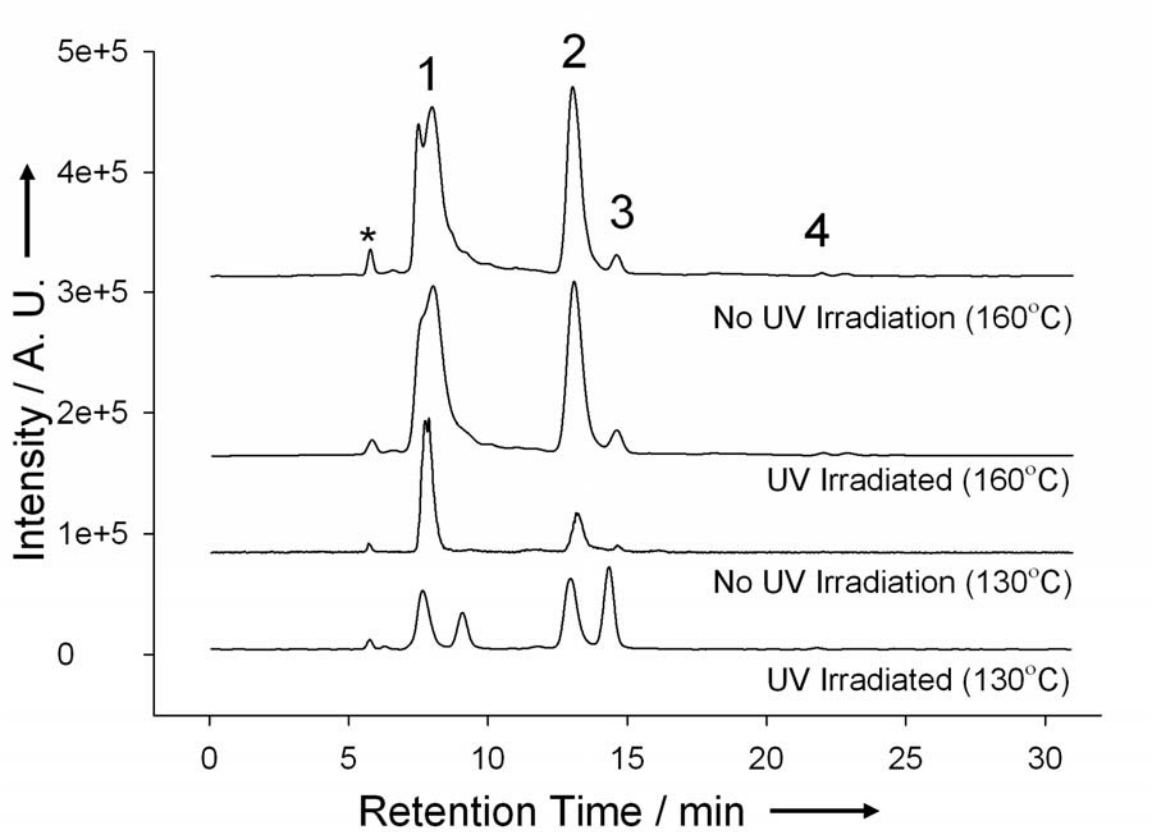

Figure 4.11. Combined selected ion chromatograms of formamide reactions with irradiated with UV light (185, 254, and 365 nm) and heated to 130 °C or 160 °C for 48 h, in the presence of sodium pyrophosphate. Offsets added for clarity. Products observed include purine (1), adenine (2), hypoxanthine (3), and guanine (4). The peak labeled (*) has the same product and precursor ion mass as adenine but is not adenine.

The same trends that are seen for calcium carbonate are also observed for sodium pyrophosphate (Figure 4.11). This includes the direct formation of adenine and purine at high temperatures (160 °C) and the direct formation of hypoxanthine when UV light is used to irradiate the sample at lower temperatures (130 °C).

4.4 Conclusions

In summary, neat formamide samples irradiated with UV light produced a larger yield and diversity of purine nucleobases than the non-UV irradiated neat formamide samples. In addition, the presence of dissolved salts and inorganic surfaces can enhance yields, but not the diversity of products when the samples are irradiated with UV light. Thus, the equalizing effect that UV light has on the yields and the product distribution further relaxes the chemical and environmental requirements for biopolymer building block formation on the prebiotic Earth.

In these simple salt reactions, the catalysts have an equalizing effect. However, the inorganic salt does have an effect on the yield and distribution of products. For example, work using other minerals has been shown to change the product distribution under thermal conditions.[19-22]

The results presented here clearly illustrate the ability for UV photons to increase the yield and diversity of nucleobases formed in model prebiotic reactions involving heated formamide, and that UV photons can work synergistically with inorganic salts or their dissolved ions in such reactions. The important observation that 254 nm UV light induces the formation of adenine, hypoxanthine and guanine from neat formamide clearly points to formamide itself as a photoactive entity. The onset of the electronic absorption spectrum of formamide is at 206 nm,[71] which corresponds to a higher energy than that of the photons used in the present study. The tail of the UV absorption spectrum of a formamide solution extends to at least 275 nm, which would allow absorption of the 254 nm photons used in these experiments. Recently, Duvernay and coworkers outlined a photochemical pathway from formamide (**1**) to formimidic acid (**2**), which then

decomposes to HCN/HNC and water (**3**).[72] HCN and HNC are believed to then undergo polymerization reactions to produce DAMN, AICN, and AICA under thermal and photochemical/thermal conditions. This multi-step process is depicted in Figure 4.5. Assuming that optical excitation of formamide is one of the important optical transitions, there will always be some water available to help initiate and facilitate the chemical steps leading to nucleobase formation.

One of the main reasons to look at the effects of the 185 nm is to note that the 185 nm photons cause the degradation or the formation of larger molecules from the purines that are analyzed in this study. This can be seen when adenine and hypoxanthine are monitored over time. The amount of adenine decreases over time when 185 nm photons are used, as does the amount of hypoxanthine, while the amount of adenine and hypoxanthine increase over the time range presented for both adenine and hypoxanthine.

CHAPTER 5

GC×GC-TOF/MS ANALYSIS OF FORMAMIDE MIXTURES

5.1 Abstract

The experimental strategy of this project first focused on the qualitative analysis of a set of expected nitrogen-bearing product compounds in formamide reactions through the systematic characterization of a set of 50 derivatized nitrogen-bearing organic standards, which included pyrimidines, purines, and related compounds. Retention coordinates (and library-matched mass spectra) were obtained for each individually prepared derivative for a protocol of operational conditions. The quantitative analysis of a mixture of these standards was then performed to determine the concentration ranges and detection limits for each standard, and to study the effect of the derivatization reaction on the formation of extraneous compounds over a period of a week. Finally, the analysis of a series of model prebiotic reactions of interest was done for the screening of expected compounds that match the standards in terms of chromatographic (first and second dimension retention) and MS information, as well as the screening of unexpected nitrogen-bearing organic compounds that exhibit similar mass spectral signatures.

5.2 Materials and Methods

5.2.1 Pre-biotic synthesis reaction conditions and sample preparation

The reactions were carried out as stated in Chapter 2, but two of the tube wells were slotted to allow calibrated exposure to a low pressure mercury lamp (Custom made Pen-ray lamp with a primary emission at 254 nm with a small amount of emission at 365 nm).

After the reaction was completed, a 200 μL aliquot was placed in a speed-vac for one day at 80 °C to evaporate the aqueous solvent and preconcentrate the reaction product analytes. The sample solutes were then reconstituted in 60 μL of pyridine and spiked with 10 μL of internal standard (100 μM concentration). This solution was derivatized with 80 μL of BSTFA/TMCS in a hot oil bath at 80 °C for 2 hours prior to GC×GC-TOF MS analysis.

5.2.2 Standards

Fifty nitrogen-bearing organic compound standards were used in this study. Pyridine solvent was used to dissolve the standards, and N,O-Bis(trimethylsilyl)trifluoroacetamide (BSTFA) with 1% trimethylchlorosilane (TMCS) was used for the derivatization of the standards into their corresponding trimethylsilyl metabolites. D_7-Quinoline from Cambridge Isotope Laboratories was used as the quantitative internal standard. Formamide, calcium carbonate, and sodium pyrophosphate were used for the prebiotic reactions. All these compounds were purchased from Sigma/Aldrich (St Louis, MO) and their retention properties are listed in Table 1.

5.2.3 GC×GC-TOF/MS analysis

A GC×GC-TOF MS (Pegasus 4D, LECO Corporation, St. Joseph, MI) was used for the analysis of the standards and samples. The instrument used helium (99.9999 % purity) as the carrier gas, and nitrogen, compressed air, and liquid nitrogen for the operation of the quad-jet thermal modulator. All gases were purchased from Air Gas (Atlanta, GA). The sample inlet was heated at 250°C, and samples were injected at a split ratio of 400:1 for the standards, and 3:1 for the samples. The carrier gas flow rate was 1 mL/min.

The GC×GC column set was comprised of a 30-meter first dimension column with a 5% phenyl-substituted, 95% methylpolysiloxane stationary phase (250 μm internal diameter, 0.25 μm stationary film thickness) that was connected to a 2-meter second dimension column with a 35% diphenyl, 65% dimethyl polysiloxane stationary phase (100 μm internal diameter, 0.1 μm stationary film thickness). The columns were purchased from Restek Corporation (Bellefonte, PA) and are commercially known as Rtx-5MS and Rtx-35, respectively. The temperature program of the first dimension column was as follows: the run started at 40°C, and was held at that temperature for 0.5 minute. A temperature ramp of 10 °C/min was used to reach the final temperature of 290 °C, where it was held for 4.5 minutes for a total run time of 30 minutes. The second dimension column was programmed as follows: the run started at 45 °C, and was held at that temperature for 0.5 minute. A temperature ramp of 10°C/min was used to reach the final temperature of 295 °C. The modulator interface between the first and second dimension columns was programmed at the following sequence: 70 °C initial temperature (for 0.5 minute), with a temperature ramp of 10°C/min to the final temperature of 320 °C.

The TOF MS transfer line was held at 280°C, and the ionization chamber was held at 200°C. Electron impact ionization was used at energy of -70 eV, and the detector voltage was 1400 V. The mass range of analysis was between 35 and 700 amu. The data acquisition rate was 200 averaged scans/sec. Data files were collected and stored on the Pegasus 4D instrument.

5.2.4 Data Processing

The basic processing of all samples was done using the ChromaTof 4.21 software (LECO Corporation, St. Joseph, MI). Additional processing to generate the peak apex plots was done on software written in-house in Igor Pro 6.04 (Wavemetrics, Portland, OR). Concentration calculations were done in Excel (Microsoft, Seattle, WA).

5.3 Results and Discussion

5.3.1 Qualitative analysis

Individual standards were run to establish the retention coordinates of the TMS-derivatives on the chosen GC×GC column set, and to monitor the artifacts that are formed during the derivatization process in order to be able to distinguish them from the compounds that may form during the prebiotic reactions. This is important because the desired compounds need to detected and monitored, as well as new or unexpected compounds. It is also important to be able to distinguish the compounds from the prebiotic reaction from the compounds of the derivatization reaction. For instance, in the analytical run for the internal standard all of the peaks in the chromatogram except for the analyte peak are artifacts from derivatization reaction. The most intense peaks are due to the solvents used in the reaction (pyridine, BSTFA, TMCS). However, a significant artifact peak, identified as 4-fluoro-2-(trifluoromethyl) benzaldehyde by the MS library, appears in the general elution region where D_7-Quinoline elutes. Knowledge of the background derivatization peaks is thus important in subtracting the artifact peaks from the formamide reaction peaks.

Table 5.1 summarizes the retention of the nitrogen-containing organic standards of interest in this study. The mass spectra for each standard were observed to confirm the

identity of the standard, and the library identification of the compound was also recorded with the similarity value provided from the library search algorithm. Most of the standards were recognized as the top library hit, however some of the compounds were similar in the electron impact MS spectra to other compounds, and were not correctly identified by the library, even though the correct library hit was present on the hit list. The retention time precision is consistent with previously reported GC×GC results, i.e. relative standard deviation values were lower in the first dimension (0.06%) than in the second dimension (1.3%), and are correlated to the analyte peak's signal to noise ratio. These reproducibility values are important because they determine the area in which the peaks in real samples exist, and allow for the confirmation of the presence of the known analytes in real samples of prebiotic reactions. The availability of the secondary retention time as confirmatory retention information is also a big advantage of GC×GC separations for this application.

Table 5.1. Retention times of the nitrogen-containing organic standards

	Nucleobases and Related Compounds	RT1	RT2	CAS of TMS-Compound	Monitor m/z
No Ring Compounds					
1	Glycine	648	1.13	3553-95-5	174
2	Biuret	504	1.27	18297-63-7	189
3	Urea	460	0.78	60615-84-1	261
4	Guanidine	664	0.63	999-97-3	347
5	Glycinamide	668	0.85	5630-81-9	188
One Ring Compounds					
6	4(6)-pyrimidone	356	1.1	18290-96-5	153
7	2-Hydroxypyrimidine	412	1.4	18290-96-5	153
8	Imidazole	380	1.53	18156-74-6	140
9	2,3-Pyrazinedicarbonitrile	524	2.43	13481-25-9	103
10	Cytosine	720	1.42	18037-10-0	240
11	5-Methylcytosine	744	1.31	32865-85-3	254
12	Thymine	632	1.13	7288-28-0	255
13	5-Azauracil	632	1.2	0-00-0	242
14	6-Azauracil	652	1.32	0-00-0	242
15	5-Azacytosine	704	1.21	10457-14-4	171
16	4,5-Diaminopyrimidine	768	1.3	5075-52-5	239
17	Cyanuric acid	784	1.23	60739-94-8	345
18	Isocytosine	656	1.13	18037-10-0	240
19	2,4,5,6-Tetraaminopyrimidine	1108	0.99	0-00-0	213
20	Urazole	676	1.15	0-00-0	302
21	2-Methylimidazole	456	1.47	75311-60-3	154
22	2,4-Diamino-6-hydroxypyrimidine	920	1.2	0-00-0	328
23	Uracil	584	1.15	10457-14-4	241
24	3,6-Dihydroxypyradizine	608	1.2	0-00-0	241
Two Ring Compounds					
25	Quinoline (Internal Standard)	496	1.87	23853-67-0	136
26	Purine	700	1.69	32865-85-3	177
27	2,6-Diaminopurine	1124	1.44	0-00-0	351
28	2,6-Diamino-8-purinol	1164	1.18	69822-65-7	441
29	Hypoxanthine	908	1.5	17962-89-9	265
30	Allopurinol	784	1.2	0-00-0	265
31	Phthalimide	748	1.58	10416-67-8	204
32	8-aminoguanine	1170	1.344	0-00-0	511
33	Adenine	944	1.46	17995-04-9	264
34	2-Aminopurine	964	1.54	17995-04-9	264
35	Xanthine	1036	1.51	0-00-0	353
36	2-Aminobenzimidazole	992	1.43	0-00-0	334
37	Isoguanine	1072	1.49	0-00-0	352
38	Uric Acid	1084	1.29	0-00-0	441
39	Guanine	1092	1.45	0-00-0	352
40	2-Hydroxy-6-aminopurine	1068	1.45	0-00-0	352
41	2-Amino-1-methylbenzimidazole	896	1.55	0-00-0	276
42	2-Amino-6-methoxybenzothiazole	1020	1.53	0-00-0	309
43	Adenosine	1340	1.28	53294-33-0	540
44	Uridine	1256	1.24	10457-16-6	518
45	Thymidine	1268	1.29	0-00-0	458
Three Ring Compounds					
46	Acridine orange	1492	3.07	494-38-2	265
47	Proflavine	1492	2.3	274691-42-8	353
48	Quinacrine	1592	2.56	83-89-6	399
49	Acridine	900	2.21	260-94-6	179
50	Methylene blue	1500	3.06	83475-40-5	271

A mixture of all 50 standards was also analyzed to verify the consistency of the retention time coordinates of the standards in a mixture of compounds, and a plot of the peak apexes of these compounds is shown in Figure 5.1. In this figure, all 50 nucleobase analogues are graphed according to their respective structure, no ring compounds (●), one ring compounds (□), two ring compounds (▲), and three ring compounds (▽). The graph at the top of Figure 5.1 shows that the GC×GC-MS separates the compounds according to structure. There are clear groups in the GC×GC-MS; the no ring compounds are located at the bottom left, the one ring compounds are located slightly to the right of the no ring compounds, and the three ring compounds are seen in the top right corner of the chromatogram.

The resolution enhancement over conventional one-dimensional GC separations is evident in several areas in the chromatogram, where a vertical line can be traced through several peak apexes that would result in peak co-elution, and is consistent with separation efficiencies that have been previously reported for GC×GC analyses. In addition, three general separation class regions are apparent in the two-dimensional separation plane that correspond to the number of aromatic rings of the nitrogen-containing aromatic compounds. The ability for GC×GC to separate these compounds in identifiable regions is particularly relevant for their screening in prebiotic reactions because the search for known and new compounds can be targeted to the zones of interest, and enhances the role of the separation to help characterize the general chemical structure of all separated analytes.

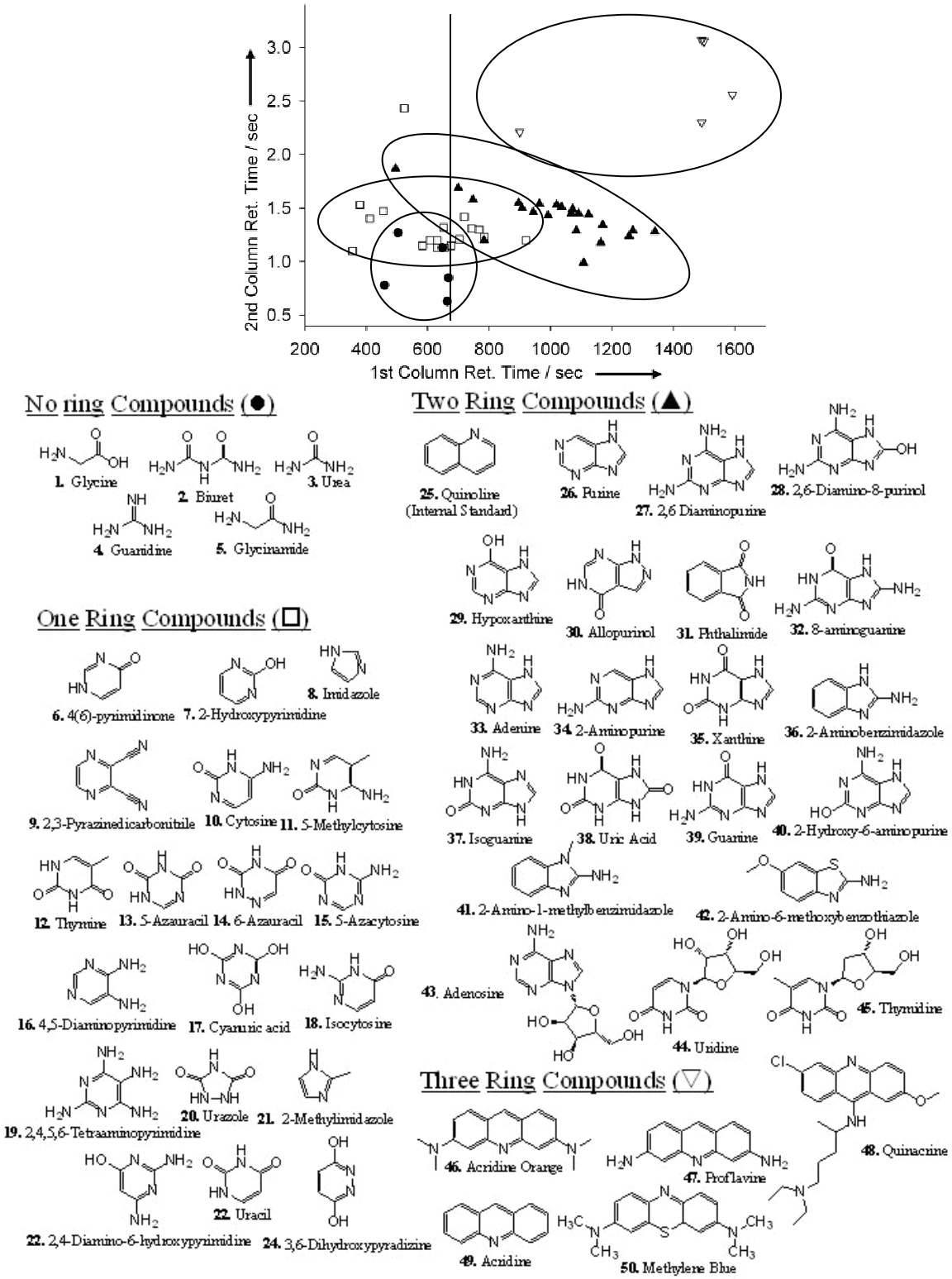

Figure 5.1. GC×GC graph of the 50 compounds shown according to their structure; no ring compounds (●), one ring compounds (□), two ring compounds (▲), and three ring compounds (▽).

.3.2 Quantative analysis

Calibration curves for four nucleobase standards (adenine, guanine, hypoxanthine and purine) were constructed. These four compounds were chosen because they have been identified as the products in the on-going HPLC analyses of formamide reactions,[19-23] and thus provide a basis of comparison in terms of the linear dynamic range and detection limits of the GC×GC method to the HPLC-UV and LC-MS/MS methods. The GC×GC/TOF MS detection limits for the N,O-Bis(trimethylsilyl)triflouroacetamide (TMS) derivatives of the four standards was established to be 5 ppb for adenine and hypoxanthine, and 10 ppb for guanine and purine. The expected concentrations of the parent compounds was expected to be in the 80 to 100 ppb range, and therefore the detection limits and dynamic ranges for the four standards was deemed satisfactory for these samples. The relative standard deviation (RSD) of the peak ratios between the internal standard and the analyte peaks were very consistent, as were the retention factor values for spiked standards in the method validation runs.

5.3.3 Formamide Reaction Analysis

HPLC-UV and LC-MS/MS were used for the anlaysis of this data in previous studies to make sure that the methods are comparable all three analyses were conducted on the same sample. Figure 5.2 shows a subset of the comparisons that were conducted to make sure that the methods were comparable. There are variations of the sample preparation that would account for any discrepancies between the three analysis methods: HPLC-UV and LC-MS/MS use water as the reconstituting agent after the formamide has been removed, whereas pyridine is used as the reconstituting agent for the GC×GC-MS analysis. Other differences in the methods such as the fact that HPLC-UV can only detect

compounds that absorb UV light, LC-MS/MS can only detect the molecules that ionize sufficiently using electrospray, and GC×GC-MS can only detect volatile molecules (except for the compounds that are derivitized) also play a role in the differences seen when the three methods quantatative data are compared.

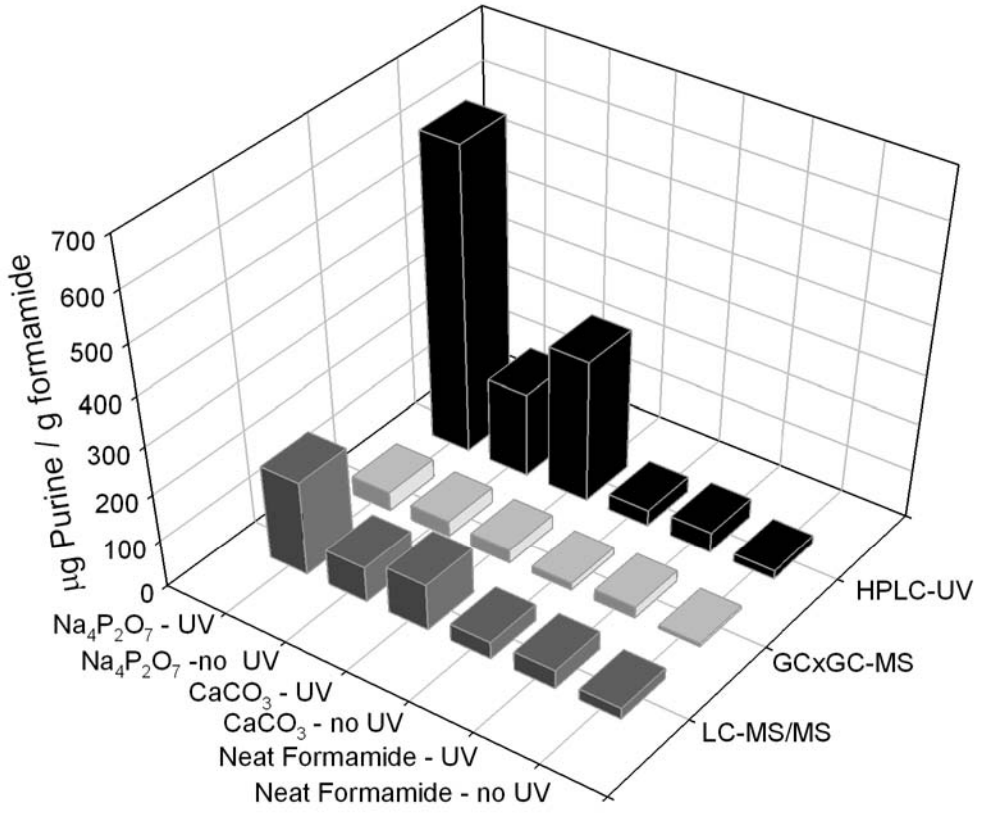

Figure 5.2. Comparison between the three different types (HPLC-UV, LC-MS/MS, and GC×GC-MS) of analyses methods used for the detection of purines in formamide pre-biotic reactions reacted for 48 hours at 130 °C: sodium pyrophosphate ($Na_4P_2O_7$), calcium carbonate ($CaCO_3$), and neat formamide.

Figure 5.2 shows that despite all of the differences in sample preparation, ionization, and detection the same trends are observed for purine production for formamide reactions. There is a slight increase in the amount of purine formed when UV light is added to a neat formamide sample heated at 130 °C for 48 hours, another increase in purine formation when formamide is reacted in the presence of calcium carbonate, and an even greater increase when neat formamide is reacted in the presence of sodium pyrophosphate.

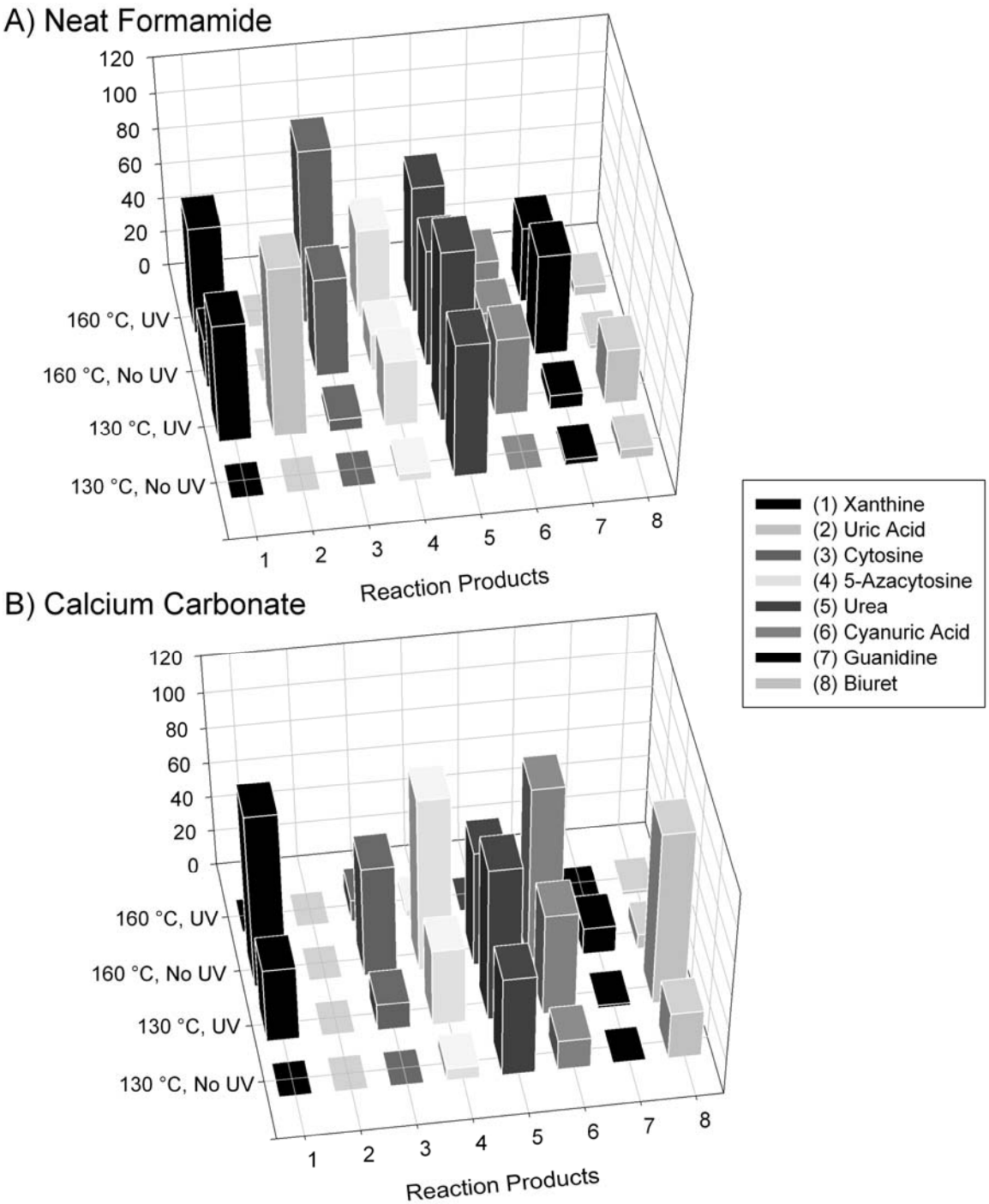

Figure 5.3. Products observed using GC×GC-MS that were not observed using HPLC-UV or LC-MS/MS. GC×GC-MS quantification of purines. Figure (A) is a neat formamide sample, Figure (B) is neat formamide reacted in the presence of calcium carbonate. The samples heated at 130 °C for 48 hours are labeled 130 °C and likewise for 160 °C, the samples irradiated with UV light (254 nm and 365 nm) are labeled UV. The additional products that were detected include (1) xanthine, (2) uric acid, (3) cytosine, (4) 5-azacytosine, (5) urea, (6) cyanouric acid, (7) guanidine, and (8) biuret.

In addition to the compounds that were known to be in the samples because of HPLC analyses, a number of other analytes were found in the samples on the basis of the retention time coordinates and the library hit lists (Figure 5.3). The screening for these compounds was not quantitative due to the lack of calibration curves for these compounds. However, response factors relative to the internal standard are recorded, such that concentrations for these compounds can be found if necessary. The nominal peak areas for these compounds suggest that they are either at trace levels in the samples, not soluble in water, or interact with the solvent in the HPLC systems, which explains why they are most likely not detected in the HPLC analyses. Their detection by GC×GC might help in refining their detection by HPLC, which will be helpful in the development of a complimentary set of analysis techniques for the reactions.

5.3.4 Sample screening for unknown compounds

For the screening of new compounds, we investigated the development of an MS script for the selective screening of nitrogen-bearing compounds. However, a number of MS filters for nitrogen-bearing compounds that were tested did not work because these compounds fall into a diverse range of categories based on the number (and position) of the nitrogen atoms in the molecule. We thus had to resort to the use of m/z 73, which is the characteristic mass of all compounds in the reaction that have been derivatized. The processing of the samples revealed a number of other compounds besides the nucleobases in the samples.

Some of the additional compounds identified in the neat formamide sample reacted at 130 ° for 48 hours based on library identification include four different uracil

derivatives including: 2-aminopyrimidine-4,6-diol, 2,6-dihydroxypyrimidine-4-carbaldehyde, pyrimidine-4,6-diol, pyrimidine-2,4,6-triol. Some of the additional compounds identified in the neat formamide sample reacted at 130 ° for 48 hours while being irradiated with UV light based on library identification include two different cytosine derivatives including: 6-aminopyrimidin-2(1H)-one and 4-aminopyrimidin-2-ol. Additional experiments using standards and spiking experiments should be done to confirm the presence of these molecules and to determine if one or more of these molecules are possible intermediates in the formation of purines or pyrimidines.

For other classes of compounds (such as organic acids, carbohydrates, and amino acids), the sample compound list was checked against the retention time coordinates of the standards to confirm the identity of the compounds with known standards that we have run in our database of 185 nitrogen-bearing compounds. The identity of other compounds in the samples will have to be checked further through their mass spectra as well as the retention zone in which they elute to give us clues as to what general structural category the analyte belongs to. Further investigations of these new compounds is thus under way.

5.4 Conclusions

The screening of model formamide reactions by GC×GC-TOF MS has shown promising results for the pre-biotic synthesis reactions that we have investigated so far, and we intend to extend the method to the analysis of other samples of prebiotic interest. As more investigations on the correlation between retention coordinate position and structural properties are pursued, a systematic mapping of the two-dimensional plane may be

possible that will be very useful in the use of GC×GC in a manner analogous to spectrometric instruments, in which the location of the signal is used to provide information on the structure of the molecule. Studies such as the translation of chromatographic retention data to thermodynamic properties (such as ΔG's of formation) by Arey et al.[73,74] will also be relevant avenues to be pursued that will provide additional information in the analysis of the products of prebiotic reactions, particularly because the mixtures contain more than the nucleobases that are the focus of this study, but also amino acids, carbohydrates, etc. for which similar chromatographic zones will have to be determined as well.

CHAPTER 6

GC×GC-TOF/MS ANALYSIS OF BIO-OILS

6.1 Abstract

GC×GC-MS is also a useful method to study other complex mixtures, such as bio-oil samples. In this chapter three different types of bio-oils were studied; Douglas-fir bark, Southern pine bark, and a Southern pine bark-wood mixture. The data shown in this chapter demonstrates that GC×GC-MS is not only a good method for the analysis of complex mixtures, it can also be used for grouping types of compounds found in any given sample for easy identification of functional group. The top 1000 compounds of these samples were analyzed via GC×GC-MS, these compounds were then divided according to the following groups: methoxy phenols, alkyl benzenes, carboxylic acids, esters, and alkanes.

6.2 Introduction

Bio-oils are a viable alternative to fossil fuel oil, and as such the study of bio-oils may lead to the development of a more sustainable fuel for transportation vehicles. Transportation vehicles are responsible for most of the consumption of fossil fuel oil today. GC×GC-TOF/MS analysis was used to determine the identities and amounts of molecules that are present in different types of bio-oils. The bio-oils that are studied are extracted from are pine bark, a mixture of pine wood and pine bark, and Douglas-fir bark.

The shortage of fossil fuels for use as fuel in the United States is growing faster than ever and the environmental issues involved with the usage of these fossil fuels has

spurred the recent interest in the development of new, clean renewable energies. The increasing demand for fuel can be quelled in a variety of ways including; enhancing vehicle efficiencies, upgrading the heavy crude reserves, further oil recovery, and the use of bio-oils.[75] Among the various methods used to produce liquid fuels, the fast pyrolysis of biomass is one of the most studied and has experienced rapid development in the last decade, mainly because it offers an alternative way to solve liquid fuel shortage issues.[76]

Fast pyrolysis of lignocellulosic biomass produces bio-oil that can be used directly for energy production. The use of bio-oils is of particular interest due to the small amount of waste produced from the production of bio-oils, even residual char can be used for fuel resources. Bio-oils are also of particular interest due to the high thermal efficiency, and the fact that they are CO_2 neutral, and greenhouse gas neutral. Further, bio-fuels are more environmental friendly and produce lower SO_X and NO_X emissions.[75] Renewable energy and locally produced bio-oil can be produced anywhere that large volumes of organic wastes are available. The thermo-chemical conversion of biomass is the most promising, non-nuclear form of energy for use in the future.

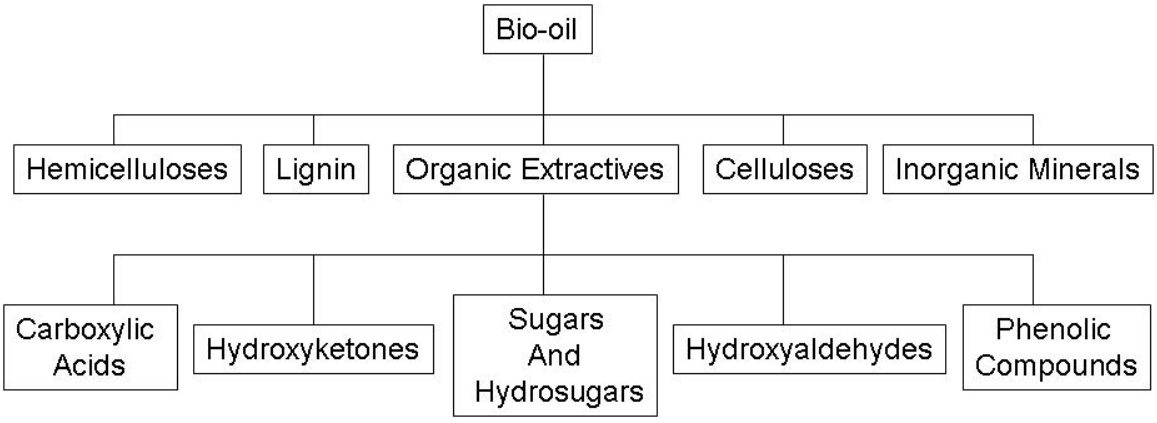

Figure 6.1. Breakdown of the bio-oil into its constituent parts

The type of material that is used to produce the bio-oil has a major impact on the indentities of chemicals analyzed and the bio-oil yield obtained. Bio-oil composition has been classified into five main substituents; cellulose, hemicelluloses, lignin, organic extractives, and inorganic materials (Figure 6.1). The organic extractives in bio-oils have been subdivided into five broad categories that can easily be identified in GC×GC-MS; hydroxyaldehydes, hydroxyketones, sugars and hydrosugars, carboxylic acids, and phenolic compounds. The organic extractives that are detected in bio-oils are fragments of the samples that are produced during the pyrolysis process. A more detailed classification of the organic extractives organizes them into the following categories; acids, alcohols, aldehydes, esters, ketones, phenols, guaiacols, syringols, sugars, furans, alkenes, aromatics, nitrogen compounds, and miscellaneous oxygenates,[75,76] of which most can be easily identified via GC×GC –MS.

Whole pyrolysis liquids have been analyzed via GC-MS for the volatile compounds[77-81], HPLC[81] and HPLC electrospray MS for the nonvolatile compounds[82,83], Fourier Transform infrared spectroscopy for determination of functional groups[83,84], gel permeation chromatography (GPC) for molecular weight distribution determination [77,80], and nuclear magnetic resonance (NMR) for determination of different types of hydrogen's and carbons and determination of specific structural groups, bonds, and areas [80,85,86].

While NMR supplies structural information for the samples, it does not allow for the determination of specific products. During HPLC analysis, the combination of polarity differences and molecular-weight differences interact to produce broadened peaks that are difficult to analyze by subsequent MS analysis.[75] GC-MS is also compound

specific, but not all compounds are detected due to co-elution of peaks and relatively low sensitivity.

GC×GC has been used extensively to study complex mixtures that have a large number of sample components. It has been applied to the separation of different matrices that are generally similar such as petroleum samples and environmental samples. GC×GC has been applied to petroleum,[87] and environmental[88,89] samples that contain many of the compounds that are seen in bio-oil samples. GC×GC-MS has previously been used for the identification of groups of acids, and methoxy phenols,[90] along with a large variety of other organic compounds. The fact that these studies have focused primarily on petroleum products makes it ideal for the study of bio-oils due to the complex nature of bio-oils and the easy comparison between bio-oils and petroleum products that can be achieved using GC×GC. Since the samples currently being analyzed are replacements for fossil fuels and are environmental sampels, GC×GC-MS is an ideal method for detection and analysis of the bio-oils. The goal of work described in this chapter is to examine the use of GC×GC for the qualitative analysis of bio-oil samples and the use of multidimensional scaling for the comparison of bio-oil samples. The differences between Southern pine bark and Douglas fir samples and bark versus a combination of Southern pine bark and Southern pine wood were examined.

6.3 Materials and Methods

6.3.1 Sample Preparation

Three samples were analyzed in this study; Douglas-fir bark, Southern pine bark, and a Southern pine bark-wood mixture. The Douglas-fir bark sample consisted solely of

bark, the Southern pine bark sample consists of pure Southern pine bark, and the Southern pine bark mixture contains a mixture of bark and wood that contained approximately 25 % wood. A moisture determination was conducted on all three bark samples and the samples were dried in a convection oven at 45 °C for one day. Three powder samples were then obtained with a Wiley Mill equipped with a 0.5 mm sieve (See Figure 6.2).

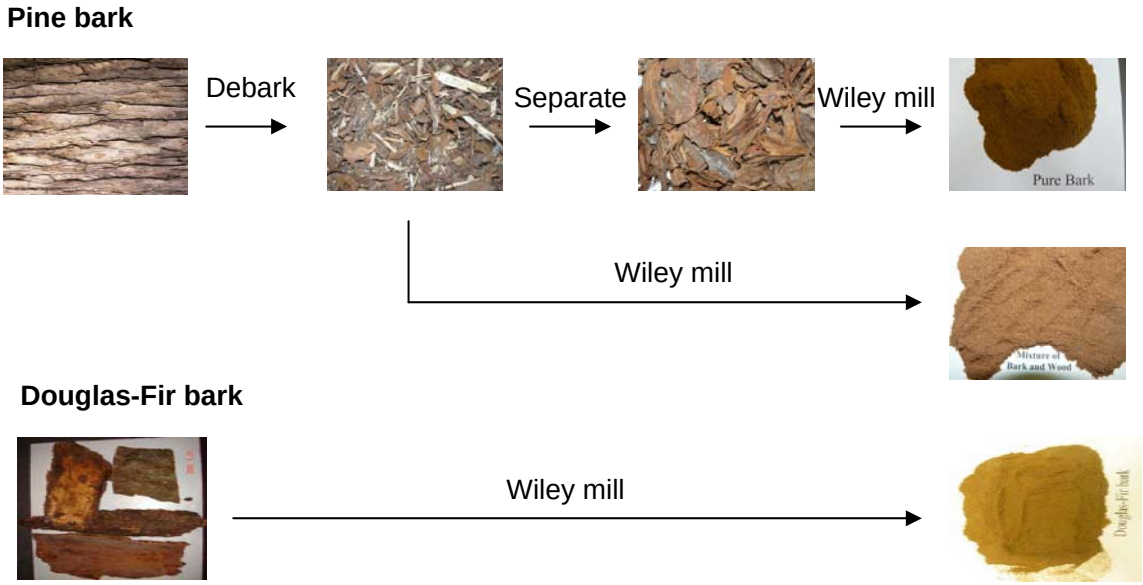

Figure 6.2. Bark sample preparation and separation

The samples were then pyrolyzed in the split furnace. The pyrolysis process was carried out using a bench-scale reactor under the pyrolytic conditions presented in Table 6.1. The samples (4.00 g) were then placed in a quartz sample boat centered in the heated zone of the furnace under nitrogen gas with a predetermined flow rate. The split-tube furnace was then preheated to the desired temperature and connected to liquid nitrogen-cooled condenser and water scrubber.

Table 6.1. Pyrolysis conditions and oil yield

	Sample GC #	Temp. (°C)	N_2 (ml/min)	Oil yield (%)
Douglas-Fir bark	1	500	200	37.46
	2	500	500	26.70
Pine bark	3	500	200	29.18
	4	500	500	24.16
Pine bark-wood mixture	5	400	200	27.51
	6	400	500	28.04
	7	500	200	30.35
	8	500	500	28.00
	9	600	200	29.03
	10	600	500	27.79

Upon completion of the reaction, the furnace was removed and the pyrolysis tube was allowed to cool down to room temperature under constant nitrogen flow. The char boat was removed and weighed, and the tar (bio-oil) was rinsed out of condenser and pyrolysis tube with acetone. The solution of tar in acetone was rotary evaporated at 40 °C under reduced pressure to remove acetone and water, and the resultant oil was weighed. The samples were then prepared for GC×GC-MS analysis by dissolving the oil in acetone at 100 mg/ ml concentrations.

6.3.2 GC×GC-TOF/MS analysis and Data Processing

The samples were then spiked with an internal standard and injected into the GC×GC-TOF/MS. The GC×GC-TOF/MS conditions and data processing were the same as those used in Chapter 5 (see Chapter 5 analysis and data processing sections).

6.4 Results and Discussion

Each bio-oil sample was analyzed and the top 1000 compounds that appeared were analyzed to determine the composition of the sample. Those 1000 compounds were then separated based on their functional groups and divided accordingly. The functional groups that had the most compounds are shown in the following figures and table. Those functional groups are methoxy phenols, alkyl benzenes, carboxylic acids, esters, and alkanes.

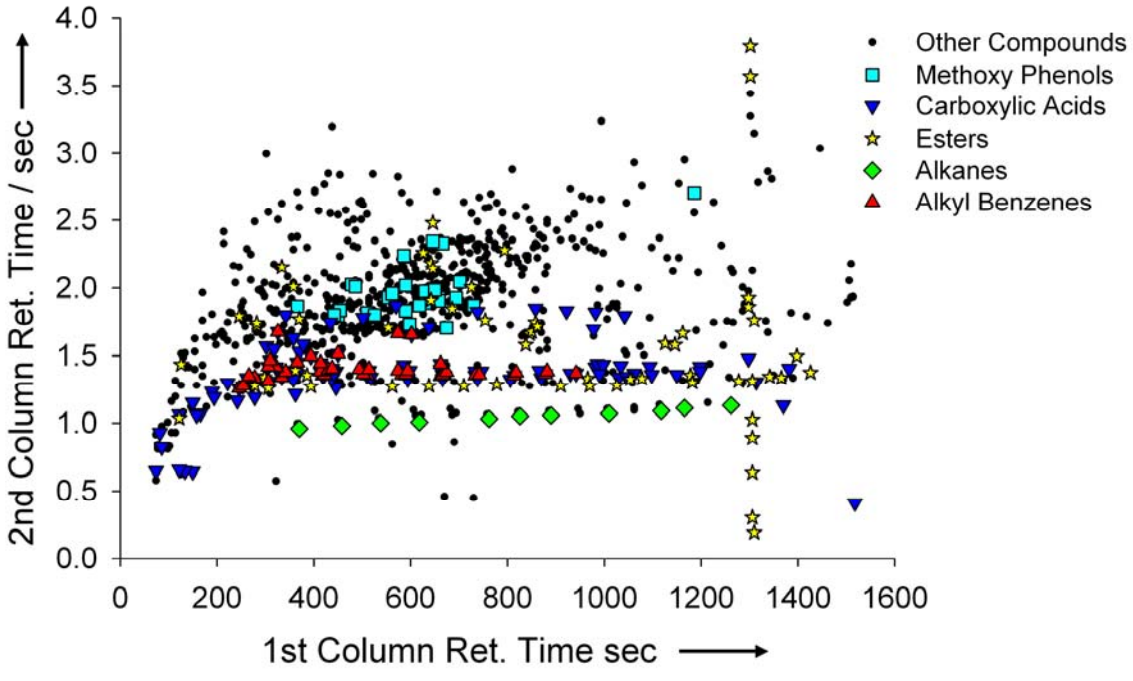

Figure 6.3. GC×GC-MS plot of retention time for the first column against retention time for the second column for Sample 1 (Douglas-fir Bark Sample). The black dots indicate the top 1000 compounds identified. The represented compounds include: methoxy phenols (■) , carboxylic acids (▼),esters (★),alkanes(◆), and benzenes(▲).

Figure 6.3 shows an example GC×GC-MS plot where the top 1000 peaks are identified, along with their composition. It is important to note in this figure that the compounds elute according to their functional group. The methoxy phenols are grouped in middle left of the plot. The carboxylic acids follow two paths, one horizontal line straight across the plot at 1.25 seconds, and one at 1.4 seconds. The Esters follow that same line at 1.25 seconds along with grouping in the center left with the methoxy phenols (note the vertical line of esters at 1300 seconds is due to oversaturation and therefore is one large peak in the center at RT1 1.90 seconds. The alkanes form a horizontal line at 0.9 seconds, and the alkyl benzenes form a line with the esters and carboxylic acids at 1.4 seconds. A representative sample of the compounds shown in Sample 1 that are indicative of the whole sample are shown in Table 6.2.

Table 6.2. A representative sample of the compounds found in bio-oil sample 1 (Douglas-fir bark), with the corresponding CAS number, the % area of the compound as a part of the detected compounds detected for that sample, the retention time for the 1st column (RT 1) and second column (RT 2) in seconds, and the similarity index for how closely that compound matches the library value.

Compounds Found in Bio-Oil Sample 1	CAS	Area %	RT 1	RT 2	Similarity
Methoxy Phenols					
2-Methoxy-4-vinylphenol	7786-61-0	0.49132	554	1.93	915
2-Methoxy-5-methylphenol	1195-09-1	0.020319	450	1.795	870
2-Methoxy-6-methylphenol	2896-67-5	0.046878	442	1.8	852
phenol, 2,6-dimethoxy-	91-10-1	0.013888	586	2.24	706
phenol, 2-methoxy-	90-05-1	1.7489	366	1.865	948
phenol, 2-methoxy-4-propyl-	2785-87-7	0.20121	598	1.73	932
phenol, 3,4-dimethoxy-	2033-89-8	0.007945	590	2.02	706
phenol, 3-methoxy-	150-19-6	0.019053	486	2.01	738
phenol, 4-ethyl-2-methoxy-	2785-89-9	0.005091	510	1.815	692
phenol, 5-methoxy-2,3-dimethyl-	34883-01-7	0.007931	630	1.975	553
Carboxylic Acids					
3-Octenoic acid	1577-19-1	0.013658	446	1.385	820
4-Pentenoic acid	591-80-0	0.002609	190	1.23	775
5-Hexenoic acid	1577-22-6	0.080842	262	1.335	869
6-Heptenoic acid	1119-60-4	0.046342	350	1.39	892
9-Decenoic acid	14436-32-9	0.010021	598	1.39	605
Acetic acid	64-19-7	0.006564	150	0.645	749
Benzoic acid	65-85-0	0.059329	434	1.745	905
cis-11-Eicosenoic acid	5561-99-9	0.039814	1198	1.42	743
cis-5-Dodecenoic acid	2430-94-6	0.016683	734	1.385	732
cis-9-Hexadecenoic acid	0-00-0	0.034542	982	1.415	812
cis-9-Hexadecenoic acid	0-00-0	0.33013	986	1.44	899
Dodecanoic acid	143-07-7	0.031761	738	1.33	865
Eicosanoic acid	506-30-9	0.073595	1198	1.385	695
Heptanoic acid	111-14-8	0.006432	362	1.215	661
Hexanoic acid	142-62-1	0.3492	274	1.285	881
Hexanoic acid, 6-hydroxy-	1191-25-9	0.016703	502	1.78	670
n-Decanoic acid	334-48-5	0.055094	594	1.325	872
n-Hexadecanoic acid	57-10-3	0.012537	1150	1.36	809
Nonanoic acid	112-05-0	0.11761	518	1.34	892
Octadecanoic acid	57-11-4	0.11297	1298	1.48	774
Octanoic acid	124-07-2	0.012643	446	1.265	659
Pentanoic acid	109-52-4	0.38317	194	1.19	860
Pentanoic acid, 3-methyl-	105-43-1	0.006277	242	1.165	498
Pentanoic acid, 4-oxo-	123-76-2	0.12818	342	1.8	907
Propanoic acid	79-09-4	0.16804	82	0.93	907
Propanoic acid, 2,3-dihydroxy-	473-81-4	0.066926	1518	0.41	426
Tetracosanoic acid	557-59-5	0.31306	1382	1.405	781
Tridecanoic acid	638-53-9	0.031415	806	1.325	860
Undecanoic acid	112-37-8	0.035651	666	1.33	810
Undecanoic acid, hydroxy-, lactone	39282-36-5	0.079948	978	1.695	825
Undecylenic acid	112-38-9	0.026706	662	1.4	838

Table 6.2. Continued

Esters					
Propanoic acid, 2-oxo-, methyl ester	600-22-6	0.15039	126	1.435	809
2-Propenoic acid, ethenyl ester	2177-18-6	0.021838	246	1.79	635
Hexanoic acid, 2-pentenyl ester, (Z)-	74298-89-8	0.013148	278	1.275	693
Heptanoic acid, methyl ester	106-73-0	0.019047	306	1.255	768
Benzoic acid, methyl ester	93-58-3	0.009942	370	1.77	726
Octanoic acid, methyl ester	111-11-5	0.032463	394	1.27	842
Decanoic acid, methyl ester	110-42-9	0.009149	562	1.27	624
Undecanoic acid, methyl ester	1731-86-8	0.00781	638	1.275	700
Formic acid phenyl ester	1864-94-4	0.008772	646	2.48	636
Dodecanoic acid, methyl ester	111-82-0	0.007349	710	1.275	734
Nonanedioic acid, monomethyl ester	2104-19-0	0.019315	754	1.76	661
Octanoic acid, methyl ester	111-11-5	0.007696	778	1.285	521
Pentadecanoic acid, methyl ester	7132-64-1	0.028302	910	1.275	807
Heptadecanoic acid, methyl ester	1731-92-6	0.006966	1026	1.28	595
Terephthalic acid, phenyl undecyl ester	0-00-0	0.004164	1054	1.325	617
Nonanoic acid, 9-hydroxy-, methyl ester	34957-73-8	0.008161	1078	1.33	670
Hexadecanedioic acid, dimethyl ester	19102-90-0	0.034618	1162	1.665	784
7-Hexadecenoic acid, methyl ester, (Z)-	56875-67-3	0.00567	1178	1.355	743
Pentadecanoic acid, 14-methyl-, methyl ester	5129-60-2	0.004344	1182	1.3	443
Hexadecanoic acid, 15-methyl-, methyl ester	6929-04-0	0.017763	1278	1.31	754
Nonadecanoic acid, ethyl ester	18281-04-4	0.012115	1306	1.31	572
Octadecanoic acid, 2-propenyl ester	6289-31-2	0.010242	1342	1.345	781
Hexadecanoic acid, 15-methyl-, methyl ester	6929-04-0	0.012788	1366	1.335	752
Alkanes					
Undecane	1120-21-4	0.03068	370	0.96	891
Dodecane	112-40-3	0.049858	458	0.98	918
Tridecane	629-50-5	0.070476	538	1	891
Tetradecane	629-59-4	0.057009	618	1.005	900
Hexadecane	544-76-3	0.057986	762	1.03	909
Heptadecane	629-78-7	0.053897	826	1.05	867
Pentadecane	629-62-9	0.010017	1262	1.13	751
Alkyl Benzenes					
Benzene, propyl-	103-65-1	0.024301	246	1.255	891
Benzene, 1-ethyl-4-methyl-	622-96-8	0.04269	254	1.275	850
Benzene, 1,2,3-trimethyl-	526-73-8	0.026236	278	1.335	890
Benzene, butyl-	104-51-8	0.032083	334	1.34	873
Benzene, 1-ethyl-2-methyl-	611-14-3	0.029345	266	1.35	816
Benzene, hexyl-	1077-16-3	0.024432	510	1.355	823
benzene, octyl-	2189-60-8	0.02288	670	1.355	822
benzene, decyl-	104-72-3	0.012547	814	1.355	750
Benzene, pentyl-	538-68-1	0.03447	422	1.36	888
benzene, nonyl-	1081-77-2	0.020086	742	1.36	772
Benzene, heptyl-	1078-71-3	0.025739	590	1.365	832
benzene, undecyl-	6742-54-7	0.010465	878	1.365	573
benzene, dodecyl-	123-01-3	0.006918	942	1.37	586
Benzene, 3-butenyl-	768-56-9	0.010516	322	1.415	780
Benzene, 1,2,4-trimethyl-	95-63-6	0.020406	306	1.42	750
Benzene, 4-pentenyl-	1075-74-7	0.007143	414	1.445	809

6.4.1 Comparisons within types of bio-oil samples

Three different types of samples were studied in this experiment: Douglas-fir bark, Southern pine bark, and a Southern pine bark/wood mixture. For the Douglas-fir bark sample there are two different pyrolysis conditions used to produce the bio-oil (See Table 6.1). The two different types of pyrolysis lead to different bio-oil yields and different compositions of the sample itself. In Figure 6.4 (A) the methoxy phenols, alkyl benzenes, carboxylic acid, ester, and alkane composition of the Douglas-fir bark samples (bio-oil sample 1 and bio-oil sample 2) is compared. While the relative amount of methoxy phenols remains the same, the amount of carboxylic acids in the sample goes up and the amount of esters significantly decreases in sample 2 compared to sample 1. This decrease in ester formation may be due to the higher N_2 flow rate used in sample 2.

In Figure 6.4 (B) the methoxy phenols, alkyl benzenes, carboxylic acid, ester, and alkane composition of the Southern pine bark samples (bio-oil sample 3 and bio-oil sample 4) is compared. In these samples the amount of methoxy phenols, esters, and alkanes in sample 4 is almost doubled the amount seen in Sample 3. This increase in methoxy phenol and ester formation may be due to the faster N_2 flow rate being used for sample 4 than was used in Sample 3.

The methoxy phenols, alkyl benzenes, carboxylic acid, ester, and alkane composition of the Southern pine bark-wood mixture samples (bio-oil sample 5, 6,7,8,9, and 10) is compared in Figure 6.4 (C). There are six different bio-oil samples in this comparison for the Pine-Bark wood mixture, Samples 5 and 6 have the same furnace temperature of 400 °C, but different flow rates, but the product distribution for the Area

% of the types of compounds produced in these samples are relatively similar. Samples 7 and 8 are reacted at a furnace temperature of 500 °C, in these reactions the flow rate for Sample 7 is 200 ml/min and the flow rate for sample 8 is 500 ml/min. For Sample 7 the amount of esters produced in the pyrolysis reaction is three times as much as that produced for Sample 8. The decrease in ester formation for the pine bark-wood mixture sample is different from the results found in the Douglas-Fir Bark and the Pine Bark samples, this difference may be due to the mixture of wood that is found in Samples 5 through 10. Samples 9 and 10 are reacted at a furnace temperature of 600 °C, and the amount of esters produced from sample 9 is larger than the amount of esters produced in sample 10. This difference in trends compared to samples 1 and 2 and samples 3 and 4 may be due to the higher furnace temperature used or the differences in bio-oils produced from barks samples to mixtures of wood and bark samples.

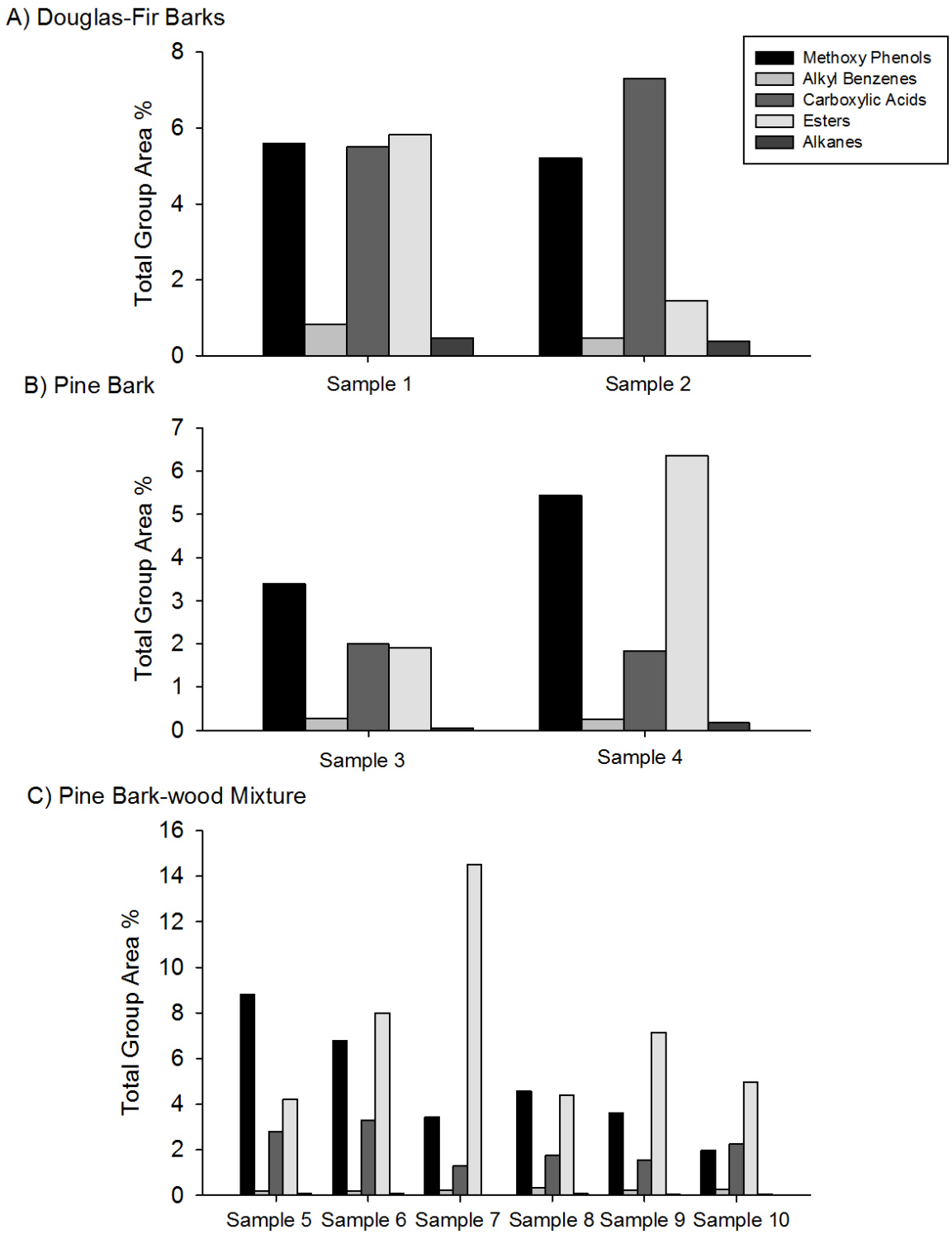

Figure 6.4. Comparison within the different types of tree bark/wood samples. Each Sample has varied pyrolysis conditions that are listed in Table 6.1. Panel (A) is Douglas-fir bark reacted under different pyrolysis conditions, panel (B) is Southern pine bark, and panel (C) is a mixture of Southern pine bark and wood.

6.4.1 Comparisons between types of bio-oil samples

As can be seen in Figure 6.3 there are large differences in the type of compounds produced from different types of bio-oils. The bio-oils samples that have the same pyrolysis conditions (500 °C furnace temperature and 200 ml/min flow N_2 rate) are bio-oil Sample 1, bio-oil Sample 3, and bio-Oil Sample 7.

The comparison between the three different types of bio-oil is shown in Figure 6.5. The type of compounds that are produced for each type of sample varies. For Bio-oil Sample 1 (Douglas-fir bark), Figure 6.5 (A), the production of methoxy phenols, carboxylic acids, and esters each take up about one-third of the total % Area covered out of the types of compounds that are selected for this analysis. There is a small amount of alkyl benzenes formed in this sample with an even smaller amount of alkanes.

For bio oil sample 3 (Southern pine bark), Figure 6.5 (B), the amount of methoxy phenols increases with respect to the other compounds formed, taking up about one-half of the total amount of type of compounds that are formed in this sample, with esters and carboxylic acids each taking up about one-quarter of the total amount of type of compounds formed.

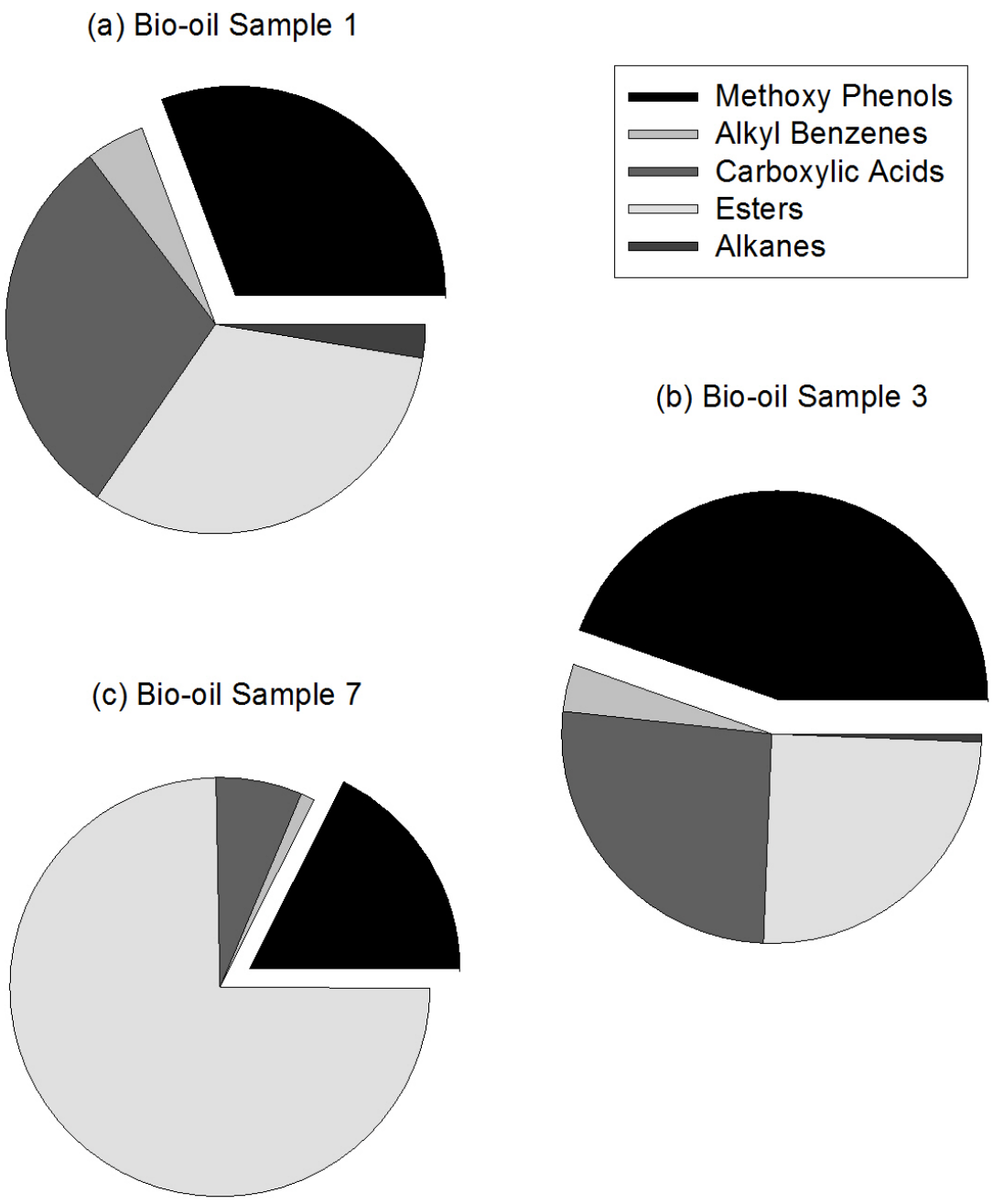

Figure 6.5 Comparisons between the different types of tree bark/wood samples. Each Sample has the same pyrolysis conditions as listed in Table 6.1. Panel (A) is Douglas-fir bark: bio-oil sample 1, panel (B) is Southern pine bark: bio-oil sample 3, and panel (C) is a mixture of Southern pine bark and wood: bio-oil sample 7.

For bio-oil Sample 7 (Southern pine Bark-wood mixture), Figure 6.5 (C), esters amount to three-fourths of the total number of compounds that are formed. This

difference with respect to sample 1 and sample 3 is quite large, due to the fact that the main type of compound detected in sample 1 and sample 3 was methoxy phenols, and methoxy phenols taking up about one-eighth of the total type of compounds formed in the Southern pine bark-wood mixture. This large difference in the type of compounds formed could be due to the introduction of wood to the Southern pine bark sample causing the large increase in the formation of esters in bio-oil Sample 7.

6.4 Conclusions

The type of matter that is reacted to form a particular type of bio-oil is important in determining the type of compounds that compose the bio-oil. The reaction conditions that are used in the production of a bio-oil also have an impact on the type of compounds that are found in a particular bio-oil sample. The results from this study indicate that a large amount of methoxy phenols are produced when a bark sample is used (Douglas-fir or Southern pine bark), and a large amount of esters are produced when a bark sample is mixed with wood (Southern pine bark-wood mixture). The results from this study also indicate that the pyrolysis conditions used to create a particular type of compound in one type of bio-oil (Douglas-fir bark) may not be the optimal conditions to create that particular type of compound in another type of bio-oil (Southern pine bark).

CHAPTER 7

CONCLUSIONS

Neat formamide samples irradiated with UV light produced a larger yield and diversity of purine nucleobases than the non-UV irradiated neat formamide samples. In addition, the presence of dissolved minerals and mineral surfaces can enhance yields, but not the diversity of products when the samples are irradiated with UV light. Thus, the equalizing effect that UV light has on the yields and the product distribution further relaxes the chemical and environmental requirements for biopolymer building block formation on the prebiotic Earth. The results presented here clearly illustrate the ability for UV photons to increase the yield and diversity of nucleobases formed in model prebiotic reactions involving heated formamide, and that UV photons can work synergistically with minerals or their dissolved ions in such reactions.

The GC×GC-MS results for the pre-biotic reaction analysis leads to easier identification and quantification of additional relevant pre-biotic molecules, along with a faster, more robust method to analyze prebiotic reactions. GC×GC-MS also allows for the identification of small molecular weight molecules that can be obtained using HPLC-UV or LC-MS/MS. The prebiotic synthesis reactions that start with only one type of molecule, formamide, not only form a large amount of molecules, they also form a wide variety of molecules, which make GC×GC-MS an ideal method to study them. The analyses presented in Chapter 5 indicate that GC×GC-MS is a valuable method for the analysis of complex pre-biotic mixtures.

GC×GC-MS is also a useful method to study other complex mixtures, such as bio-oil samples. The bark and bark-wood bio-oil samples studied in Chapter 6 show that

GC×GC-MS is not only a good method for the analysis of complex mixtures, it can also be used for grouping types of compounds found in any given sample for easy identification of functional group, and eventually the entire molecule. The results from this study indicate that not only does the different type of bark used lead to the formation of different molecules, the N_2 flow rate and the furnace temperature also have an effect on the type of compounds that are formed.

REFERENCES

(1) Gesteland, R. F.; Cech, T. R.; Atkins, J. F. *The Rna World*; 3rd ed.; Cold Spring Harbor Laboratory Press: Cold Spring Harbor, NY, 2006.

(2) Battersby, T. R.; Albalos, M.; Friesenhahn, M. J. *Chemistry & Biology* **2007**, *14*, 525-531.

(3) Crick, F. H. C. *Journal of Molecular Biology* **1968**, *38*, 367-379.

(4) Heuberger, B. D.; Switzer, C. *Chembiochem* **2008**, *9*, 2779-2783.

(5) Tso, P. O. P.; Melvin, I. S.; Olson, A. C. *Journal of the American Chemical Society* **1963**, *85*, 1289-1296.

(6) Benner, S. A. *Accounts of Chemical Research* **2004**, *37*, 784-797.

(7) Miller, S. L. *Science* **1953**, *117*, 528-529.

(8) Oro, J. *Nature* **1961**, *191*, 1193-1194.

(9) Ehrenfreund, P.; Irvine, W.; Becker, L.; Blank, J.; Brucato, J. R.; Colangeli, L.; Derenne, S.; Despois, D.; Dutrey, A.; Fraaije, H.; Lazcano, A.; Owen, T.; Robert, F.; Intl Space Sci, I. I. T. *Reports on Progress in Physics* **2002**, *65*, 1427-1487.

(10) Ferris, J. P.; Orgel, L. E. *Journal of the American Chemical Society* **1965**, *87*, 4976-&.

(11) Ferris, J. P.; Orgel, L. E. *Journal of the American Chemical Society* **1966**, *88*, 1074.

(12) Ferris, J. P.; Orgel, L. E. *Journal of the American Chemical Society* **1966**, *88*, 3829-3831.

(13) Fuller, W. D.; Orgel, L. E.; Sanchez, R. A. *Journal of Molecular Evolution* **1972**, *1*, 249-257.

(14) Hill, A.; Orgel, L. E. *Origins of Life and Evolution of the Biosphere* **2002**, *32*, 99-102.

(15) Joyce, G. F. *Nature* **1989**, *338*, 217-224.

(16) Levy, M.; Miller, S. L.; Oro, J. *Journal of Molecular Evolution* **1999**, *49*, 165-168.

(17) Orgel, L. E. *Origins of Life and Evolution of the Biosphere* **2004**, *34*, 361-369.

(18) Roy, D.; Najafian, K.; Schleyer, P. V. *Proceedings of the National Academy of Sciences of the United States of America* **2007**, *104*, 17272-17277.

(19) Saladino, R.; Crestini, C.; Ciambecchini, U.; Ciciriello, F.; Costanzo, G.; Di Mauro, E. *Chembiochem* **2004**, *5*, 1558-1566.

(20) Saladino, R.; Crestini, C.; Ciciriello, F.; Costanzo, G.; Di Mauro, E. *Chemistry & Biodiversity* **2007**, *4*, 694-720.

(21) Saladino, R.; Crestini, C.; Costanzo, G.; Negri, R.; Di Mauro, E. *Bioorganic & Medicinal Chemistry* **2001**, *9*, 1249-1253.

(22) Saladino, R.; Crestini, C.; Neri, V.; Brucato, J. R.; Colangeli, L.; Ciciriello, F.; Di Mauro, E.; Costanzo, G. *Chembiochem* **2005**, *6*, 1368-1374.

(23) Sanchez, R. A.; Ferris, J. P.; Orgel, L. E. *Journal of Molecular Biology* **1967**, *30*, 223-253.

(24) Schopf, W. J. *Earth's Earliest Biosphere: Its Origin and Evolution*; Princeton University Press: Princeton, NJ, 1983.

(25) Senanayake, S. D.; Idriss, H. *Proceedings of the National Academy of Sciences of the United States of America* **2006**, *103*, 1194-1198.
(26) Voet, A. B.; Schwartz, A. W. *Bioorganic Chemistry* **1983**, *12*, 8-17.
(27) Yamada, H.; Hirobe, M.; Higashiyama, K.; Takahashi, H.; Suzuki, K. T. *Tetrahedron Letters* **1978**, 4039-4042.
(28) Yamada, H.; Okamoto, T. *Chemical & Pharmaceutical Bulletin* **1972**, *20*, 623-624.
(29) Zubay, G.; Mui, T. *Origins of Life and Evolution of the Biosphere* **2001**, *31*, 87-102.
(30) Costanzo, G.; Saladino, R.; Crestini, C.; Ciciriello, F.; Di Mauro, E. *Bmc Evolutionary Biology* **2007**, *7*.
(31) Schopf, J. W. *Life's Origin: The Beginnings of Biological Evolution*; University of California Press: Berkeley, 2002.
(32) Zubay, G. *Origins of Life on the Earth and in the Cosmos*; 2nd ed.; Academic Press: Orlando, 2000.
(33) Orgel, L. E. *The Origins of Life: Molecules and Natural Selection*; John Wiley & Sons: New York, 1973.
(34) Campos, V.; Marigliano, A. C. G.; Solimo, H. N. *Journal of Chemical and Engineering Data* **2008**, *53*, 211-216.
(35) Bernstein, M. P.; Allamandola, L. J.; Sandford, S. A. In *Life Sciences: Complex Organics in Space*; Raulin, F., Greenberg, J. M., Eds. 1997; Vol. 19, p 991-998.
(36) Chen, Y. J.; Nuevo, M.; Hsieh, J. M.; Yih, T. S.; Sun, W. H.; Ip, W. H.; Fung, H. S.; Chiang, S. Y.; Lee, Y. Y.; Chen, J. M.; Wu, C. Y. R. *Astronomy & Astrophysics* **2007**, *464*, 253-257.
(37) Gerakines, P. A.; Moore, M. H.; Hudson, R. L. *Icarus* **2004**, *170*, 202-213.
(38) Hudson, R. L.; Khanna, R. K.; Moore, M. H. *Astrophysical Journal Supplement Series* **2005**, *159*, 277-281.
(39) Raunier, S.; Chiavassa, T.; Duvernay, F.; Borget, F.; Aycard, J. P.; Dartois, E.; d'Hendecourt, L. *Astronomy & Astrophysics* **2004**, *416*, 165-169.
(40) Woon, D. E. *International Journal of Quantum Chemistry* **2002**, *88*, 226-235.
(41) Millar, T. J. *Astrobiology: Future Perspectives* **2004**, *Kluwer Eds*.
(42) Bockelee-Morvan, D., Lis, D.C., Wink, J.E. *Cometary and Interstellar Material* **2000**, *353*, 1101-1114.
(43) Schutte, W. A.; Boogert, A. C. A.; Tielens, A.; Whittet, D. C. B.; Gerakines, P. A.; Chiar, J. E.; Ehrenfreund, P.; Greenberg, J. M.; van Dishoeck, E. F.; de Graauw, T. *Astronomy and Astrophysics* **1999**, *343*, 966-976.
(44) In *ECT Kirk-Othmer Encyclopedia of Chemical Technology* Wiley-Interscience: 1978; Vol. 11, p 258-262.
(45) Miller, S. L. a. L. E. O. *The Origins of Life on the Earth*; Prentice-Hall: Englewood Cliffs, 1974.
(46) *Principles of Atmospheric Chemistry*; Osford University: Oxford, 1995.
(47) Vaida, V. *International Journal of Photoenergy* **2005**, *7*, 61-70.
(48) Saladino, R.; Ciambecchini, U.; Crestini, C.; Costanzo, G.; Negri, R.; Di Mauro, E. *Chembiochem* **2003**, *4*, 514-521.

(49) Saladino, R.; Crestini, C.; Neri, V.; Ciciriello, F.; Costanzo, G.; Mauro, E. *ChemBioChem* **2006**, *7*, 1707-1714.

(50) Saladino, R.; Neri, V.; Crestini, C.; Costanzo, G.; Graciotti, M.; Di Mauro, E. *Journal of the American Chemical Society* **2008**, *130*, 15512-15518.

(51) Michalkova, A.; Tunega, D.; Nagy, L. T. *Journal of Molecular Structure-Theochem* **2002**, *581*, 37-49.

(52) Costanzo, G.; Saladino, R.; Crestini, C.; Ciciriello, F.; Di Mauro, E. In *BMC Evol. Biol.* 2007, p (Suppl 2): S1.

(53) Gomez, A.; Tang, K. Q. *Physics of Fluids* **1994**, *6*, 404-414.

(54) Dole, M.; Mack, L. L.; Hines, R. L. *Journal of Chemical Physics* **1968**, *49*, 2240-&.

(55) Iribarne, J. V.; Thomson, B. A. *Journal of Chemical Physics* **1976**, *64*, 2287-2294.

(56) Dimandja, J. M. D. *American Laboratory* **2003**, *35*, 42-+.

(57) Dimandja, J. M. D. *Analytical Chemistry* **2004**, *76*, 167A-174A.

(58) Dimandja, J. M. D.; Grainger, J.; Patterson, D. G.; Turner, W. E.; Needham, L. L. *Journal of Exposure Analysis and Environmental Epidemiology* **2000**, *10*, 761-768.

(59) Dalluge, J.; Beens, J.; Brinkman, U. A. T. *Journal of Chromatography A* **2003**, *1000*, 69-108.

(60) Mayadunne, R.; Nguyen, T. T.; Marriott, P. J. *Analytical and Bioanalytical Chemistry* **2005**, *382*, 836-847.

(61) Junge, M.; Huegel, H.; Marriott, P. J. *Chirality* **2007**, *19*, 228-234.

(62) Mohler, R. E.; Dombek, K. M.; Hoggard, J. C.; Young, E. T.; Synovec, R. E. *Analytical Chemistry* **2006**, *78*, 2700-2709.

(63) Sinha, A. E.; Hope, J. L.; Prazen, B. J.; Nilsson, E. J.; Jack, R. M.; Synovec, R. E. *Journal of Chromatography A* **2004**, *1058*, 209-215.

(64) Tranchida, P.; Donato, P.; Dugo, P.; Dugo, G.; Mondello, L. *Trac-Trends in Analytical Chemistry* **2007**, *26*, 191-205.

(65) McGuigan, M.; Waite, J. H.; Imanaka, H.; Sacks, R. D. *Journal of Chromatography A* **2006**, *1132*, 280-288.

(66) Hyotylainen, T.; Kallio, M.; Hartonen, K.; Jussila, M.; Palonen, S.; Riekkola, M. L. *Analytical Chemistry* **2002**, *74*, 4441-4446.

(67) Groger, T.; Welthagen, W.; Mitschke, S.; Schaffer, M.; Zimmermann, R. *Journal of Separation Science* **2008**, *31*, 3366-3374.

(68) Harrison, T. M.; Blichert-Toft, J.; Muller, W.; Albarede, F.; Holden, P.; Mojzsis, S. J. *Science* **2006**, *312*.

(69) Watson, E. B.; Harrison, T. M. *Science* **2005**, *308*, 841-844.

(70) Boden, J. C.; Back, R. A. *Transactions of the Faraday Society* **1970**, *66*, 175-&.

(71) Gingell, J. M.; Mason, N. J.; Zhao, H.; Walker, I. C.; Siggel, M. R. F. *Chemical Physics* **1997**, *220*, 191-205.

(72) Duvernay, F.; Trivella, A.; Borget, F.; Coussan, S.; Aycard, J. P.; Chiavassa, T. *Journal of Physical Chemistry A* **2005**, *109*, 11155-11162.

(73) Arey, J. S.; Nelson, R. K.; Xu, L.; Reddy, C. M. *Analytical Chemistry* **2005**, *77*, 7172-7182.

(74) Arey, J. S.; Nelson, R. K.; Xu, L.; Reddy, C. M. *Analytical Chemistry* **2007**, *79*, 4736-4736.

(75) Mohan, D.; Pittman, C. U.; Steele, P. H. *Energy & Fuels* **2006**, *20*, 848-889.

(76) Lu, Q.; Li, W. Z.; Zhu, X. F. *Energy Conversion and Management* **2009**, *50*, 1376-1383.

(77) Garcia-Perez, M.; Chaala, A.; Pakdel, H.; Kretschmer, D.; Roy, C. *Biomass & Bioenergy* **2007**, *31*, 222-242.

(78) Garcia-Perez, M.; Chaala, A.; Pakdel, H.; Kretschmer, D.; Roy, C. *Journal of Analytical and Applied Pyrolysis* **2007**, *78*, 104-116.

(79) Wu, L.; Guo, S. P.; Wang, C.; Yang, Z. Y. *Bioresource Technology* **2009**, *100*, 2069-2076.

(80) Ingram, L.; Mohan, D.; Bricka, M.; Steele, P.; Strobel, D.; Crocker, D.; Mitchell, B.; Mohammad, J.; Cantrell, K.; Pittman, C. U. *Energy & Fuels* **2008**, *22*, 614-625.

(81) Mullen, C. A.; Boateng, A. A. *Energy & Fuels* **2008**, *22*, 2104-2109.

(82) vanderHage, E. R. E.; Boon, J. J. *Journal of Chromatography A* **1996**, *736*, 61-75.

(83) Zhou, L.; Zong, Z. M.; Tang, S. R.; Zong, Y.; Xie, R. L.; Ding, M. J.; Zhao, W.; Zhu, X. F.; Xia, Z. L.; Wu, L.; Wei, X. Y. *Energy Sources Part a-Recovery Utilization and Environmental Effects*, *32*, 370-375.

(84) Yuan, X. Z.; Tong, J. Y.; Zeng, G. M.; Li, H.; Xie, W. *Energy & Fuels* **2009**, *23*, 3262-3267.

(85) Fukushima, M.; Yamamoto, M.; Komai, T.; Yamamoto, K. *Journal of Analytical and Applied Pyrolysis* **2009**, *86*, 200-206.

(86) Kuznetsov, B. N.; Efremov, A. A.; Levdanskii, V. A.; Kuznetsova, S. A.; Polezhayeva, N. I.; Shilkina, T. A.; Krotova, I. V. *Bioresource Technology* **1996**, *58*, 181-188.

(87) Mao, D.; Van De Weghe, H.; Lookman, R.; Vanermen, G.; De Brucker, N.; Diels, L. *Fuel* **2009**, *88*, 312-318.

(88) Gaquerel, E.; Weinhold, A.; Baldwin, I. T. *Plant Physiology* **2009**, *149*, 1408-1423.

(89) Perera, R. M. M.; Marriott, P. J.; Galbally, I. E. *Analyst* **2002**, *127*, 1601-1607.

(90) Hamilton, J. F.; Webb, P. J.; Lewis, A. C.; Hopkins, J. R.; Smith, S.; Davy, P. *Atmospheric Chemistry and Physics* **2004**, *4*, 1279-1290.